MINIATURE AMBULATORY SKIN CONDUCTANCE MONITOR AND METHODS FOR INVESTIGATING HOT FLASH PHENOMENA

by

Dennis Edmund Bahr

A dissertation submitted in partial fulfillment of

The requirements for the degree of

Doctor of Philosophy

(Biomedical Engineering)

at the

UNIVERSITY OF WISCONSIN-MADISON

2012

Date of final oral examination: 5/2/12

The dissertation is approved by the following members of the Final Oral Committee:

Willis Tompkins, Professor, Biomedical Engineering
Walter Block, Professor, Biomedical Engineering
Oliver Wieben, Professor, Biomedical Engineering
Heidi Ploeg, Professor, Mechanical Engineering
John Webster, Professor Emeritus, Biomedical Engineering
Everett Smith, Professor Emeritus, Population Health Sciences

MINIATURE AMBULATORY SKIN CONDUCTANCE MONITOR AND METHODS FOR INVESTIGATING HOT FLASH PHENOMENA

Dennis Edmund Bahr

Under the supervision of Professor Willis J. Tompkins
At the University of Wisconsin-Madison

The purpose of this research was to design, build, and test a system to measure hot flash events in ambulatory women during menopause. Hot flash events were measured using changes in skin conductance on the upper torso. The underlying reason for the development of the system was to have a user friendly system that could accurately record hot flash events as they related to the efficacy of intervention therapies such as estrogen and those using various Complementary and Alternative Medicine (CAM) therapies.

A skin conductance monitoring system was developed and tested and was shown to acquire and record hot flash events in both supervised laboratory and unsupervised ambulatory conditions. The efficacy of the system was proven by comparing the results from algorithms developed during this research and experts who marked the hot flash events in the data. The experts had years of experience doing hot flash clinical research and well versed in the morphology of hot flash events.

The developed monitoring system of a reusable, miniaturized, enclosed electronic circuit board that snaps onto two hydrogel electrodes affixed to a disposable adhesive patch. Three components work together to provide improved hot flash recordings: the Ag/AgCl electrode, the

hydrogel to skin interface, and the breathable cloth dressing. Data collected by the monitor are downloaded directly from the monitor to a computer using customized software for displaying and processing the data.

The system required the development of sophisticated software algorithms to properly process the data for reliable, reproducible, and accurate measurement of hot flash events. Signal processing algorithms were investigated including matched filters or template matching and artificial neural networks. These two methods were chosen for implementation because each of them treats data in a different and unique way and expectations were that one or both of them would provide a method that could be used for computer scoring of the hot flash data.

The algorithm with the best statistics was the matched filter which demonstrated an average sensitivity of 0.92 and an average specificity of 0.90 in a development cohort of 17 women between the ages of 40 and 60 who experienced hot flashes over a three day period. The monitor and algorithm were then validated on a similar but different cohort of 20 women. The results showed an average sensitivity of 0.92 and a specificity of 0.87.

Hardware and software was developed by a team of three engineers in the Madison, Wisconsin area. A women's health research team at the University of California at San Francisco (UCSF) Women's Health Clinical Research Center did all of the recruiting and data collection.

Advisor: Willis J. Tompkins, PhD Date: May 8, 2012

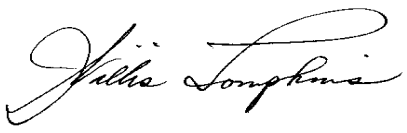

_____

Keywords

Hot flash, hot flush, recorder, monitor, matched filter, template matching, pattern matching, electrode, hydrogel, Pearson, correlation coefficient, artificial neural networks, menopause

Definitions

True Positive: TP False Positive: FP

True Negative: TN False Negative: FN

Sensitivity: A measurement of the proportion of true positives (positives based on a gold standard identified as such by a diagnostic test) out of the total number of positives identified by the gold standard test. SENS = TP / TP+FN

Specificity: A measurement of the proportion of true negatives (negatives based on a gold standard identified as such by a diagnostic test) out of the total number of negatives identified by the gold standard test. SPEC =TN / TN + FP

Positive Predictive Value: A measure of the rate at which a hot flash is truly positive.

PPV = TP / TP + FP

Negative Predictive Value: A measure of the rate at which a hot flash is truly negative.

PPV = TN / TN + FN

Collaboration Statement

The research reported in this thesis was completed in collaboration with Professor John G. Webster who is with the Biomedical Engineering Department at the University of Wisconsin in Madison, Wisconsin and Mark Shults who is an expert in medical materials and a Madison, Wisconsin resident. During the development of the signal processing phase of the work, collaborators included Professor Willis J. Tompkins who is with the Biomedical Engineering Department at the University of Wisconsin in Madison Wisconsin and Professor John L. Semmlow from the Robert Wood Johnson Medical School and the Department of Biomedical Engineering at Rutgers University in New Jersey.

A collaborative agreement was established with a team of researchers, clinicians, and statisticians at the University of California at San Francisco (UCSF) Women's Health Clinical Research Center. Their job was to recruit women subjects, do the human studies, and collect the hot flash data for subsequent processing. It was my job to oversee the design, development, and testing of the new hot flash monitor system.

The research and subsequent development of the system was funded by two SBIR Phase I grants R43AT3183-01 and R43AT4070-01, and also by one SBIR Phase II grant 2R44AT3183-02 from the National Institutes of Health National Center for Complementary and Alternative Medicine (NCCAM).

Acknowledgments

First of all, I would like to thank my advisor and mentor, Professor Willis J. Tompkins whose help and guidance brought this research to a very satisfactory conclusion. His continual encouragement and support is much appreciated. He allowed me to do my own work, but occasionally made suggestions that were very helpful. I was also very fortunate to be able to work with Professor John Webster of the Biomedical Engineering Department at the University of Wisconsin who is an expert in medical instrument and electrode design, and a team of clinical researchers from the Women's Health Clinical Research Center at the University of California at San Francisco, who did the clinical studies that were necessary to complete this work.

I wish to thank fellow team members including Mark Shults who is a biomedical engineer experienced in the design and development of miniature medical instruments and conductive adhesive polymer materials as well as Mitchell Tyler who helped with the human interface and ergonomics of the monitor.

A collaborative agreement was set up with a team of researchers, clinicians, and statisticians at the University of California at San Francisco (UCSF) Women's Health Clinical Research Center. Their effort complemented the engineering team and proved to be a valuable component in this effort. I wish especially to thank Dr. Deborah Grady for her direction in setting up the human studies and Judy Macer for managing the clinical studies and for her very insightful feedback on the performance and design of the monitor. Dr. Fredi Kronenberg's vast experience with hot flash monitoring and women's clinical studies added an important component by continually

reviewing the work as it progressed and providing valuable feedback. I learned a great deal from Dr. Kronenberg and Dr. Grady on how to do good human clinical studies that would pass peer review and I thank them both for this. I also wish to thank statistician and mathematician Jennifer Creasman for helping me sort through ideas for algorithms and ultimately checking my work in coding and testing the algorithms.

I would not have pursued my PhD this late in life if it were not for the continuous and persistent efforts of Professor Everett Smith to finish my PhD and the encouragement of my children Aaron and Angela. For this they all deserve a very special thank you. Finally, I would like to thank the National Institutes the Health for funding this work to its completion.

I wish to acknowledge the clinical researcher who made this statement regarding the hot flash monitor.

Yes! This is the best hot flash monitor in existence, and more to the point it is an order of magnitude improvement on what came before. (Biolog etc).
So that's a great accomplishment and the engineers are to be commended for their creative design in what could become the next fashion statement for menopausal women (all you need is multicolor covers like phones and people won't worry about hiding it under their clothes....)

Fredi

Table of Contents

Keywords iii

Definitions iii

Collaboration Statement iv

Acknowledgments v

Table of Contents vii

List of Figures xi

List of Tables xvi

List of Appendices xvii

Chapter 1 1

1 Literature Review and Background 1

1.1 Introduction and Overview 1

1.2 Motivation and Objectives 2

Chapter 2 6

2 Body Surface Recording 6

2.1 Introduction and Overview 6

2.2 Characteristics of Human Skin 6

2.3 Sweat Glands and Sweat Pores 8

Chapter 3 11

3 Hot Flash Electrodes 11

3.1 History and Introduction 11

3.2 The Metal Electrode 12

3.3 The Hydrogel Electrode 14

3.4 Hydrogel Electrode Testing 15

Chapter 4 22

4 System Hardware 22

4.1 Introduction and Overview 22

4.2 Electrical Design 22

4.3 Mechanical Design 24

4.4 Ergonomic Design 26

Chapter 5 28

5 System Firmware 28

5.1 Introduction and Overview 28

5.2 Embedded Software 28

5.3 Signal Sampling 29

5.4 Hot Flash Data Storage 31

Chapter 6 32

6 Research Methodology 32

6.1 Introduction and Overview 32

6.2 Human Subjects 32

6.3 Data Collection 34

6.4 The Diagnostic Grade Monitor 38

6.5 Data Processing Algorithms 40

Chapter 7 42

7 Human Safety and Data Monitoring 42

7.1 Human Safety 42

7.2 Data Safety Monitor 43

Chapter 8 46
8 Matched Filter and Pattern Matching 46
8.1 Introduction and Overview 46
8.2 Matched Filter Template 47
8.3 Matched Filter Template Selection 51
8.4 Pearson Correlation Coefficient 52
8.5 Matched Filter Data Processing 56
Chapter 9 60
9 Adaptive Neural Networks 60
9.1 Introduction and Overview 60
9.2 Neural Network Theory 61
9.3 Neural Network Structure 63
9.4 Neural Network Implementation 65
9.5 Neural Network Training 69
9.6 Using the Trained Neural Network 74
Chapter 10 80
10 Conclusion and Discussion 80
10.1 Data Reduction Results 80
10.2 Production Hot Flash Monitor 81
Bibliography 83
Appendix I 88
Appendix II 92
Appendix III 93
Appendix IV 120

Appendix V.....123

Appendix VI.....125

Appendix VII.....126

Appendix VIII.....127

Appendix IX.....128

Appendix X.....131

List of Figures

Figure 2-1: Section of human skin showing the various layers (Ebling, Eady, and Leigh, 1992.) ……..……7

Figure 2-2: An electrical circuit model that shows the layers in the skin and depicts the equivalent circuit elements that match these layers. Included is a model for an electrode to gel interface with the epidermis. (Neuman 2008) …….……...…….…...8

Figure 2-3: The three most common characteristics of hot flash conductance waveforms are a rapid rise in conductance, the gently rounded peak, and the exponential like fall. The scale for the abscissa is the number of 10 s samples and the ordinate has been normalized to the peak of the hot flash. ……..10

Figure 3-1: In general, skin impedance decreases (skin conductance increases) with frequency for metal electrodes. The unit of conductance used in this dissertation is the μS. (Neuman 2008). ……...12

Figure 3-2: Shown is the impedance versus frequency of a pure Ag electrode as well as Ag electrodes with electrolytically deposited layers of AgCl. The electrode area is 0.25 cm^2 and the letters-numbers indicate the amount of deposition in mA·s. (L.A. Geddes, L.E. Baker, and A.G. Moore, "Optimum electrolytic chloriding of silver electrodes." *Medical and Biological Engineering, 1969, 7, 49-56.*) ……..…..13

Figure 3-4: An assembled hydrogel electrode patch used during the early experimentation to provide data on hydrogel formulations. The Ag/AgCl metal electrodes were standard ECG electrodes with a male snap on the opposite side. ……...17

Figure 3-5: Abscissa units are in hours and ordinate units are in μS. Left half shows AG603 hydrogel with a conductance averaging 10 μS and erratic recordings. Right half shows AG803 hydrogel yielding a conductance averaging 1 μS with clean recordings. Blue circles show where exercise increases conductance. ……19

Figure 3-6: Abscissa units are in hours and ordinate units are in μS. Shown is a comparison of two electrodes worn by the same subject at the same time. Top: The cream used with the Biolog monitor causes about a 6 μS baseline conductance. Sweating generated by exercise (marked by circles) causes about a 30% change. Bottom: Conductive adhesive gel causes about a 0.8 μS baseline conductance and has less motion artifact. Sweat created by exercise causes a 400% change. During a shower (at about 16:00), the recorder was detached (0 μS). After the shower, electrode was wet recording about 20 μS and recovering in about 30 min. ..……...20

Figure 3-7: Abscissa units are in hours and ordinate units are in μS. The electrode patch shows a baseline conductance of about 0.2 μS. The typical hot flash rises to about 3.0 μS and lasts about 5 to 10 min. ……..……..21

Figure 4-1: Schematic diagram showing the circuit used to apply a voltage to the skin and measure the resulting current flow. Complete schematics for both the diagnostic grade and production monitors can be found in Appendix I. ……..……..23

Figure 4-2: Exploded view of the production hot flash monitor showing all of the components. The small 10 pin header on the right side of the circuit board is the JTAG connector used for programming the microprocessor. On the front of the unit are the USB connector and a battery holder for a small coin cell. …….…….…….……...25

Figure 4-3: The size of the monitor is 7.2 cm × 3.8 cm × 1.2 cm and it has a mass of 16 g or a weight of 0.56 oz including the battery. The battery has a useful life of more than 1 week. The conductance range is from 0 to 30 μS. ……..……...…26

Figure 4-4: Proposed enclosure designs and color schemes for future production. ……....27

Figure 5-1**:** Biphasic waveform that is applied to the skin. The peak-to-peak amplitude is 1.0 V. ……...…….……30

Figure 5-2**:** Positive waveform showing where the voltage is applied to the skin and where the current is sampled. ……..……...…31

Figure 6-1: Samples of the hot flash data that was marked by the experts. ….……..…...35

Figure 6-2: The internal circuitry of the diagnostic grade hot flash monitor that was used in the initial hydrogel electrode investigations. A complete schematic can be found in Appendix I. ……..….……38

Figure 8-1: Abscissa units are in hours and the ordinate units are in μS. The hot flash events can be clearly seen with the blue circles showing subject markings. The large event near the end of the trace shows the effects of exercise or bathing. ……...46

Figure 8-2: Poisson distribution functions. Abscissa units are the number of events and the ordinate units show the probability of an event occurring. *www.wikipedia.org* 48

Figure 8-3: Log-Normal distribution functions with a mean of 10 and variances of 2 and 6. Abscissa units are the number of events and the ordinate units show the probability of an event occurring. *www.google.com* …...……...…….……...……..50

Figure 8-4: The five templates used for the filter kernels. Where *c* is the center parameter and *w* is the width parameter. The values for these parameters were chosen using ROC curves. ……52

Figure 8-5: Pearson Correlation using the data from subject 3024. The red line is an empirically chosen cut point to maximize the statistics. The data above the line are considered hot flash events. ……...……53

Figure 8-6: A comparison between the unprocessed data and the results from the Pearson correlation algorithm. Two false positives are indicated just before hour 3. However, these will ultimately be rejected because the size of the event in the unprocessed data is too small to be a hot flash. ……. ……..……....54

Figure 8-7: Product coefficient returned from the Pearson correlation calculations. The amplitude is representative of the energy in the subject data. Any peak below 5.0 is rejected as subject data that is too small to be a hot flash. …….…....55

Figure 8-8: A receiver operating characteristic (ROC) curve showing the results of varying the kernel parameters. Each circle represents the results of processing the data with a fixed center and width. The best center and width generated the circled point. ……..56

Figure 9-1: Similarity between a neuron (a) and a simple neural network (b) with a single output classifier. www.wikipedia.com www.codeproject.com …….……..…61

Figure 9-2: Sigmoid function and its derivative. While the sigmoid has a range of 0 to 1 the derivative has a range of 0 to 2.5. These functions were normalized before using them. www.wikipedia.com …….……...63

Figure 9-3: A signal flow diagram of the neural network used in this research. ……...…..64

Figure 9-4: Forward response of the neural network written in MatLab. The input is a 60 point vector containing the hot flash data. The hidden values are a vector of length 35 while the output is a single value between 0 and 1 that describes the probability of the input being a hot flash. The variables acc1 and acc2 contain the accumulated weighted sums of the input and hidden layers respectively before the sigmoid discriminator is applied. ……66

Figure 9-5: Back propagation algorithm implemented in MatLab using the gradient method. ……...68

Figure 9-6: An overlay of the 295 true hot flash events used to train the neural network. ....…..70

Figure 9-7: An overlay of the 118 false hot flash events used to train the neural network. …..70

Figure 9-8: Neural network learning curves showing the results from 5 training runs. An epoch is the entire training set having been passed once through the neural network. The rms error is calculated using the errors from the true and false data sets using equations 9.12 and 9.13. The differences in the learning curves are caused by the weights having been randomly initialized. ……..……..…71

Figure 9-9: Neural network learning curve for the training run that produced the best statistical results. The values of the weights generated from this run were used to process both the development and validation data sets. For this run the learning coefficient was set to 0.0005. ..72

Figure 9-10: Learning curve when a learning constant of 0.01 and a true error gain of 5 were used. The oscillations continued even if more epochs were used in the training process. ……..74

Figure 9-11: The classification from the neural network. The cut point of 0.3 produced the best overall statistics on both the development and validation cohort. The data came from subject 3024. ……..……75

Figure 9-12: Comparison between subject data 3024 and the neural network classification response. The blue circles indicate events that were marked by the experts as a hot flash. ..…..76

Figure 10-1: Commercialized Hot Flash monitor. Placement of the monitor is usually done vertically over the sternum but it can be placed on either side. ……....81

List of Tables

Table I - Characteristics of the Hydrogel Materials Manufactured by AmGel……16

Table II - Characteristics of the Women in the Development and Evaluation Cohorts……....33

Table III - Development Cohort Marked by Experts…….…....36

Table IV - Validation Cohort Marked by Experts…….....…..37

Table V - Statistics using the Matched Filter on the Development Cohort……..……....57

Table VI - Statistics using the Matched Filter on the Evaluation Cohort…….…….58

Table VII - Errors Generated during Best Training Run……...…….…..…..73

Table VIII - Statistics using the Neural Network on the Development Cohort…….....77

Table IX - Statistics using the Neural Network on the Validation Cohort…….....….78

Table X - Collective Results using the matched Filter and the Neural Network……..…….80

List of Appendices

Appendix I - Hot Flash Monitor Schematics…….…...…….88

Appendix II - Participant/Staff Instructions for Wearing the Bahr Hot Flash Monitor….....92

Appendix III - FLASH Monitor Evaluation Studies II Clinical Trial Protocol……..……93

Appendix IV - IRB Application and Approval…….....120

Appendix V - Instructions for Expert Rating of Hot Flashes from the Development Set…..…123

Appendix VI - Rules for Marking Hot Flashes……...…….....125

Appendix VII - Hot Flash Storage……...126

Appendix VIII - Derivation of Sigmoid Derivative Equation 9.3…….....127

Appendix IX - North American Menopause Society Poster…….……..…128

Appendix X - Miniature ambulatory skin conductance monitor and algorithm for investigating hot flash events…….……...131

Chapter 1

1 Literature Review and Background

1.1 Introduction and Overview

A hot flash event is the sudden onset of intense flushing in the upper torso and face, often followed by profuse sweating and chills (Kronenberg 1990). The etiology of hot flashes is thought to be related to abnormalities of thermoregulation associated with changes in hormone levels that occur at menopause, but the mechanism is not clearly understood (Freedman *et al.* 1998). There are currently about 45 million women in the United States between the ages of 45 and 65 years. At least two thirds of these women will experience hot flashes and approximately 20% will seek medical relief for debilitating vasomotor symptoms (Kronenberg 1990). Vasomotor symptoms, including hot flashes and night sweats, are frequently reported by menopausal women as well as breast cancer survivors and men undergoing androgen deprivation therapy. Until recently, estrogen and other forms of hormone therapy were used to treat vasomotor symptoms among menopausal women. However, findings from the Women's Health Initiative (WHI) indicated that the benefits of hormone-based therapies for hot flashes were outweighed by the risks of increased incidents of breast cancer, coronary heart disease, stroke, and pulmonary embolism.

Clinicians are continually turning to other means to manage hot flashes, including Complementary and Alternative Medicine (CAM) therapies. There is a long history of the use of

CAM therapies for hot flashes, but the empirical base to assess safety and efficacy is neither extensive nor very strong. The Food and Drug Administration (FDA) has recommended that hormones for the treatment of hot flashes be used at the lowest dosage and for the shortest period of time. However, little is known about risks and benefits for smaller doses, shorter treatment times, and different routes of administration. Thus, investigators who are conducting research on a range of treatments to reduce hot flashes are searching for methods to objectively measure hot flash events as a result of intervention treatments.

1.2 Motivation and Objectives

For some time now there has been an intense interest in the research and medical communities regarding the etiology of hot flash events and in finding safe and effective treatments. However, research in 2005 (when this research was initiated) was limited by the lack of adequate technology to reliably and accurately obtain objective measures of hot flash frequency and severity. Most studies used a 7-day self-reported hot flash diary (Sloan *et al.* 2001). This measure was subjective, often inaccurate, and unreliable because participants forgot or failed to enter hot flashes in the diary and especially at night when many hot flashes occur. The severity of hot flash events for self-reporting usually was and still is defined on a scale of (mild, moderate, severe), and the exact timing of the hot flash is often not recorded at all (Miller *et al.* 2004). In addition, keeping a daily diary is labor intensive and inconvenient so most participants are unwilling to do this for more than a few days at a time.

Another method of monitoring sternal skin conductance in 2005 was to use a belt mounted electronic skin conductance monitor (the UFI Model 3991/1-SCL Single-Channel Hot Flash

Monitor Biolog) that had wires leading to the attached electrodes. While the correlation between sternal skin conductance events and self-reported hot flashes was high under controlled laboratory conditions, the correlation between these measures was always lower in ambulatory studies due to under reporting of subjective hot flashes. Ambulatory hot flash monitors that were available in 2005 were simply not statistically accurate (Carpenter *et al*. 2005). In addition these devices were too bulky or weighed too much and thus interfered with daily activities and sleep. The electrodes that were used were problematic because the electrodes would loosen or release with excessive sweating and bathing. Placement and attachment of electrodes required trained personnel, thus requiring the subject to return to the study site for reattachment. These monitors could only collect and store small amounts (1 to 2 days worth) of data for later processing. Thus, the scientists assessing existing measures of hot flashes demanded improved sternal skin conductance monitors to capture hot flash data.

In January of 2004 the National Institutes of Health's (NIH) National Center for Complementary and Alternative Medicine (NCCAM) along with several other NIH Institutes and Centers convened a meeting to assess the current state of measurements for hot flashes events (Miller 2004). This meeting was attended by scientists, researchers, and engineers from around the country. As a result of this meeting and the pressing need for adequate monitoring of hot flash events, NCCAM, the National Institute on Aging (NIA), the National Institute of Biomedical Imaging and Bioengineering (NIBIB), and the Office of Research on Women's Health (ORWH) issued a request for Phase I Small Business Innovative Research (SBIR) grant applications to conduct research to improve hot flash monitoring systems. A proposal was written and submitted by John Webster, Mark Shults, and myself. We were awarded the grant and subsequently were

asked by our NIH program manager to collaborate with a team of researchers and physicians at the University of California at San Francisco (UCSF) Women's Health Clinical Research Center. NIH believed that our engineering team and the team at UCSF would be the best combination of resources and talent to guarantee success of this research.

The guidelines that NIH (NCCAM) gave to grant awardees were to interface with an existing piece of equipment or to modify an existing system, but the device or system was to be specifically designed to collect data on hot flashes and night sweats during ambulatory conditions. Specifically:

1. Identify characteristics of existing sternal skin monitors that limit use under ambulatory conditions and develop modifications or new systems that would improve the characteristics that currently limit data collection of hot flash events;

2. Develop a prototype for clinical testing;

3. Conduct pilot studies of that device in the laboratory in individuals experiencing hot flashes, noting correlation between self reported hot flashes and those identified by the tool or device;

4. Conduct a pilot study of the device under ambulatory conditions, noting correlation between self reported data on hot flashes and those identified by the tool or device;

5. Develop software to process the acquired data and present the results in a fashion that is appropriate for use in a research environment.

6. Determine subsequent steps needed to refine or improve this device for use in larger scale studies.

These objectives provided a clear path as to what needed to be accomplished. The first and most important step was to develop an electrode that provided artifact free signals with little or no base line wandering. Secondly, develop improved measurement devices that were reliable, user-friendly, accurate, and would collect data for three to seven days under ambulatory conditions. This was necessary in order to monitor subjects in intervention studies. The monitor must be able to collect data under conditions of daily life, during waking and sleeping hours, without interfering with daily activities. These devices would be used to evaluate the efficacy of various therapies, including complementary and alternative medicine (CAM) modalities, to record hot flashes under ambulatory conditions in clinical studies.

It was decided to use skin conductance as a measure of a hot flash events because it had been demonstrated by Freedman (1989) that an increase in sternal skin conductance due to sweating was an accurate measure of the occurrence of hot flashes in temperature controlled laboratory settings. Molnar (1975) demonstrated in extensive studies that the temperature of the upper anterior torso increased during a hot flash event causing mild to perfuse sweating. Thus, this site was chosen as the best place to monitor skin conductance and the sternum was chosen because it was easy to affix electrodes over the bone like structure.

Chapter 2

2 Body Surface Recording

2.1 Introduction and Overview

Developing a model that described the construction and characteristics of human skin proved extremely useful in developing an effective electrode. The nature of skin is quite complex and the model that was developed used approximations to represent capacitance and voltage sources that did not have any actual functional entity.

2.2 Characteristics of Human Skin

Human skin consists of three main layers of tissue; the *epidermis*, the *dermis*, and the *subcutaneous layer*. Figure 2-1 shows the various layers in a section of skin.

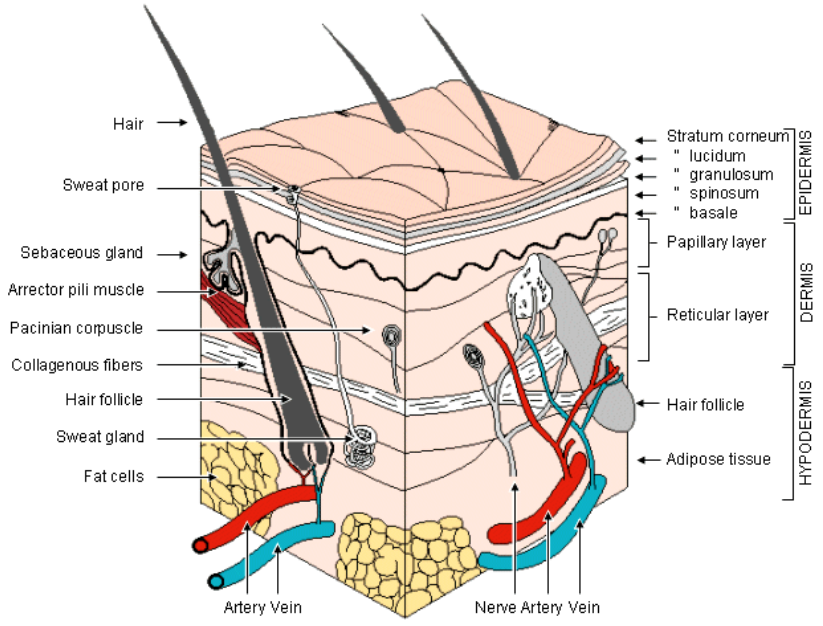

Figure 2-1: Section of human skin showing the various layers (Ebling, Eady, and Leigh, 1992.)

These layers provide a barrier to the interior of the body, provide a surface that can help maintain thermal equilibrium through vasodilatation and sweating, and provide a sense of feeling or touch. Human skin consists of the outermost layer, or *epidermis*, that is made up of three sublayers. These are the *stratum germinativum*, the *stratum granulosum*, and the *stratum corneum*.

In the deepest layer stem cells divide, grow, and become skin cells. As these cells pass through to the *stratum granulosum* stage they gradually lose their nuclear material and begin to die forming a dead layer of keratinous material. The outer *stratum corneum* layer is continually being worn away and replaced by cells from the layers below. Therefore, the epidermis is a continuously changing layer of our skin. The *stratum corneum* has the highest electrical resistance of the three layers because it consists primarily of dead cells. The deeper layers are more conductive and contain the hair follicles, the sweat glands, the sweat ducts, the vascular bead, and the nerves. Figure 2-2 shows an electrical model that reflects the characteristics of the various layers and components in the skin.

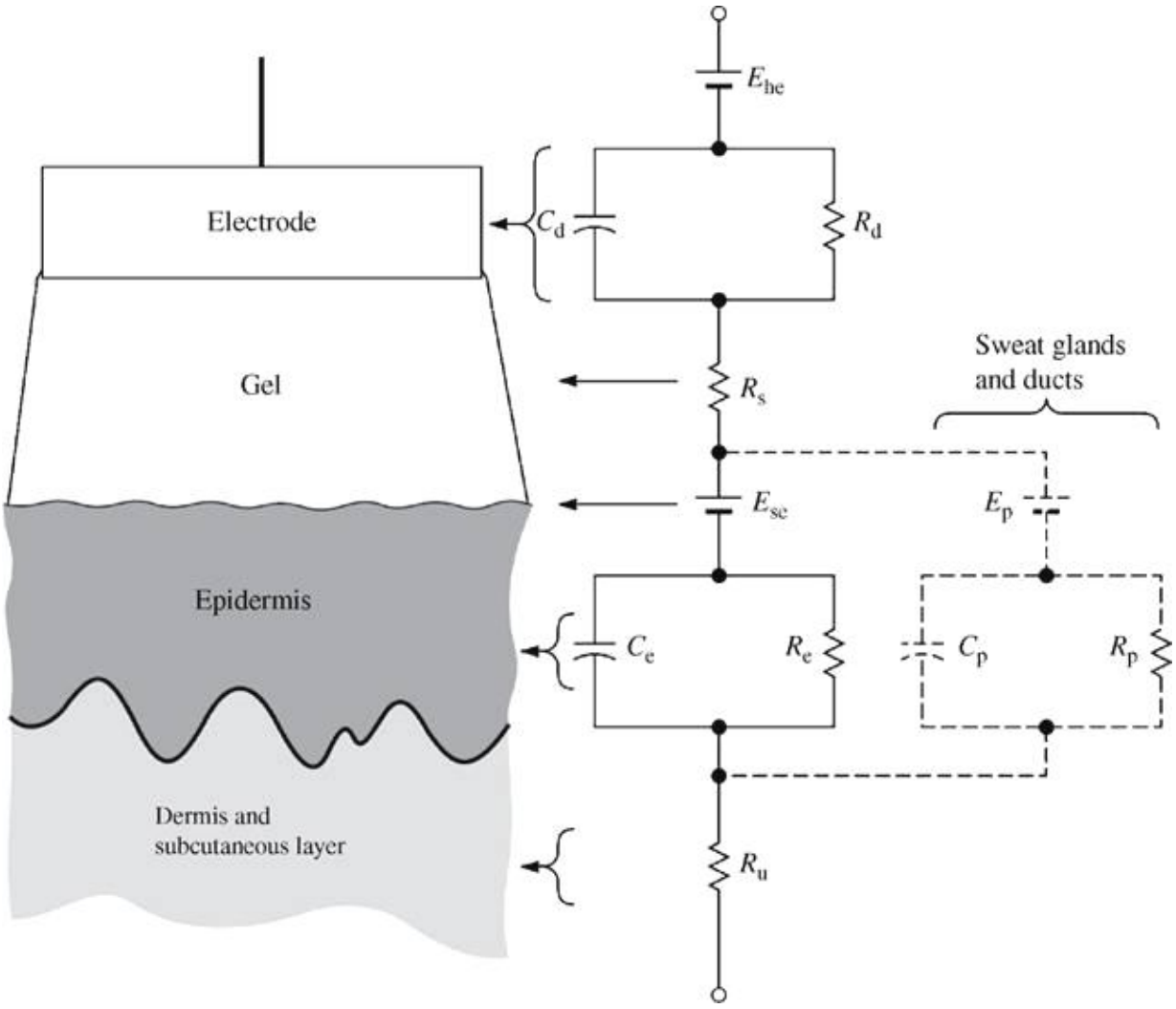

Figure 2-2: An electrical circuit model that shows the layers in the skin and depicts the equivalent circuit elements that match these layers. Included is a model for an electrode to gel interface with the epidermis. (Neuman 2008)

2.3 Sweat Glands and Sweat Pores

There are two well known mechanisms that the human body uses to cool itself. One is vasodilatation and the other is sweating when vasodilatation alone cannot accomplish the task. Freedman (1989) demonstrated that an increase in sternal skin conductance due to sweating was

an accurate measure of the occurrence of hot flashes in temperature controlled laboratory settings. Sweat initiates in the sweat glands and is modulated by body temperature, hormones, and neural activity and carried to the surface through the sweat ducts. Immediately after the initiation of the hot flash event, the pores on the skin surface begin opening and exuding sweat that has been channeled to the surface by the sweat ducts from the sweat glands below the surface. Full sweat pore recruitment takes approximately 1 min. Once the skin surface is covered in a layer of fluid the skin begins to cool and the pores close over a period that usually lasts about 10 min. The rate of cooling is directly related to the environment. If it is humid and the skin does not evaporate the sweat, the cooling is much slower.

The action of the sweat pores opening provides electrical access to the layers below the epithelium. A small voltage of less than 1 V applied to the surface of the skin by a pair of closely spaced electrodes will cause a current to flow. It is postulated that the current flows from electrode to electrode mostly through the sweat pores under the electrode surfaces. This current will be approximately 10 to 30 times the baseline leakage and roughly proportional to the cross-sectional area of the recruited sweat pores. There will be a small surface leakage current due to the layer of sweat on the skin below the electrode, but the majority of the current is assumed to come from the sweat ducts and sweat pores. Figure 2-3 shows the normalized conductance vs. number of 10 s samples for a typical hot flash event.

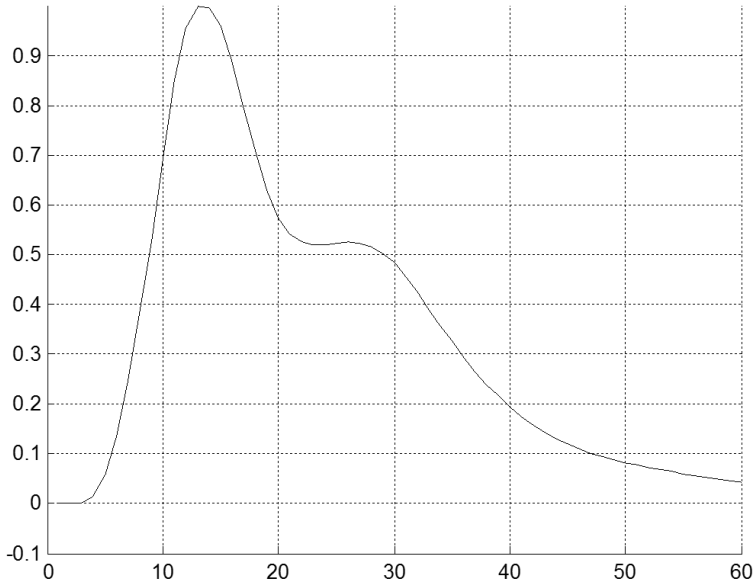

Figure 2-3: The three most common characteristics of hot flash conductance waveforms are a rapid rise in conductance, the gently rounded peak, and the exponential like fall. The scale for the abscissa is the number of 10 s samples and the ordinate has been normalized to the peak of the hot flash.

The rapid rise in the conductance, the gently rounded peak, and the exponential like fall are three common characteristics found in hot flash conductance waveforms. These three characteristics were the most important in detecting the hot flash events in the conductance data recorded from the cohorts. The plateau between sample numbers 20 and 30 occurred in 15% to 20% of the hot flash waveforms that were collected during this research. No explanation as to what causes this could be found in the literature or from the research that was done for this dissertation.

Chapter 3

3 Hot Flash Electrodes

3.1 History and Introduction

A major challenge in any type of data collection system is developing the sensing method or in this case, the electrode. Electrodes used for electrocardiogram (ECG) signals require a very good electrical connection through the epidermis to the underlying tissue. To provide this, the gel usually contains up 5% of a salt such as NaCl. The salt enters the sweat pores and provides a 'salt bridge' to the lower layers of the skin where the conductivity is higher than at the surface.

One method of measuring hot flashes is to use an electrode with isotonic sodium chloride based semi-liquid gel or cream that approximates perspiration (0.1 to 0.3% NaCl). This formula is substituted for the higher salt content (~5% NaCl) gel and sponge in a standard ECG electrode. A constant 0.5 V is applied to a pair of these electrodes and the current is measured. Conductance is current divided by voltage. These electrodes have a number of major limitations. The gel between the skin and the electrode will begin migrating almost immediately causing motion artifacts and the conductance to drift without physiological involvement. A second major limitation is that the impermeable plastic patches trap sweat under the electrode increasing hydration causing a continual rise in conductance over time thus rendering the electrode essentially useless after a few days of use. This was mostly due to salt and water diffusing into the skin. A third problem is that the stickiness or tack was designed for a few days of use and was very aggressive often leaving a large welt on the skin after removal.

3.2 The Metal Electrode

Olsen et al. (Olsen 1979) studied the impedance of a metal electrode-skin interface with respect to frequency and time. They found that the impedance decreased with time but more importantly they found a very large drop in impedance with frequency. Therefore, as shown in Figure 3-1 any measurement of the real component of conductance must to be done below 5 to 10Hz.

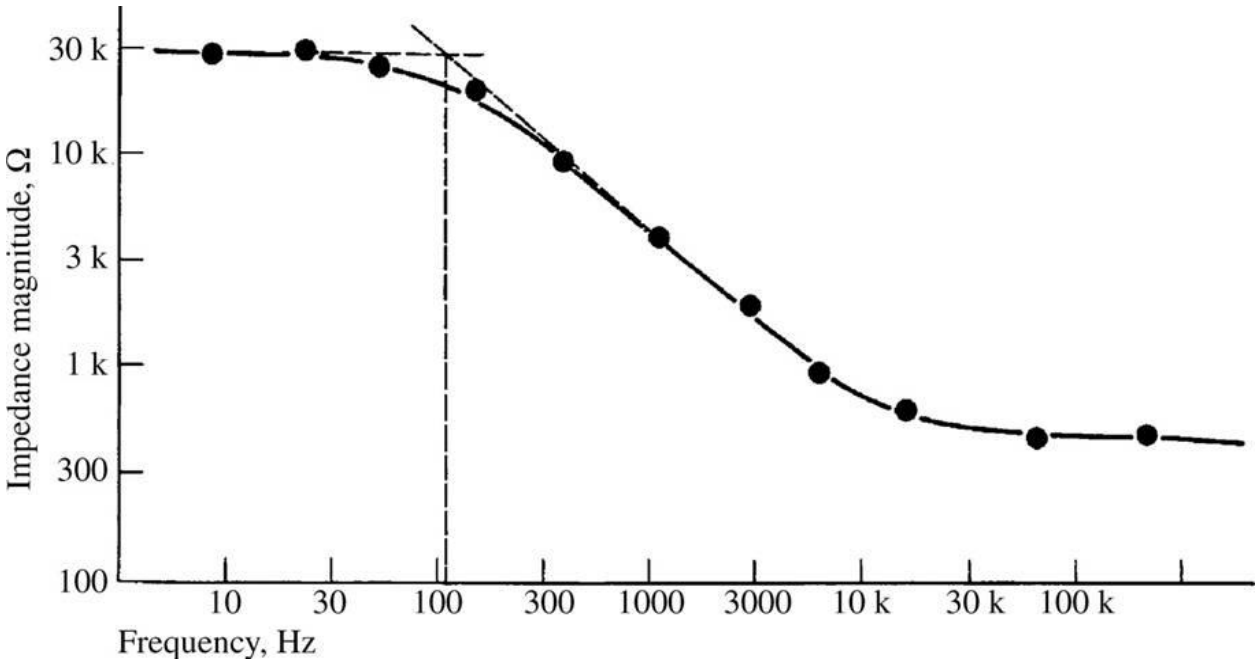

Figure 3-1: In general, skin impedance decreases (skin conductance increases) with frequency for metal electrodes. The unit of conductance used in this dissertation is the μS. (Olson 1979).

The time constant τ for a signal can be calculated using equation 2.1. For a frequency of 5 Hz the time constant is 32 ms.

$$\tau = RC = 1/2\pi f \qquad 2.1$$

To get a signal that had the least amount of effect from the various tissue capacitances the sampling should be done at least 5 times the time constant or 160 ms. A sampling time of 250

ms was chosen for this research to provide time to do the actual sampling. The metal electrode of choice in most cases is the Ag/AgCl electrode since the impedance of a silver electrode with a coating of silver chloride produces an electrode with an impedance that varies much less with respect to frequency. Figure 3-2 shows Ag electrodes with various depositions of AgCl.

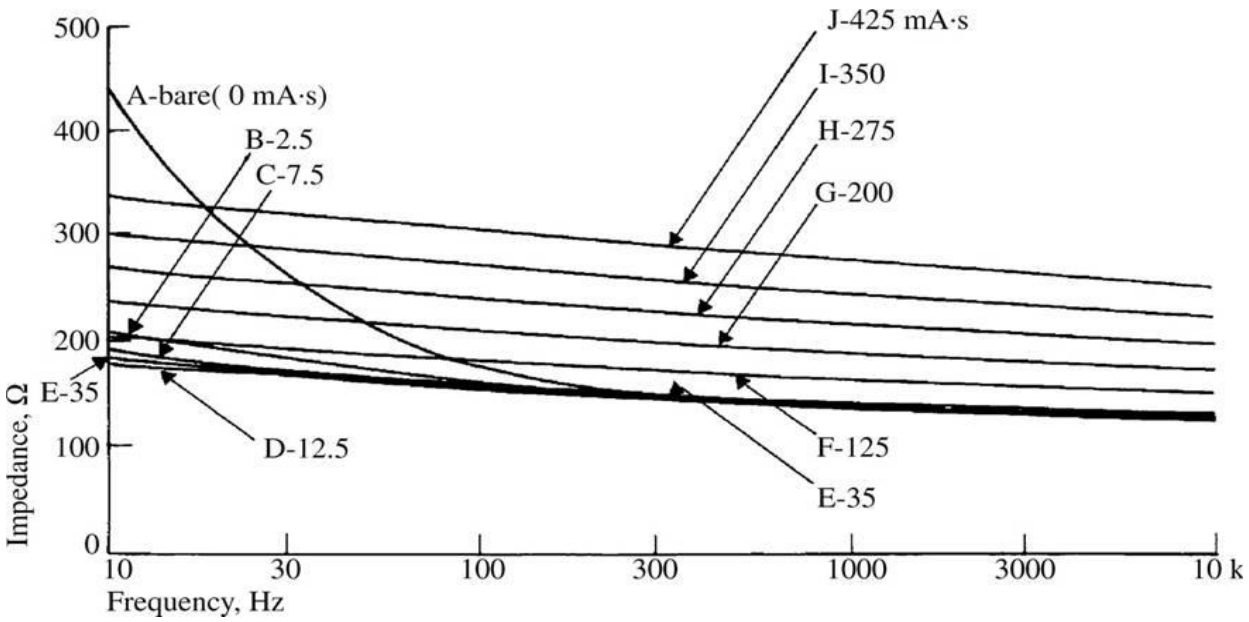

Figure 3-2: Shown is the impedance versus frequency of a pure Ag electrode as well as Ag electrodes with electrolytically deposited layers of AgCl. The electrode area is 0.25 cm^2 and the letters-numbers indicate the amount of deposition in mA·s. (L.A. Geddes, L.E. Baker, and A.G. Moore, "Optimum electrolytic chloriding of silver electrodes." *Medical and Biological Engineering, 1969, 7, 49-56.*)

A pure Ag electrode has a capacitive component that is dominant at lower frequencies creating problems when using low frequency voltages to measure conductance. Applying a layer of AgCl significantly reduces the low frequency impedance eliminating the problem. Since hot flash data samples were taken with a window of 250 ms, an Ag/AgCl metal electrode was required and was chosen for this research.

The AgCl electrode is a non-polarizable electrode, which means that a current will pass freely across the electrode-electrolyte interface and the half-cell potential is stable in an isotonic solution. The metal portion of the electrode must be interfaced to the skin with a material that provides skin contact and maintains a cross-sectional area that does not migrate with time or motion. Another issue is the interface with this material and the metal portion of the electrode. A double layer is produced between the material and metal and this surface must be physically stable or motion will create electrical artifacts in the signal. The ECG electrodes measure voltage and the cross sectional area of the interface material is of no consequence. However, hot flash electrodes measure current and the cross-sectional area of the interface material does matter and it must be stable.

The interface between metal and an electrode gel can be described using the Nernst equation that describes the half cell potentials of the materials. For this research these half-cell potentials were of minor interest as they were electrically stable and did not contribute to motion artifacts. The half cell potential of one electrode was effectively balanced by the half-cell potential of the second electrode.

3.3 The Hydrogel Electrode

A new type of electrode had to be developed to eliminate or minimize the problems that were inherent in the then current hot flash electrodes. This electrode needed to be isotonic and hypoallergenic as well as maintaining its physical shape to prevent base line artifacts. It needed to be able to remove the sweat that accumulated at the electrode surface and transport it to the outer surface where it could be evaporated. This would prevent erratic base-line drift over time

because of skin hydration. The electrode patch needed a surface tact that would stay adhered for three or more days without causing skin irritation.

Jossinet and McAdams (1990) had showed that when electrodes using semi-liquid gels as the skin electrode interface were used, the skin was well hydrated and skin resistance decreased (conductance increased) with time. They also showed that for hydrogel electrodes, the skin resistance did not decrease with time because these materials do not actively hydrate the skin. Their investigations demonstrated that skin conductivity is best measured using a hydrogel (or very mild wet gel) electrode interface that does not actively modify the skin's properties. Hydrogels are water-containing polymers that incorporate either natural or synthetic hydrocolloids and are therefore "solid" and hydrophilic. They maintain their shape providing an interface to the skin that has a constant area for electrical conduction.

3.4 Hydrogel Electrode Testing

Hydrogel materials looked very promising, so samples of hydrogels were acquired and tested for conductivity, base line drift, and motion artifact rejection. There are many varieties of hydrogel materials and many manufactures of hydrogel materials, but it was decided to acquire hydrogel samples from AmGel, Inc. a major manufacturer of medical hydrogel materials. If the results of these experiments proved unsatisfactory, other manufacturers with other hydrogel formulations would be investigated. Table I shows a chart of the materials that AmGel manufactures.

Table I Characteristics of the Hydrogel Materials Manufactured by AmGel

AmGel TECHNOLOGIES

GELS FOR VARIOUS APPLICATIONS

	AG500	AG600 SERIES		AG700 SERIES			AG800	AG900 SERIES	
GEL FEATURES	AG501	AG602	AG603	AG702	AG703	AG704	AG803	AG901	AG902
SENSING		X	X						
DEFIBRILLATION		X	X						
STIMULATION				X	X	X	X		
SURGICAL GROUNDING PADS								X	X
FIXATION	X	X	X	X	X	X			
IONTOPHORESIS / D.C. CURRENT							X		
OPTIMIZED FOR SILICON / CARBON (RUBBER) ELECTRODES						X			
DRY OUT RESISTANCE *	HIGH	HIGH	MOD	HIGH	MOD	MOD	HIGH	HIGH	HIGH
ADHESIVE TACK	HIGH	HIGH	HIGH	HIGH	MOD	MOD	MOD	MOD	MOD
GEL THICKNESS	44mil	35mil	25mil	35mil	30mil	30mil	35mil	36mil	22mil
ROLL LENGTH	300 ft (91 m)	300 ft (91 m)	300 ft (91 m)	300 ft (91 m)	300 ft (91 m)	300 ft (91 m)	300 ft (91 m)	300 ft (91 m)	400 ft (120 m)
SUBSTRATE	Polyester Liner	Polyester Liner	Polyester Liner	Polyester Liner	Polyester Liner	Polyester Liner	Polyester Liner	Polyester Liner	Aluminum Foil
VOLUME RESISTIVITY	6,000 ohm-cm max	1,000 ohm-cm max	1,000 ohm-cm max	1,500 ohm-cm max	1,500 ohm-cm max	1,500 ohm-cm max	15,000 ohm-cm min 30,000 ohm-cm max	7,000 ohms-cm max	15 ohms max***
PROCESS SHELF LIFE **	Non-Slit 1 year Slit 6 months	Non-Slit 1 year Slit 6 months	Non-Slit 1 year Slit 6 months	Non-Slit 1 year Slit 6 months	Non-Slit 1 year Slit 6 months	Non-Slit 1 year Slit 6 months	Non-Slit 1 year Slit 6 months	Non-Slit 1 year Slit 6 months	1 year

* Ability to maintain moisture and adhesive tack

*** Impedance per pad @ 500k Hz

** Proper Storage Conditions of Packaged Rolls: Short Term (less than one month) Temperatures: 32°-104°F (0-40°C) Humidity: 35-50%
Long Term and Optimal Temperatures: 41°-80.6°F (5-27°C) Humidity: 35-50%

10/2008

Samples were chosen from three of AmGel's major hydrogel Series and included AG603, AG703, and AG803. Samples in the AG900 series were not chosen because these materials are usually used for surgical grounding pads. The hydrogel materials were cut into 1.5 cm^2 squares and placed in pairs on a 4 cm by 7 cm oval skin colored polyester with a surface adhesive and containing two pre-assembled Ag/AgCl metal electrodes. Figure 3-4 shows an assembled electrode patch.

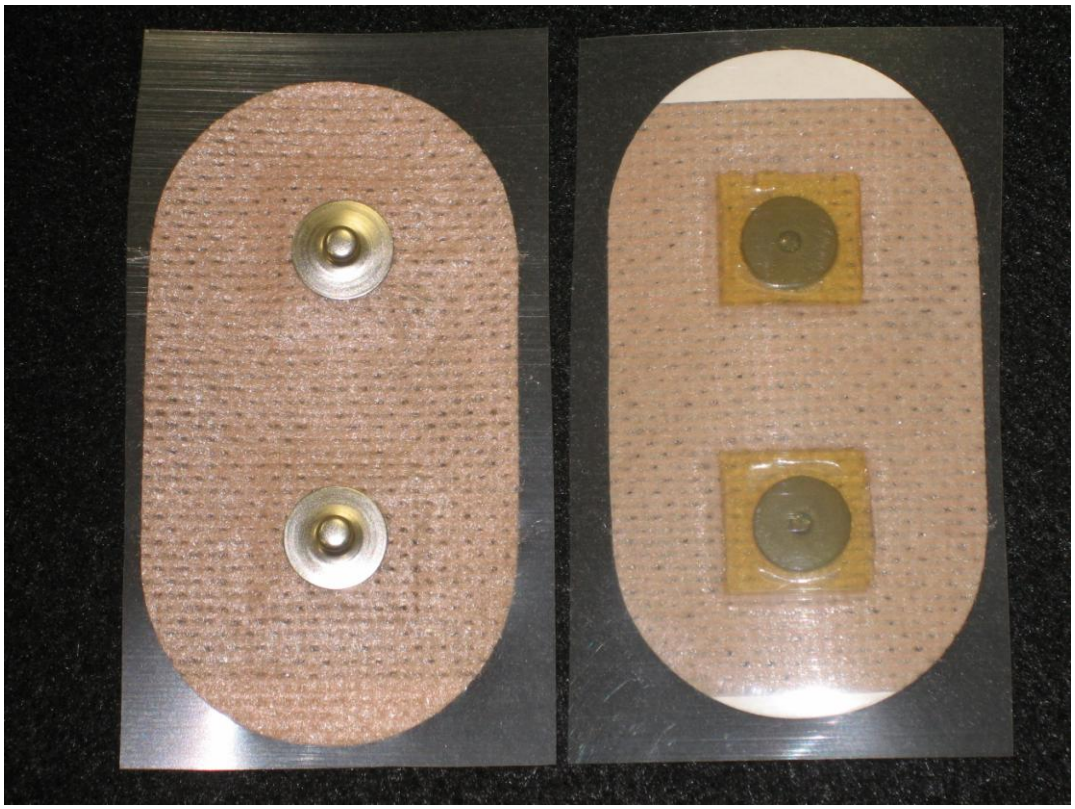

Figure 3-4: An assembled hydrogel electrode patch used during the early experimentation to provide data on hydrogel formulations. The Ag/AgCl metal electrodes were standard ECG electrodes with a male snap on the opposite side.

In order to find the best hydrogel material specific attention was paid to baseline values, baseline drift, and signal-to-noise ratios when measuring hot flash episodes. It was found that the AmGel AG703 and AG803 adhesive hydrogels were superior to AG603 hydrogel, BIOLOG gels, or 0.1% or 0.9% saline in hydrogels. Both AG703 and AG803 showed the best results as to low baseline drift, low artifact, and fast recovery back to baseline. The best overall results were obtained using AG803 which is a specially formulated hydrogel material usually used for electrophoresis.

Electrodes were tested with various adhesive properties or tacks to ensure that the electrode

conductor made good contact with the skin for several days, yet caused minimal irritation while worn or when removed. Modern chronic use skin adhesives were tried in the size of large Band-Aids similar to “Scar Solution” and were found that the tack is too low for one-week use. No electrode could be found with a tack that adhered adequately for two weeks and not damage the skin.

The patch material chosen is spunlaced polyester (MacTec, Inc - TM-9478) and coated on one side with 594 acrylic-based hypoallergenic pressure-sensitive adhesive. The adhesive material is a medical grade adhesive and is formulated for sustained contact with human skin. It is protected by a 70# dense, semi-bleached Kraft release liner. The TM-9478 material is designed for use as a breathable medical tape. One reason the polyester patch material was chosen was because it could absorb water without undergoing any physical changes. The hydrogel and the polyester absorb the sweat from the skin and the breathable feature allows the sweat to evaporate. That way, the electrode will always recover back to a low base line between hot flash events in which sweating is a major aspect of the event.

The baseline conductance changed a few μS over the 3 day testing periods usually increasing in magnitude. This was assumed to be caused by the accumulation of salt content under the electrode. If the electrode patch became wet as in taking a shower, it dried off in about 1 h and was ready to continue collecting hot flash data. Figure 3-5 shows graphs of some of the results of the experimental studies.

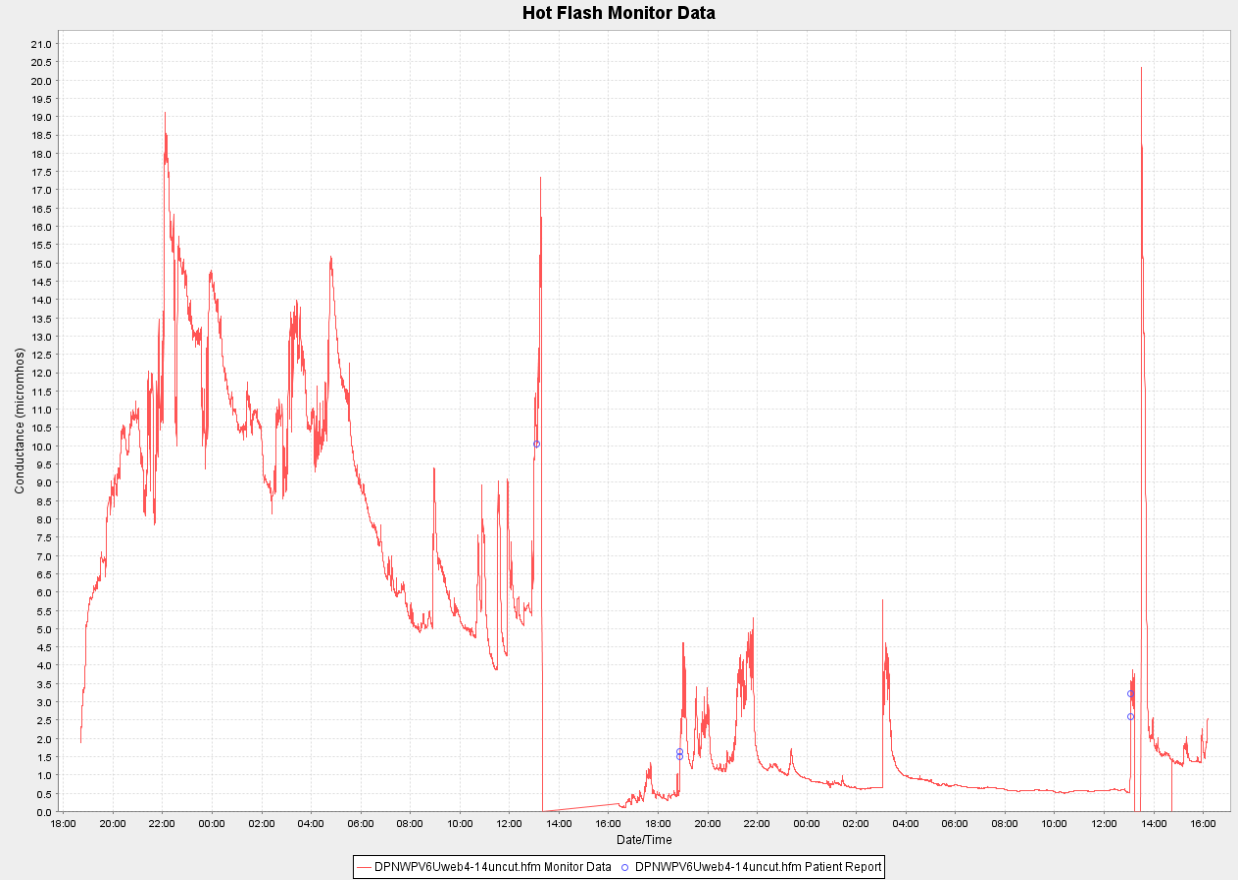

Figure 3-5: Abscissa units are in hours and ordinate units are in μS. Left half shows AG603 hydrogel with a conductance averaging 10 μS and erratic recordings. Right half shows AG803 hydrogel yielding a conductance averaging 1 μS with clean recordings. Blue circles show where exercise increases conductance.

The hydrogel material that was chosen (AG803) was compared with the cream recommended by BIOLOG for hot flash monitoring using two of the monitors designed for this research. The monitors were placed on the same subject and post experiment the data was synchronized in time and plotted as shown in Figure 3-6.

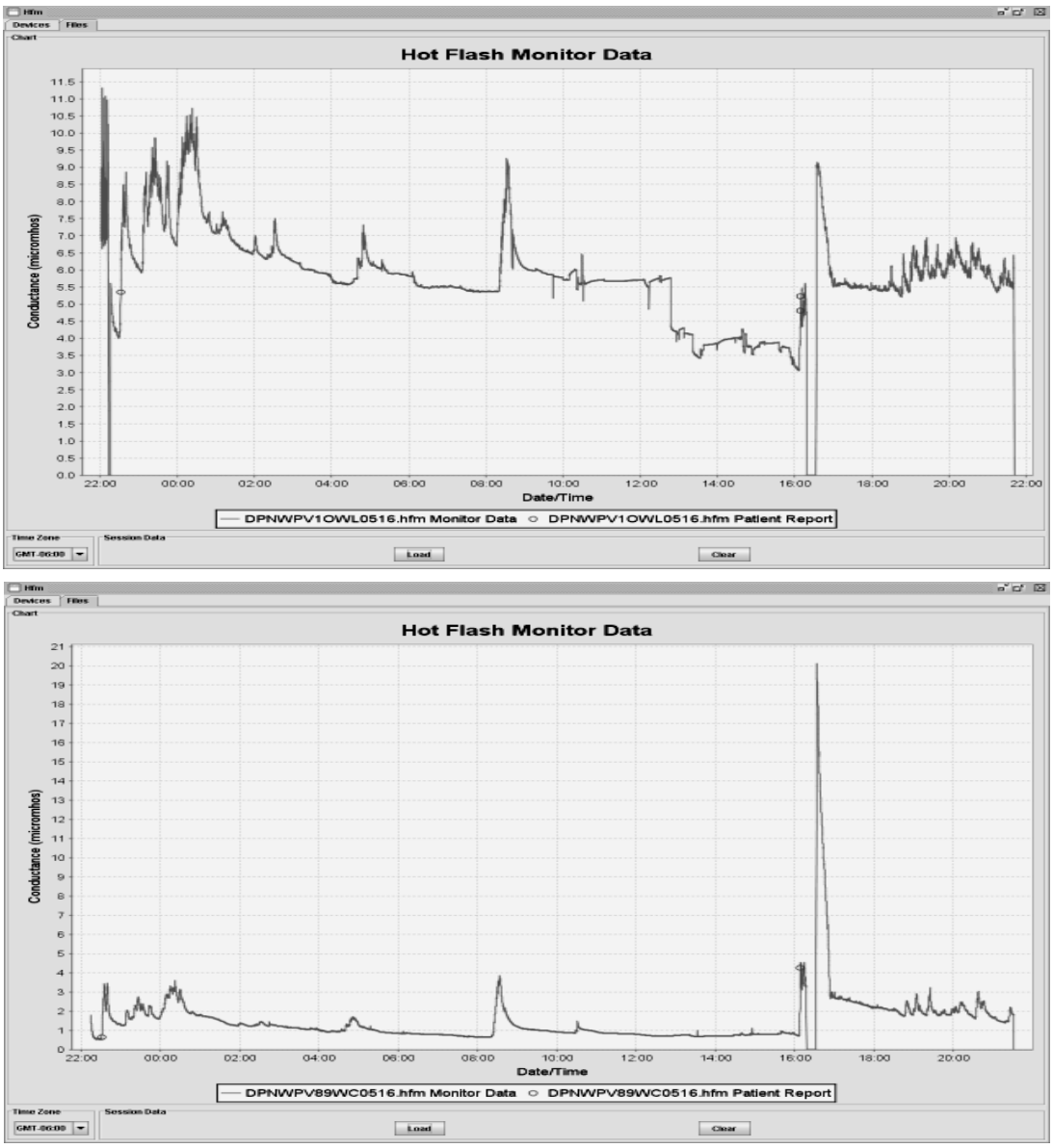

Figure 3-6: Abscissa units are in hours and ordinate units are in μS. Shown is a comparison of two electrodes worn by the same subject at the same time. Top: The cream used with the Biolog monitor causes about a 6 μS baseline conductance. Sweating generated by exercise (marked by circles) causes about a 30% change. Bottom: Conductive adhesive gel causes about a 0.8 μS baseline conductance and has less motion artifact. Sweat created by exercise causes a 400% change. During a shower (at about 16:00), the recorder was detached (0 μS). After the shower, electrode was wet recording about 20 μS and recovering in about 30 min.

Figure 3-7 shows recorded hot flash events using the chosen hydrogel and tack. The lack of motion artifact and low baseline drift show the superiority of this electrode patch.

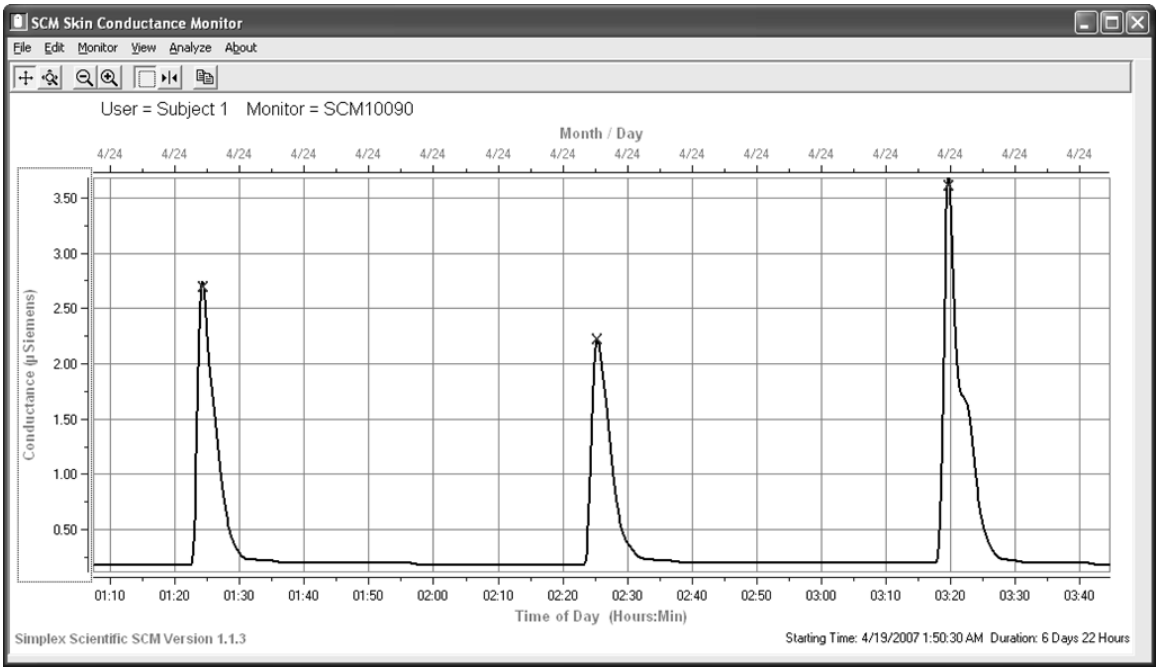

Figure 3-7: Abscissa units are in hours and ordinate units are in µS. The electrode patch shows a baseline conductance of about 0.2 µS. The typical hot flash rises to about 3.0 µS and lasts about 5 to 10 min.

Chapter 4

4 System Hardware

4.1 Introduction and Overview

Good portable medical instrument design practice requires a blend of choices that produce a product that is effective, reliable, low power, inexpensive, and has good human machine interface (HMI) ergonomics. The method used most often is to pick a microprocessor, design hardware around it and, write embedded software to tie the whole thing together. Important requirements for a portable hot flash monitor are low power and light weight. The Texas Instruments (TI) MSPF4302272 microprocessor was chosen for use in this monitor because it is one of the lowest power devices on the market and because of the high quality of available embedded software programming tools.

4.2 Electrical Design

The electrical design entails applying a low voltage (~0.5 V) to the skin using a pair of electrodes and measuring the resultant current flow. Since $i = e/r$ (voltage e divided by resistance r) and conductance is the reciprocal of resistance, the equation for current can be rewritten as $i = eS$ where the unit of conductance is in Siemens or in the case of this research micro Siemens (μS). There is a linear relationship between the measured current and changes in skin conductance. Implementation was accomplished using the electronic circuit shown in Figure 4-1.

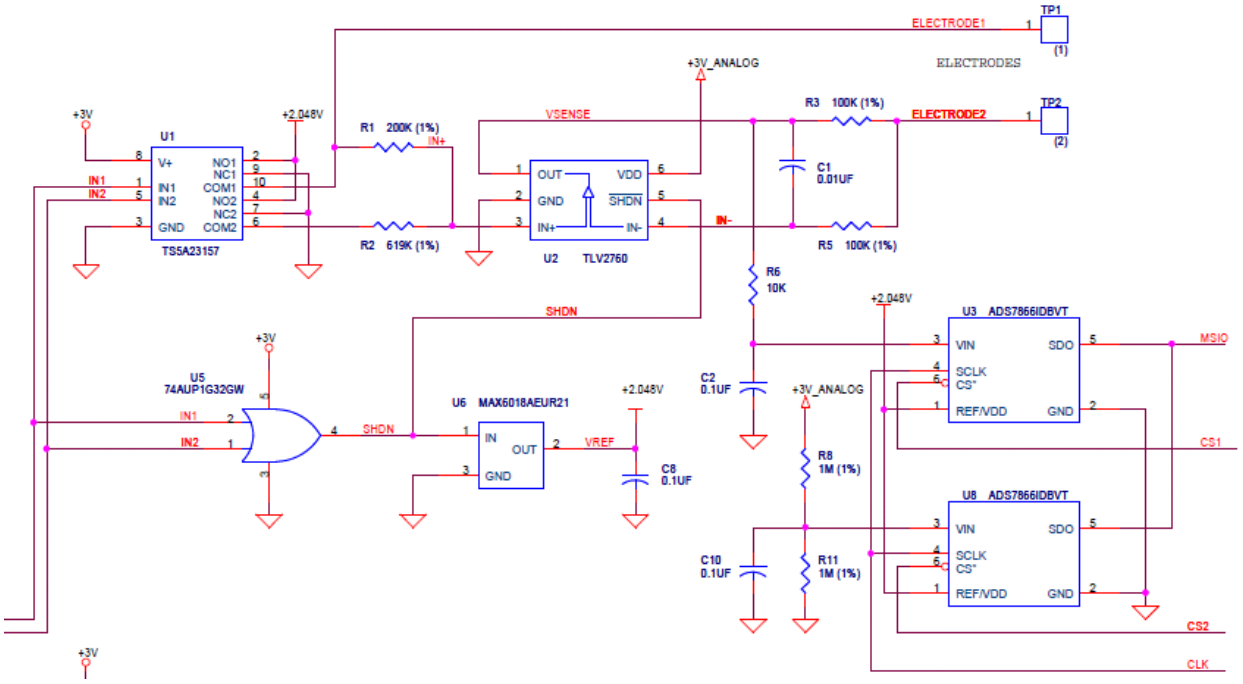

Figure 4-1: Schematic diagram showing the circuit used to apply a voltage to the skin and measure the resulting current flow. Complete schematics for both the diagnostic grade and production monitors can be found in Appendix I.

When amplifier U11 (TLV2760) is turned ON by control line SHDN it applies a voltage to the skin and keeps the voltage constant by varying the current flow in direct response to the changes in skin conductance. The process begins by turning ON voltage reference U6 producing a regulated +2.048 V that is used as a reference by the rest of the circuit. To prevent electrode polarization, two pulses are used with one having a positive polarity and the second occurring at a later time with a negative polarity. The portion of the hot flash conductance signal that has the highest frequency component is the rise time and takes place in 1 to 2 min. With this information it was decided to sample using a positive pulse and a negative pulse 5 s apart. The integrated circuit U10 alternately switches the reference voltage and ground between COM1 and COM2 with a 5 s period and a duty cycle of 250 ms. The signals that do this switching (IN1 and IN2)

originate from the microprocessor and cause the voltage between ELECTRODE1 and ELECTRODE2 to alternate between $+0.5$ V and -0.5 V with the same period and duty cycle. Resistor R19 measures the voltage output of the operational amplifier. The voltage across resistor R14 is proportional to the current flowing from the amplifier's output and to electrode 2. A resistance value of 100 kΩ provides a 1 V signal for a current flow 10 μA through the electrodes when the electrodes are connected to a conductance of 10 μS. Analog-to-digital converter U8A measures this voltage. The two pulses are averaged, and the resultant stored to memory.

4.3 Mechanical Design

The hot flash monitor mechanical design went through a number of iterations before settling on a design where the printed circuit board was entirely enclosed and designed to be water and sweat resistant. The material of choice for the enclosure was an ABS plastic that is durable and yet flexible enough such that dropping it on a hard surface like concrete would not fracture the unit. Figure 4-2 shows the final design that went into production.

The portion of the case top covering the largest portion of the circuit board was connected to the case bottom using torx screws that require a special screwdriver with a star shaped head. This was done to deter subjects from opening the unit exposing the entire printed circuit board. The item marked door is for user access to download the data, erase the memory, and set the onboard real time clock. The door is fastened using a standard Phillips head screw.

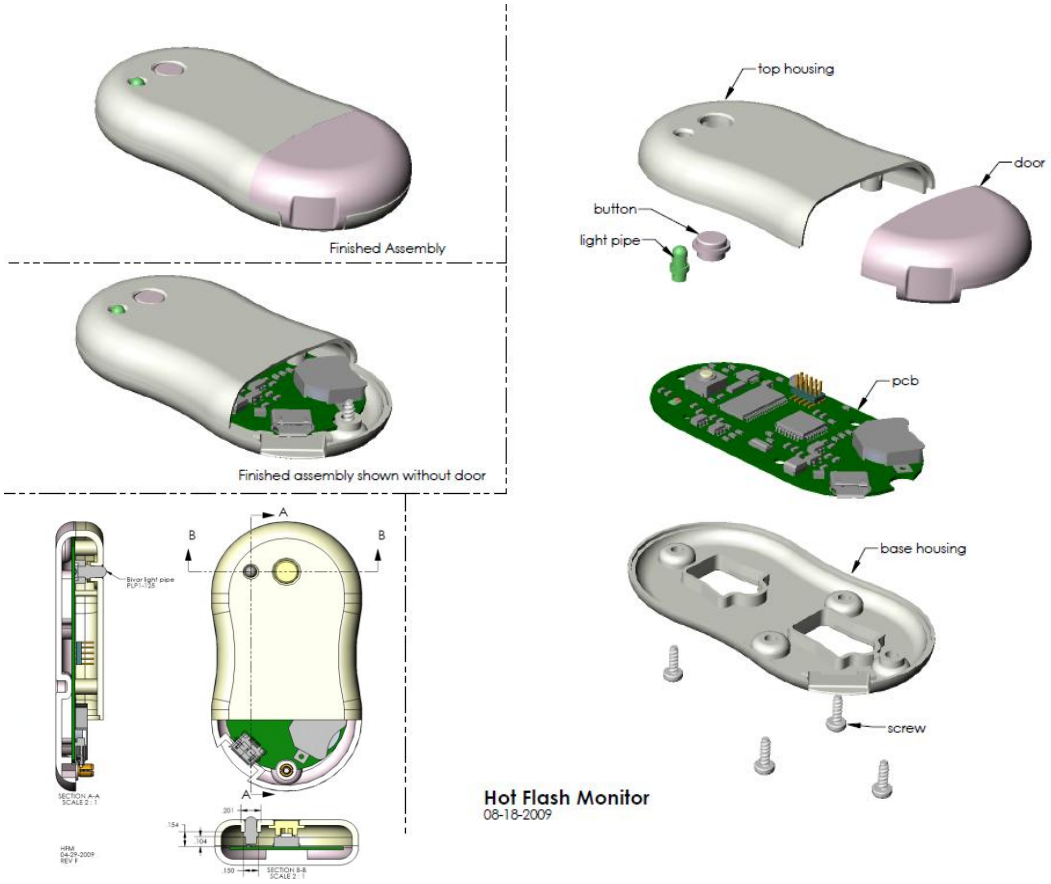

Figure 4-2: Exploded view of the production hot flash monitor showing all of the components. The small 10 pin header on the right side of the circuit board is the JTAG connector used for programming the microprocessor. On the front of the unit are the USB connector and a battery holder for a small coin cell.

The electrode connectors are affixed to the bottom portion of the case and connected to the circuit board using a pair of short wires. The original design used a floating set of electrode snaps, where the male side was allowed to slide in the female portion, however this proved to be problematic and generated a great deal of motion artifact. The fixed electrodes do not create significant shear stresses on the electrode patch as the skin flexes under the patch. An assembled unit can be seen in Figure 4.3.

Figure 4-3: The size of the monitor is 7.2 cm × 3.8 cm × 1.2 cm and it has a mass of 16 g or a weight of 0.56 oz including the battery. The battery has a useful life of more than 1 week. The conductance range is from 0 to 30 μS.

4.4 Ergonomic Design

Since these monitors were to be worn mostly by women it was decided to include designs that would have esthetic appeal to the women who wore them. The shape of the monitor was given the general shape of the female human torso with significant contouring to prevent chafing and abrasion to the adjacent skin surfaces. Thus far the only color produced has been the off color ivory; however future shapes and color schemes have been developed and can be seen in Figure 4-4.

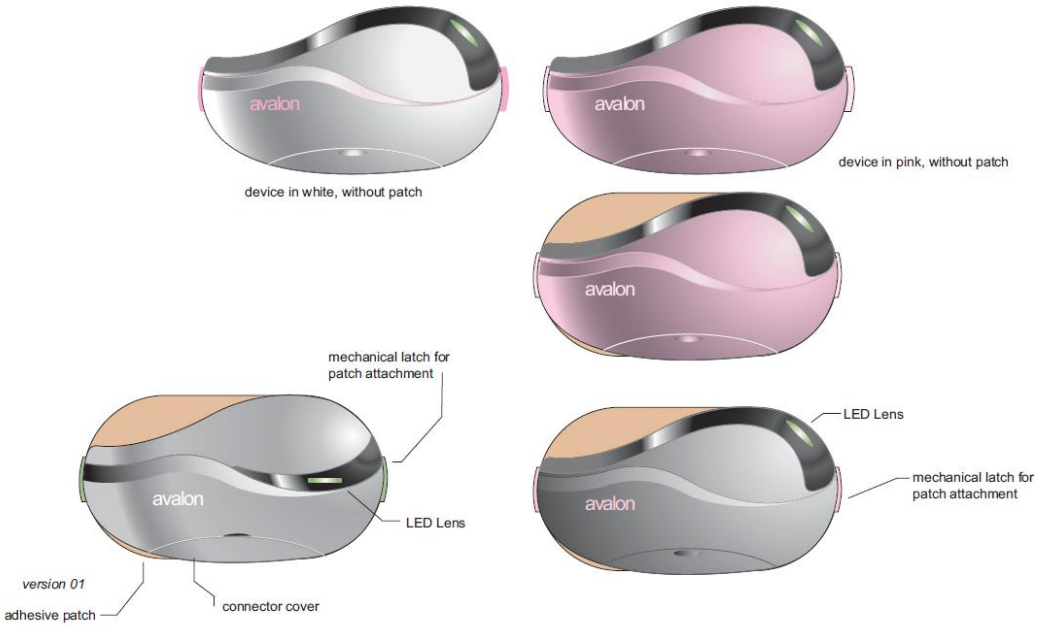

Figure 4-4: Proposed enclosure designs and color schemes for future production.

Chapter 5

5 System Firmware

5.1 Introduction and Overview

Embedded software design and development requires programming tools that are easy to use, free of problems, and have been designed or adapted for use with the microprocessor of choice. When using microprocessors from the TI MSP430F family programmers usually choose the TI programming tool suite because it is inexpensive and very functional. The choice made for this research was to use a version of Linux gcc that had been especially adapted for the MSP430 microprocessor family. This product, called *mspgcc*, contains an assembler, a compiler, and a linker. It does require the user to build the make files giving it a somewhat steep learning curve. The reason that this product was chosen was that it had the stability of Linux gcc and had features not found in the TI tool suite. Important features included the ability to place a function within a function allowing one to more easily develop cooperative multi-tasking kernels and debugging tools not found in the TI suite. The source code was developed using Code Wright® version 7.5 that was originally developed by Borland, Inc. This software editor was designed specifically for developing firmware.

5.2 Embedded Software

Embedded or Real Time software development is both difficult and complex primarily because it must be responsive to temporal events and provide some action to service these events in a timely fashion. This is accomplished using independent modules or service routines called tasks.

If events occur too quickly the software must decide how the events will be serviced. Does the software switch between the tasks giving each task a small slice of time before moving on to the next (preemptive multi-tasking) or does the software allow the tasks to decide when to switch (cooperative multi-tasking). Preemptive multi-tasker kernels can be very complex and are usually added using off-the-shelf software. A simpler way to manage the tasks is to use a cooperative multi-tasker. The tasks are switched when the currently running task is waiting for something or has finished running. The time when events get serviced depends heavily on what the tasks are doing and their priority. Sampling may need to be done at a fixed rate such as when the software is controlling an A/D converter. This is usually done using a timer interrupt and an Interrupt Service Routine (ISR) that executes a small set of instructions to gather samples and then pass them to the appropriate task when that task executes. The hot flash firmware versions used cooperative multi-tasking together with a round robin multi-tasker where the internal timers in the microprocessor took on the task of servicing events. This allowed the microprocessor to spend most of its time sleeping since the timers did almost everything except actually manipulating and storing the data.

5.3 Signal Sampling

The embedded software controlled the sampling process, local data storage, and the data download process. All timing was controlled by an on board timer paced by a 32.768 kHz watch quality crystal with drift errors between 0.1% and 0.01%. The microprocessor was placed in a sleep mode with only the timer, interrupts, and watchdog timer running. The watchdog was set to an 8 s interval. The timer provided the waveforms for the data collection and generated an

interrupt every 5 s waking the microprocessor. The first order of business was to pet the watchdog timer preventing it from triggering. The conductance value was sampled, stored, and the microprocessor was put back to sleep. The fraction of the time that the microprocessor was fully active was about 10% of the total time thus saving large amounts of battery power allowing the monitor to run continuously for nearly 10 days on a CR1220 Lithium coin cell battery. The voltage waveform that was used to measure the skin conductance was generated by onboard microprocessor timers. Figure 5-1 shows the waveform timing and amplitude. The voltage was held constant at 0.5 V. during the time the pulse was applied. Figure 5-2 shows where the microprocessor control signals apply the voltage to the skin. Sampling of the electrical current was done approximately 50 ms before the end of the pulse.

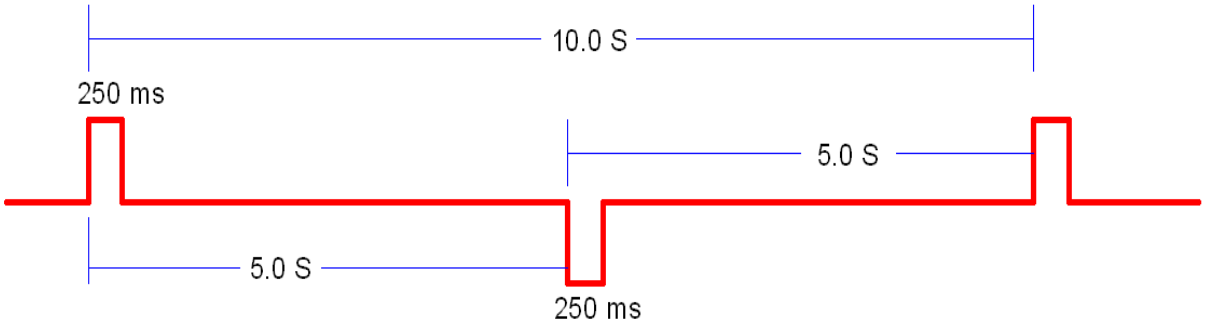

Figure 5-1: Biphasic waveform that is applied to the skin. The peak-to-peak amplitude is 1.0 V.

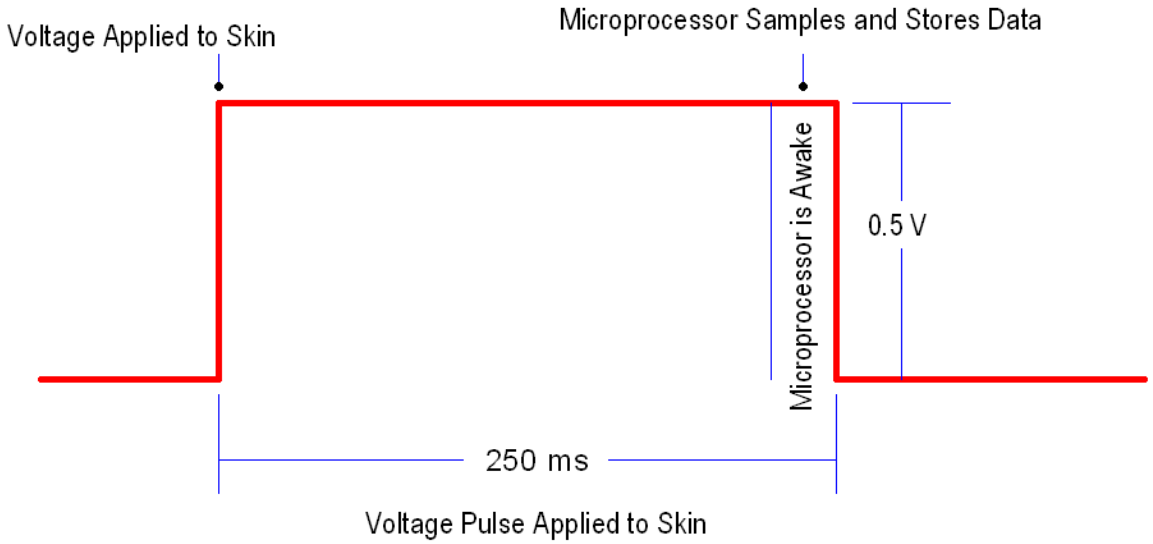

Figure 5-2: Positive waveform showing where the voltage is applied to the skin and where the current is sampled.

5.4 Hot Flash Data Storage

Three versions of the hot flash monitor were built each with its own version of firmware. The first version was a laboratory grade monitor that stored the data in byte format with 17 bytes per record. The second version of monitor stored data in binary using 12 bits for the hot flash data which gave the monitor a range between 0 and 40.95 µS Heart rate was stored as 17 bits which gave the monitor a resolution of 1 ms and a range between 20 and 180 beats per min. The third version was the production version and it stored data the same way the as the second version except it did not include heart rate. All three monitors used one bit to indicate when the subject experienced a hot flash event and pressed the button on the monitor. This data was stored at the next 10 second storage interval. A complete description of the data storage can be found in Appendix VII.

Chapter 6

6 Research Methodology

6.1 Introduction and Overview

Two cohorts of 20 women each between the ages of 45 and 60 years and who had 10 or more hot flashes per day over a three day period were recruited for this research. The subjects were split into two groups, the development cohort and the validation cohort. A production grade hot flash monitoring system was used to sample, record, and process the hot flash data from these women. The processed data was compared with scored data from experts who had many years of experience doing hot flash studies and who were familiar with hot flash morphology. The development cohort data was used to adjust various parameters in the algorithms until they produced sensitivities in the low to mid 0.90's and specificities in the upper 0.80 to lower 0.90. The algorithms were then used to process the data from the validation cohort with expectations that the statistics would be somewhat less than those of the development set.

6.2 Human Subjects

There are currently about 45 million women in the United States between the ages of 45 and 65 years. At least two thirds of these women will experience hot flashes and approximately 20% will seek medical relief for debilitating vasomotor symptoms (Kronenberg 1990). For the purpose of this dissertation, the population was considered as the approximate 6.0 million individuals who would ultimately seek medical relief. Due to limitations of time and money it was only possible to use a small subset of this population so it was decided to use two cohorts of

20 women each. Other than money and time, there was no other justification as to the number and size of the cohorts. The individuals recruited for these studies were from the population in the San Francisco area who volunteered for the studies. The Table II shows the demographics of the two cohorts. Three subjects were dropped from the development cohort were it was clear that the electrodes did not have good contact with the skin.

Table II Characteristics of the Women in the Development and Evaluation Cohorts

Characteristic	**Development Cohort**	**Evaluation Cohort**
Age, mean (SD)	55.1 (4.0)	54.9 (3.2)
Ethnicity, % white	65.0	63.2
Education, % college graduate	50.0	47.4
Relationship status, % married	55.0	47.4
Body mass index, mean (SD)	28.8 (6.0)	28.0 (4.4)
Alcohol use, % $\leq$ 3 drinks in prior month	35.0	57.9
Smoker, % current	10.0	21.0
Hot flashes per day, mean (SD)	9.0 (5.2)	9.3 (5.0)

6.3 Data Collection

During hot flash events the conductance rises rapidly as the sweat pores open and begin exuding sweat. The conductance reaches a peak with full sweat pore recruitment and the conductance then falls slowly as the sweat pores close and the sweat evaporates from the electrode. This morphological shape varies in rise time, height, width, and fall time within subject records and across subject records. Hot flashes have a rise time of approximately 1 min and duration of no more than ten min. The task was to locate the hot flashes events in the data among the motion artifacts such as those produced by exercise and bathing.

The miniature ambulatory monitor and software were tested by collecting data on two cohorts of 20 subjects who had an average of 10 hot flashes per day over a three day period. The results from the first or development cohort had the data from three subjects discarded because the electrodes were clearly intermittent and not making proper contact with the surface of the skin. Because the skin conductance data usually contained artifacts and noise and often had a slow baseline drift, the data was filtered with two separate filters. This is done by passing the filter kernels over the data in one direction and then in the other, doing half of the required math operations in each of the two directions. Since the data was post processed with stored causal data, it was possible to use centering on both filters to eliminate all phase shift errors.

The noise was minimized without significant distortion by using a centered moving average convolution filter with a width of 7 points (±1 min). To minimize the base line drift in the data, it was filtered using a 361 point (±30 min) centered median filter. This type of filter has the characteristic of eliminating drift without distorting the sharp peaks.

Since it is known that subject marked data cannot be considered to be reliable (Miller *et al*. 2004) experts that had years of doing hot flash studies and familiar with hot flash morphology were used to mark the data. Figure 6-1 shows the results of hot flash data marked by experts as to where they thought a hot flash had occurred.

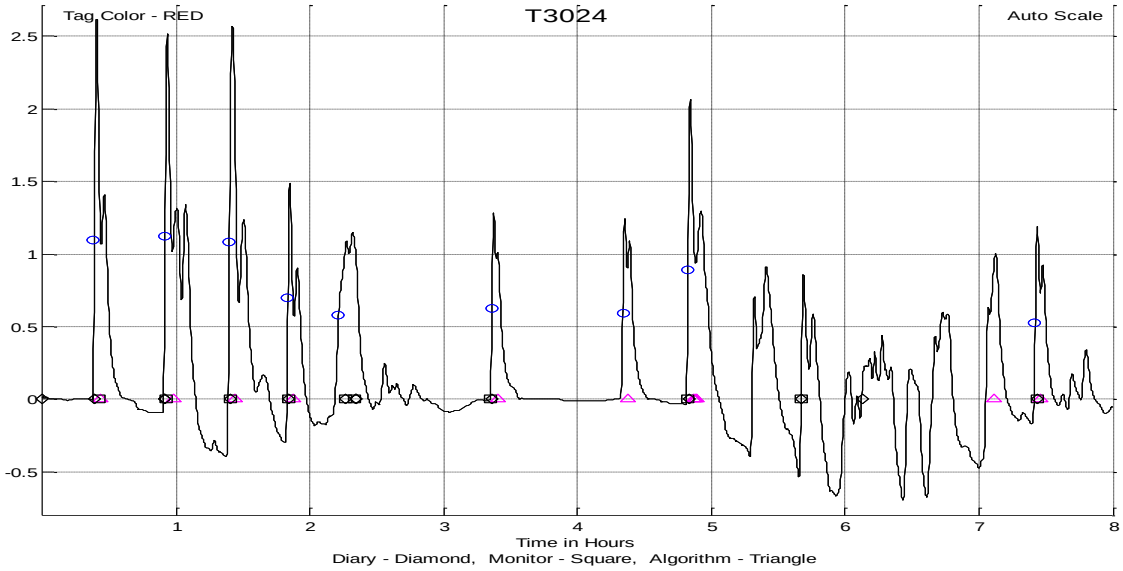

Figure 6-1: Sample of the hot flash data that was marked by the experts.

Tables III and IV shown below indicate which expert marked what data and appendices V and VI contain the instructions and rules for marking hot flash events. Comparisons were made between the ways these experts marked the data. Some of the experts were relatively cautious marking only perfect hot flashes while others somewhat less conservative. However, the differences were not significant enough to warrant the use of this information when training the algorithms.

Table III Development Cohort Marked by Experts							
Development Cohort	**DG**	**FK**	**JW**	**MT**	**JM**	**DB**	**JC**
H3001	√	√	√	√	√		√
H3002		√	√	√	√		√
H3003			√	√	√		√
H3004			√	√	√		√
H3005				√	√		√
H3008		√		√	√		√
H3009		√		√	√		√
H3011			√	√	√		√
H3012		√		√	√		√
H3013		√		√	√		√
H3014				√	√		√
H3016				√	√		√
H3017				√	√		√
H3020				√	√		√
H3022			√	√	√		√
H3024			√	√	√		√
H3025			√	√	√		√

Table IV Validation Cohort Marked by Experts							
Validation Cohort	**DG**	**FK**	**JW**	**MT**	**JM**	**DB**	**JC**
H4001		√	√	√			
H4002			√	√	√		
H4008				√	√	√	
H4014					√	√	√
H4015		√				√	√
H4019		√	√				√
H4020		√	√	√			
H4021			√	√	√		
H4026				√	√	√	
H4033					√	√	√
H4041		√				√	√
H4042		√	√				√
H4043		√	√	√			
H4044			√	√	√		
H4048				√	√	√	
H4049					√	√	√
H4051		√				√	√
H4058		√	√				√
H4059		√	√	√			
H4062					√	√	√

6.4 The Diagnostic Grade Monitor

When this research began there were many unknowns that needed to be answered such as how much would the skin conduction change during a hot flash event, how would conduction vary over time, and how long would the event persist. The monitor needed to have a wide dynamic range and the ability to vary the sensing voltage amplitude and shape using the onboard microprocessor. The monitor had to have very high precision and accuracy such that the measurements of conductivity would not be degraded in any way by the monitor. The monitor would use the existing method of measuring skin conductance by applying a small potential (~0.5 V) to a pair of electrodes place within 2cm of each other and measure the resultant current flow. To address these issues, a number of medium sized (10 cm × 5 cm × 2.5 cm) diagnostic grade skin conductance monitors with a dynamic range of 40 μS, a precision of 0.025%, and an accuracy of 0.1% were designed and built as shown in Figure 6-2.

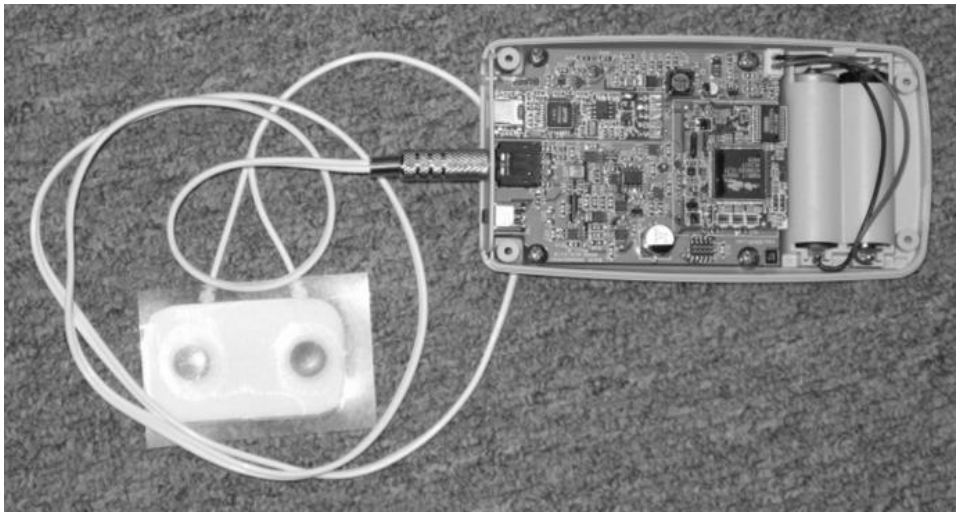

Figure 6-2: The internal circuitry of the diagnostic grade hot flash monitor that was used in the initial hydrogel electrode investigations. A complete schematic can be found in Appendix I.

Five of these diagnostic grade monitors were designed and built so that we could research electrode-to-skin interface materials and collect data for testing various data reduction algorithms. The monitors were calibrated using 0.1% precision resistors at 20 μS and then tested with 0.1% precision resistors at 5, 10, 20, 30, and 40 μS. All of the monitors met the required precision and accuracy. After a few weeks of testing by the engineering team, who did not have hot flashes, a number of the units were sent to the collaborators at the University of California, San Francisco (UCSF) for testing in their bioelectrical laboratory and on ambulatory participants in clinical research studies. All of the participants were members of the research team at UCSF with a number of the individuals having daily hot flashes.

The purpose of these early studies was to determine how well hydrogel electrodes performed when compared to the then current semi-liquid gels in laboratory and ambulatory conditions. The manufacturer (AmGel, Inc.) of the hydrogel material had three material types that were routinely used as electrode to skin interfaces. The material (AG803) that proved to provide the best results as to low background drift, low motion artifact, and good skin adherence without damage was a material that is often used in electrophoresis treatments.

The human studies using the miniature hot flash monitor was approved by the UCSF IRB and the Committee for Human Research (CHR). The CHR approved the proposed research prior to enrollment of any human participants. Copies of the request and approval documents can be found in Appendix IV.

6.5 Data Processing Algorithms

The hot flash skin conductance data collected during this research consisted of 72 h of data from each of the 40 women in the two cohorts. Sampling the conductance every 10 s generated 25,920 samples from each subject over the 3 day period. These data may be described as time ordered continuous signals that contain hot flash events, base line drift, and motion artifact. Algorithms needed to be developed that could process these data allowing the algorithm to move along the data by shifting or sliding over the data. It was possible to isolate and extract hot flash events for training purposes but not for the general determination of hot flash events.

Four signal processing algorithms were investigated including matched filters or template matching, support vector machines, hidden Markov models, and artificial neural networks. All of these methods are pattern classifiers; however each has a unique way of processing data. Support vector machines and neural networks do class discrimination using hyperplanes or hyperspace and both use a learning process with a set of training templates usually composed of a subset of the actual data set.

Support vector machines have been used for hot flash studies (Thurston 2009). The data from this research showed relatively good sensitivity and specificity of 0.89 and 0.96 respectively. However, the women were monitored over a 4 h period in a temperature controlled laboratory setting and not in an ambulatory environment. Support vector machines also ignore the time dependence of hot flash events.

Observed skin conductance with hidden hot flash states closely follows the Hidden Markov Model making this method a good candidate for processing hot flash events. Hidden Markov models use state machines where the transition between states is determined by stochastic processes. The hidden Markov model was eliminated because there have been studies using this method on hot flash data (Creasman, et al. 2011). Her results were modest at best with large amounts of false positives.

Instead of Markov models, I decided to use neural networks as one algorithm to process hot flash events. Both models use probabilities when moving from state to state, but the neural network provided many orders of magnitude higher classification boundaries. The second algorithm that I decided to use was the Matched Filter. The matched filter correlated the hot flash data with a parameterized template on a point by point basis providing a goodness-of-fit coefficient. For this research the templates consisted of a set of parameterized patterns using the log-normal as the basis function.

Chapter 7

7 Human Safety and Data Monitoring

7.1 Human Safety

A total of 20 healthy women, aged 45 to 60 years were studied during this research. Because of the focus on menopausal symptoms, children and men were not appropriate subjects. Also some minority women were recruited to improve representation in the sample, although all participants needed to be English speaking since there was no capacity to translate the research documents and PDA programs into other languages. All data was collected for research purposes only and was kept confidential, following IRB and HIPPA guidelines. The Participant/Staff instructions used during this research is shown in Appendix II. Appendix III contains the Clinical Trial Protocol followed during this research. The IRB request and approval forms can be found in Appendix IV.

Risk to the human subjects was minimal. This research used physical sensors that were applied to the surface of the body and did not involve input of significant amounts of energy. The electrodes were similar to electrodes routinely used in electrocardiography or polygraph studies. Similar electrodes have been used by several hot flash investigators measuring skin conductance. Electric currents were by design inherently less than 10 μA. Whereas other investigators applied electrical voltages continuously, the new monitor applied the voltage with a low duty cycle of less than 10%. The hydrogels that were used were applied to the skin in a similar fashion to those already in use for medical skin applications. These hydrogels had already passed all tests

for cytotoxicity, primary skin irritation, and delayed contact hypersensitivity. However, additional tests were run by the researchers for possible skin irritation. There were some mild skin irritations similar to the mild erythema that appears when medical adhesive tape is removed from skin.

All participants provided informed consent according to the guidelines of the University of California, San Francisco, and we took great care to ensure that participants understand the requirements of participation. We protected the identification of subjects by using coded numbers when labeling the data. We carefully assessed and reviewed findings on skin irritation after each participant wore the sternal and wrist-watch devices. There were no direct benefits to the participants. The research was expected to contribute to a better technology to study menopausal symptoms.

7.2 Data Safety Monitor

The progress of this study and participant safety was evaluated by an independent Data and Safety Monitor by the name of Dr. Andrew Avins. He is a senior researcher at Kaiser Permanente of Northern California with experience in study design, research ethics, and statistics. He periodically reviewed the timeline, conduct and outcomes of the study and provided feedback to the NIH and study investigators on the overall performance of the study with particular attention to protecting the safety of participants. Dr. Avins is entirely independent of the institutions and investigators participating in these studies and has no financial ties to the outcome of the study and no financial ties to other companies developing similar medical devices.

Prior to implementation of the proposed study, the Data Safety Monitor evaluated the study design, review informed consent documents, data collection forms and plans for recruitment, study procedures, outcome measurements and safety monitoring. At periodic intervals during the course of the study he:

- evaluated the adequacy and timeliness of participant recruitment, adherence to the protocol, data quality, and the potential of the study to meet the stated goals;
- evaluated participant safety;
- considered factors external to the study when relevant information, such as scientific developments, could have an impact on the safety of the participants or on the ethical conduct of the study;
- ensured that we had data integrity;
- made recommendations, as necessary, to the NIH, study Investigators, and the UCSF Institutional Review Board on continuation, termination, or other modifications of the study protocol.

Since this study was not blinded or controlled, all Data and Safety Monitoring meetings were open and could be attended by all investigators, the study biostatistician and NIH staff, and the clinical site principal investigators. A meeting schedule was developed by the investigators and the Data Safety Monitor based on the final protocol design and testing stages of the new devices. An emergency meeting of the DSM could have been called at any time by the NIH or PI should questions of participant safety arise, but this did not occur.

Reports to the Data Safety Monitor and NIH staff were prepared by the PI for the clinical site (Dr. Grady). The contents and format of the report followed guidelines established prior to the

start of the study. Additions and other modifications to these reports were directed by the Data and Safety Monitor and generally include information on:

- participant safety and satisfaction
- recruitment and projected completion dates,
- adherence to the protocol,
- quality and timeliness of data,
- baseline characteristics of participants
- study drop-outs by phase, including number, reason, and baseline characteristics
- modifications to the monitor and timeliness of prototype iteration
- a display version of the monitor and data on reproducibility and accuracy

The PI of the clinical site (Dr. Grady) prepared minutes of the Data and Safety Monitoring meetings, including any recommendations for changes in the protocol, and these were sent to the NIH and all investigators within 2 weeks of the meeting. The minutes of each meeting concluded with recommendations to continue, terminate or alter the study. Such recommendations were transmitted to all investigators and to the NIH and reviewed immediately. Recommendations that were accepted by the NIH were transmitted by the Project Scientist to PIs and business officials of the grantee institutions as rapidly as possible. It was the responsibility of the PIs to assure that DSM recommendations are sent to the IRB. All materials, discussions, and proceedings of the Data and Safety Monitor were kept completely confidential.

Chapter 8

8 Matched Filter and Pattern Matching

8.1 Introduction and Overview

The morphological shape of hot flash events varies in rise time, height, width, and fall time within subject records and across subject records. However, the variations all maintain the look of a negative exponential squared curve skewed to the right. The hot flashes have a rise time of approximately one minute and duration of no more than ten minutes. The task was to locate the hot flashes amongst the motion artifacts and instances of false hot flash patterns such as those produced by exercise and bathing. Figure 8.1 shows a hot flash data record with subject marked hot flashes.

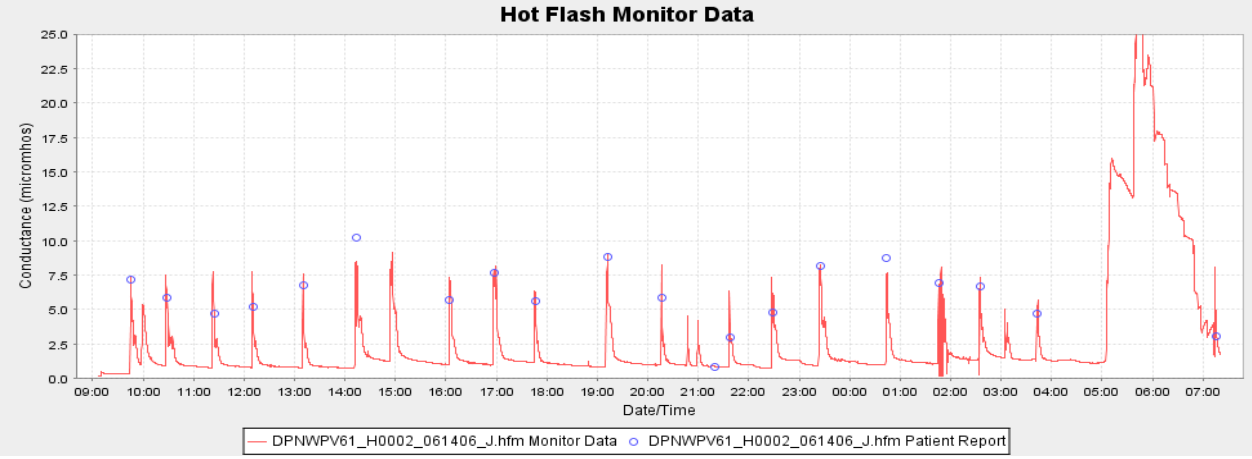

Figure 8-1: Abscissa units are in hours and the ordinate units are in µS. The hot flash events can be clearly seen with the blue circles showing subject markings. The large event near the end of the trace shows the effects of exercise or bathing.

Immediately after the initiation of the hot flash event, the pores on the skin surface begin opening and exuding sweat from the sweat glands below the surface. The electrical current seen by the electrodes begins to increase due to the increase in conductivity since sweat is far more conductive than the epithelium. This current increases approximately linearly with the cross-sectional area of the active sweat pores and is seen as a rapid rise in the conductivity waveform. If the person is already sweating the baseline is usually shifted upward and the hot flash event is simply added to this offset. After a brief period of time the sweat pores begin to close causing the conductance waveform to crest and then descend in a quasi exponential drop back to the base line. This descent is thought to be caused by the absorption of the liquid sweat by the electrode patch and finally its evaporation. The task was to find a function to model this pattern.

8.2 Matched Filter Template

Pattern matching requires using a known pattern for the filter kernel. I could have used the hot flash data that we had collected and chosen an average of many samples for each subject or an average of samples from the entire cohort. Such a choice may have generated great statistics for the development cohort but may not have functioned properly over other population samples collected in the future. This is akin to an over trained development set.

A second choice was to use a parameterized kernel where the shape could be altered by modifying the parameters of the chosen shape. I wanted a kernel that would perform properly with the development data set, the test data set, and data collected during future work. I needed a function that had the characteristics of a hot flash, but was general in nature and not tied to a specific cohort. The function needed to rise rapidly from the baseline to a crest and then descend

back to the baseline over a longer period of time. In other words it needed to be skewed to the right. Functions that contained negative exponential squared terms seemed to be the best candidates. There are many such functions but I chose to limit my search to the Poisson distribution and the log-normal distribution since they met the general criteria I needed. Even though these were probability density functions I knew that I could perform a substitution of variables on the standard deviation and mean in these equations and morph them into functions of time. The Poisson distribution is described as a discrete probability function that describes the probability of a given number of events occurring in a fixed interval of time if these events occur with a known average rate and are independent of the time that the last event occurred. The equation describing the Poisson distribution is shown in equation 8.1.

$$f(k;\lambda) = \frac{\lambda^k e^{-\lambda}}{k!} \qquad 8.1$$

This function had the exponential decay that I wanted but the rise time appeared to rise quickly only when the variance λ had a relatively low value. See Figure 8-2.

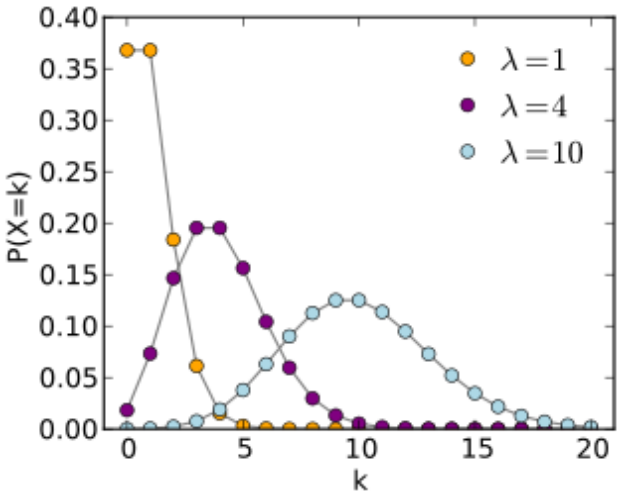

Figure 8-2: Poisson distribution functions. Abscissa units are the number of events and the ordinate units show the probability of an event occurring. *www.wikipedia.org*

The second problem with the Poisson distribution function is that the variance and the mean are equal to each other in all cases. This made it all but impossible to alter the rise time, width, and fall time independently as I needed to do. After some consideration, I decided to abandon any further consideration of the Poisson distribution. The second function that I investigated was the log-normal distribution. The equation for the one dimensional log-normal function is shown in equation 8.2.

$$fx(x;\ \mu,\sigma) = \frac{1}{x\sigma\sqrt{2\pi}}\ e^{\frac{-(lnx-\mu)^2}{2\sigma^2}}\ ,\ x > 0 \qquad 8.2$$

This function is usually called the log-Gaussian, but it is sometimes referred to as the Galton distribution after Francis Galton. This function is useful in modeling naturally occurring variables that are the product of many naturally occurring independent variables rather than the sum of these variables. The symbol σ is the standard deviation when describing this probability density function and the square, σ^2 is the variance. The symbol μ is the mean value and the x symbol is the independent variable and can range from $-\infty$ to $+\infty$. The term $\frac{1}{x\sigma\sqrt{2\pi}}$ in front of the exponential is the normalization constant and comes from the fact that the integral over the exponential function is not unity but rather $x\sigma\sqrt{2\pi}$. With this normalization constant the log-normal function is a normalized function such that the integral over its full domain is unity. Examples of log-normal plots are shown in Figure 8-3.

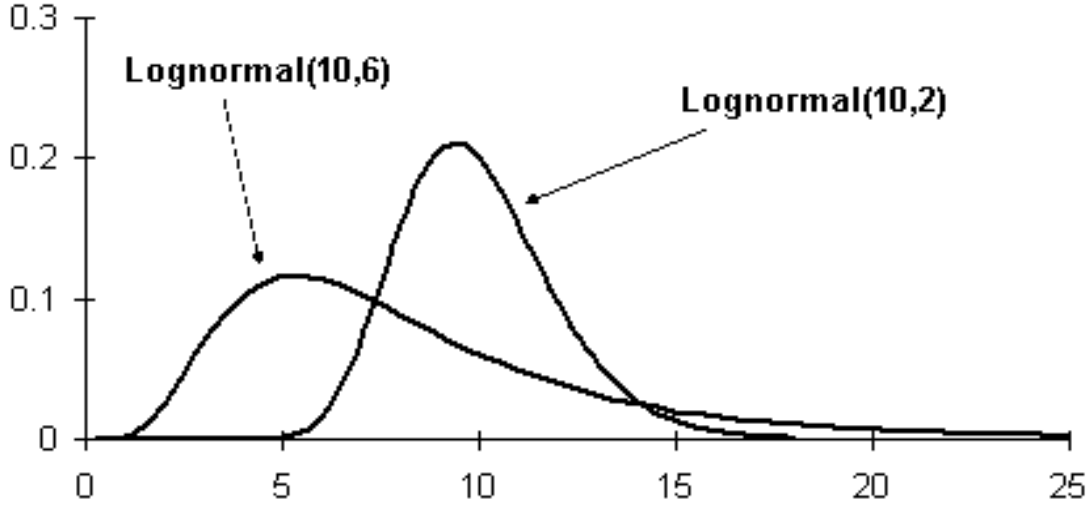

Figure 8-3: Log-Normal distribution functions with a mean of 10 and variances of 2 and 6. Abscissa units are the number of events and the ordinate units show the probability of an event occurring.
www.google.com

This function has the mean and standard deviation as two separate variables and it seemed more plausible to use this function since I could modify this equation into an equation where rise time, peak value, function width, and fall time were essentially independent of each other yet the equation had the exponential decay that I felt necessary to have. Such a kernel should give more consistent results and provide better overall statistics. What I needed was simpler equation that had a similar shape but for my purpose I wanted a form of the equation where the mean and standard deviation could be replaced with just two terms, such as center and width. The empirical equation that I ultimately used is shown as equation 8.3.

$$template(x + offset) = \left[\exp\left[-0.8 \times \left(\frac{\ln\left(\frac{x}{center}\right)}{width}\right)\right]\right]^2 \qquad 8.3$$

The term x is the value along the abscissa with a range from 0 to 90. Since the data was sampled and stored every 10 s. the range spanned $[90 * 10/60]$ or 15 minutes. The center is where the peak occurs and the width is a measure of the skew or drop in the tail. Offset is the amount of time from zero to where the function's rising edge begins. The equation 8.3 is nothing more than an empirical approximation to equation 8.2. The variables center and width in equation 8.3 were chosen to produce the best statistical results when compared with experts who marked the data sets for hot flash events. The variable segment is a vector of the subject data and the template is a vector of the matched filter template to be used on the data. The results are two arrays where one is the correlation between the data (CC) and the template while the other (CP) is the product of the template and data. This product information is used to eliminate events where the CC indicated a hot flash event, but where the amplitude of the data was too small to be an event.

8.3 Matched Filter Template Selection

Initially, it was hoped that a single kernel could be developed with fixed constants for the center and width that could be used for all subjects. But, this was not to be and it was necessary to use five separate kernels all with unique values for the center and width as shown in Figure 8-4. These curves were chosen by using different values for the both the center and width parameters and plotting the results on receiver operating characteristic (ROC) curves. The width was varied between 0.1 and 4.0 in steps of 0.1 and the center was varied between 1 and 25 in steps of 1 providing 1000 filter kernels. This was done on the entire development cohort.

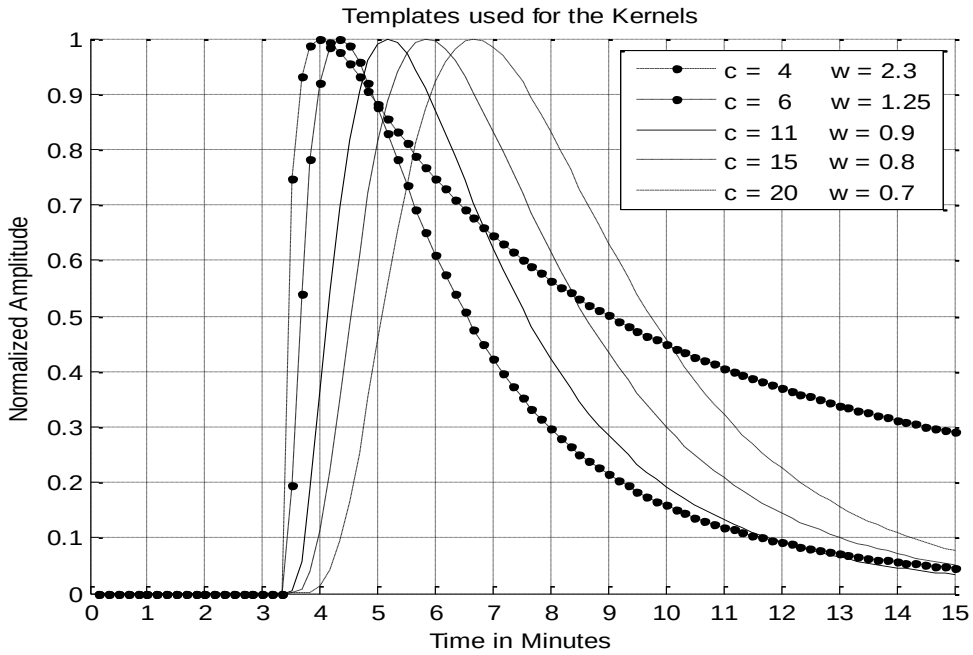

Figure 8-4: The five templates used for the filter kernels. Where *c* is the center parameter and *w* is the width parameter. The values for these parameters were chosen using ROC curves.

8.4 Pearson Correlation Coefficient

The Pearson Product-Moment Correlation Function was implemented as a sliding or moving algorithm and was used to determine the best values for the center and width parameters. A function was written in MatLab to calculate the sliding Pearson correlation coefficient.

The Pearson correlation function returns a vector of $25920 \times (72 \times 360)$ data points with a temporal spacing of 10 s. These data points indicate the probability of a hot flash event in the raw data. A cut point was empirically selected to maximize the statistics. Figure 8-5 shows the results from one of the members of the development cohort and the cut point as a red line.

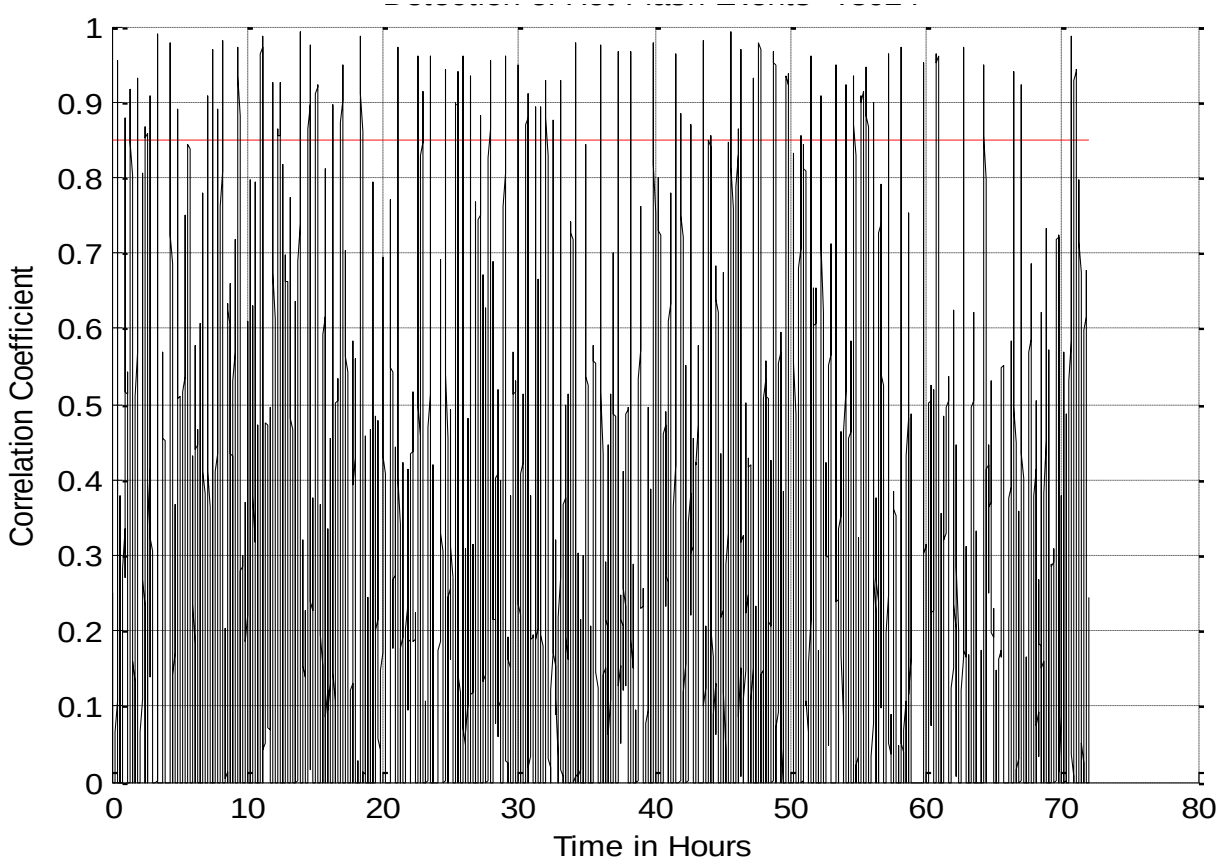

Figure 8-5: Pearson Correlation using the data from subject 3024. The red line is an empirically chosen cut point to maximize the statistics. The data above the line are considered hot flash events.

Figure 8-6 draws a comparison between the correlation coefficient vector and the raw data. The correlation function also returns a product vector with the same 72 h length. If a positive correlation is indicated, but the product returned from the correlation function is less than 5.0, the event is rejected. Figure 8-7 shows the plot of the correlation product.

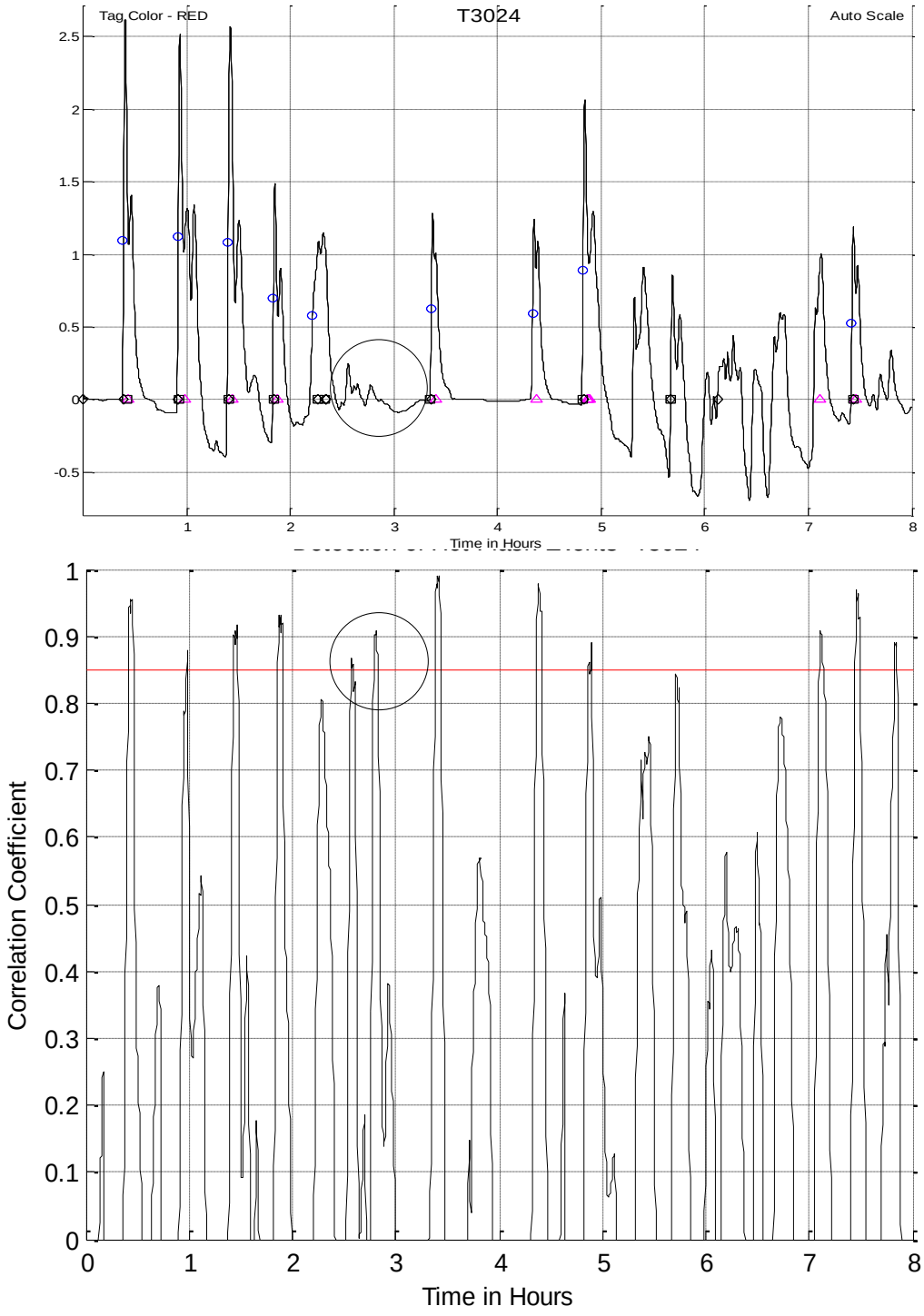

Figure 8-6: A comparison between the unprocessed data and the results from the Pearson correlation algorithm. Two false positives are indicated just before hour 3. However, these will ultimately be rejected because the size of the event in the unprocessed data is too small to be a hot flash.

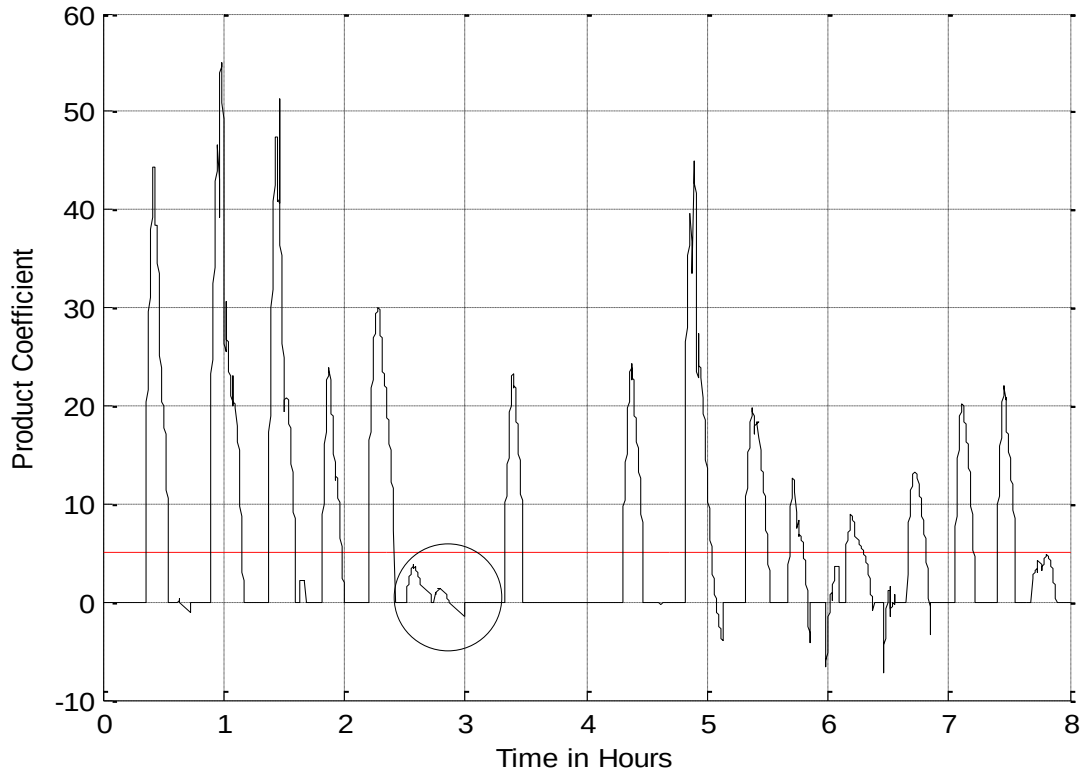

Figure 8-7: Product coefficient returned from the Pearson correlation calculations. The amplitude is representative of the energy in the subject data. Any peak below 5.0 is rejected as being too small to be a hot flash.

Initially, each of the parametric log-normal patterns was used as the filter kernel in conjunction with the Pearson correlation coefficient to determine the best parameters for that kernel. The parameters were varied and the statistics were calculated using the expert marked data. Extensive use was made of Receiver Operating Characteristic (ROC) curves to determine what values to use for the center and width for the parameterized kernels. An example of one of these curves is shown in Figure 8-8.

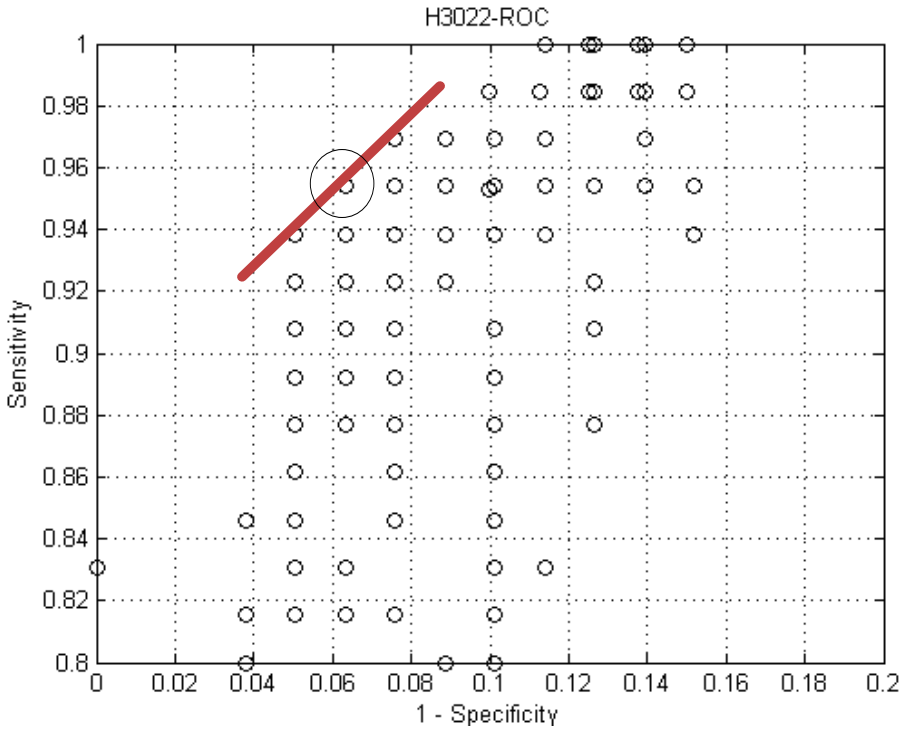

Figure 8-8: A receiver operating characteristic (ROC) curve showing the results of varying the kernel parameters. Each circle represents the results of processing the data with a fixed center and width. The best center and width generated the circled point.

ROC curves were run for each of the 17 subjects in the development set and the points (circles on the graph) that were clustered in the upper left hand corner were considered likely candidates. The parameters of the kernels that generated these points and were common across the subjects were the values chosen as the working parameters. Five templates were chosen as the best fit to the development data set. A match occurred if one or more of the five templates found a match.

8.5 Matched Filter Data Processing

The data from each of the subjects in the development data set was processed using the five kernels and if just one of them indicated a hot flash, it was considered a hot flash. This method

was shown to produce good results with a mean sensitivity of 0.92 and a mean specificity of 0.90 using the development cohort as shown in Table V.

Table V Statistics using the Matched Filter on the Development Cohort

Subject	TP	TN	FP	FN	SENS	SPEC	PPV	NPV
H3001	16	111	14	3	0.84	0.89	0.53	0.97
H3002	36	90	16	2	0.95	0.85	0.69	0.98
H3003	65	64	10	5	0.93	0.86	0.87	0.93
H3004	54	81	9	0	1.00	0.90	0.86	1.00
H3005	33	93	14	4	0.89	0.87	0.70	0.96
H3008	17	119	5	3	0.85	0.96	0.77	0.98
H3009	22	104	9	9	0.71	0.92	0.71	0.92
H3011	61	77	5	1	0.98	0.94	0.92	0.99
H3012	62	72	8	2	0.97	0.90	0.89	0.97
H3013	44	77	16	7	0.86	0.83	0.73	0.92
H3014	35	100	9	0	1.00	0.92	0.80	1.00
H3016	13	114	15	2	0.87	0.88	0.46	0.98
H3017	22	116	4	2	0.92	0.97	0.85	0.98
H3020	30	91	20	3	0.91	0.82	0.60	0.97

H3022	65	69	10	0	1.00	0.87	0.87	1.00
H3024	59	76	8	1	0.98	0.90	0.88	0.99
H3025	16	124	4	0	1.00	0.97	0.80	1.00
Mean	**38**	**93**	**10**	**3**	**0.92**	**0.90**	**0.76**	**0.97**

Using the same algorithm and kernels on the evaluation cohort of 20 individuals produced an average sensitivity is 0.92 and the average specificity is 0.87 as shown in Table VI.

Table VI Statistics using the Matched Filter on the Evaluation Cohort

Subject	TP	TN	FP	FN	SENS	SPEC	PPV	NPV
H4001	42	84	18	0	1.00	0.82	0.70	1.00
H4002	27	96	17	4	0.87	0.85	0.61	0.96
H4008	23	94	27	0	1.00	0.78	0.46	1.00
H4014	28	101	11	4	0.88	0.90	0.72	0.96
H4015	33	88	16	5	0.88	0.85	0.69	0.95
H4019	11	116	16	1	0.92	0.88	0.41	0.99
H4020	47	84	9	4	0.92	0.90	0.84	0.95
H4021	29	100	10	5	0.85	0.91	0.74	0.95
H4026	47	63	30	4	0.92	0.68	0.61	0.94

H4033	34	102	7	1	0.97	0.94	0.83	0.99
H4041	38	90	13	3	0.93	0.87	0.75	0.97
H4042	24	92	23	5	0.83	0.80	0.51	0.95
H4043	19	116	5	4	0.83	0.96	0.79	0.97
H4044	3	126	15	0	1.00	0.89	0.17	1.00
H4048	57	71	13	3	0.95	0.85	0.81	0.96
H4049	20	110	14	0	1.00	0.89	0.59	1.00
H4051	38	79	24	3	0.93	0.77	0.61	0.96
H4058	5	136	2	1	0.83	0.99	0.71	0.99
H4059	51	81	12	0	1.00	0.87	0.81	1.00
H4062	4	131	8	1	0.80	0.94	0.33	0.99
Mean	**29**	**98**	**15**	**2**	**0.92**	**0.87**	**0.63**	**0.97**

Chapter 9

9 Adaptive Neural Networks

9.1 Introduction and Overview

An adaptive neural network is a mathematical method for pattern classification that uses complex decision boundaries and yet can generalize to any particular problem. This method was developed in the 1940's by McCullough and Pitts. They built a mathematical model that simulated the biological neuron by multiplying the inputs to the network with a series of weights and then summing these values to produce a single output that is either true or false. This is similar to how the dendrites and axons function in our brains. The dendrites collect electrical signals from other neurons often applying a weight to these signals, summing the results, and sending the resultant signal along the neuron axon to other neurons.

An adaptive neural network is a method of identifying patterns in new observations where the identity of these patterns has been learned on the basis of a training set containing a subset of these observations and where the groupings of these patterns has been previously established. The groupings are determined by using quantitative information that describes various implied traits or characteristics. The neural network is presented with individual training patterns along with the classification information describing to which group the pattern belongs. Part of the learning process is to determine which of the traits or characteristics are important to the classification process using arrays of weighting coefficients. This type of identification is called

a statistical classification since the classification will show a variable behavior that is statistical in nature, and when accomplished using machine learning it is often called supervised learning.

9.2 Neural Network Theory

The similarity between a single neuron and a neural network with a single output can be seen in Figure 9-1.

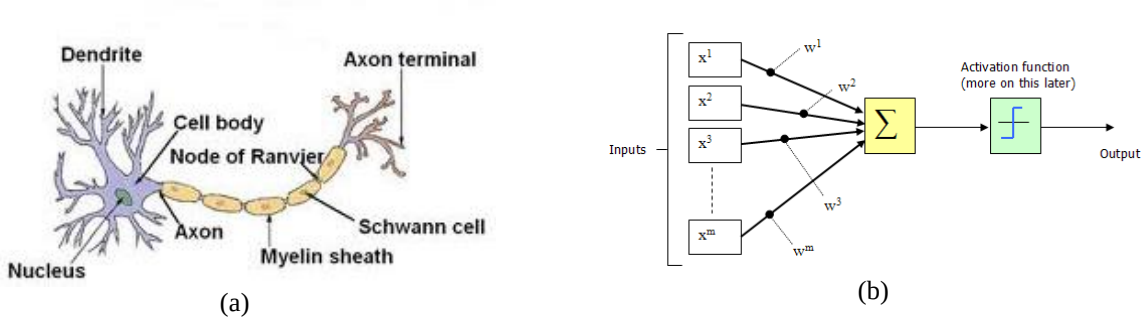

Figure 9-1: Similarity between a neuron (a) and a simple neural network (b) with a single output classifier. www.wikipedia.com www.codeproject.com

The signals entering the dendrites of the neuron are modified by various chemical and electrical processes before being summed and sent along the axon where the signal is presented to other neurons. Modifications of the input signals are done continously as the biological system adapts to various local and external stimuli. The neural network, on the other hand, uses weights to modify the input signals, but only does this during a training session and does not modify these weights when the neural network is being used to classify signals not used for training. In a neuron the connection to the dendrite can be either excitatory or inhibitory and in the artificial neural network this is accomplished by having weights that can be either positive or negative. Equation 9.1 describes the neural network process.

$$a = \sum_{i=1}^{N} w_i x_i + b \qquad 9.1$$

The term x is the input symbol, w is the multiplier weights, i is the input sample number, b is a bias term, N is the total number of inputs, and a is the output. This equation is identical to the equation of a linear discriminator.

The output a is often passed to a non-linear discrimination or activation function with an output of ±1, 0-1, or some non-linear mathematical output. There are a number of such mathematical discriminator functions each with its own special characteristics including a vertical line with a range from 0-1, a sloped line, the hyperbolic tangent, and the sigmoid function. The sigmoid is usually the function of choice because it is a monotonic function and has the ability to compress the output giving its networks greater stability. The sigmoid also happens to be a differentiable function with a derivative that is easy to calculate. The sigmoid function and its derivative are shown mathematically in equations 9.2 and 9.3 and graphically in Figure 9-2.

(Sigmoid function) $$y(z) = \frac{1}{1+e^{-z}} \qquad 9.2$$

(Sigmoid derivative) $$y'(z) = y(z) \times [1 - y(z)] \qquad 9.3$$

The first derivative of the sigmoid function is often found in the literature without explanation of its derivation and is often considered an approximation to the true derivative. However, equation 9.3 is not an approximation and the derivation can be found in Appendix VIII.

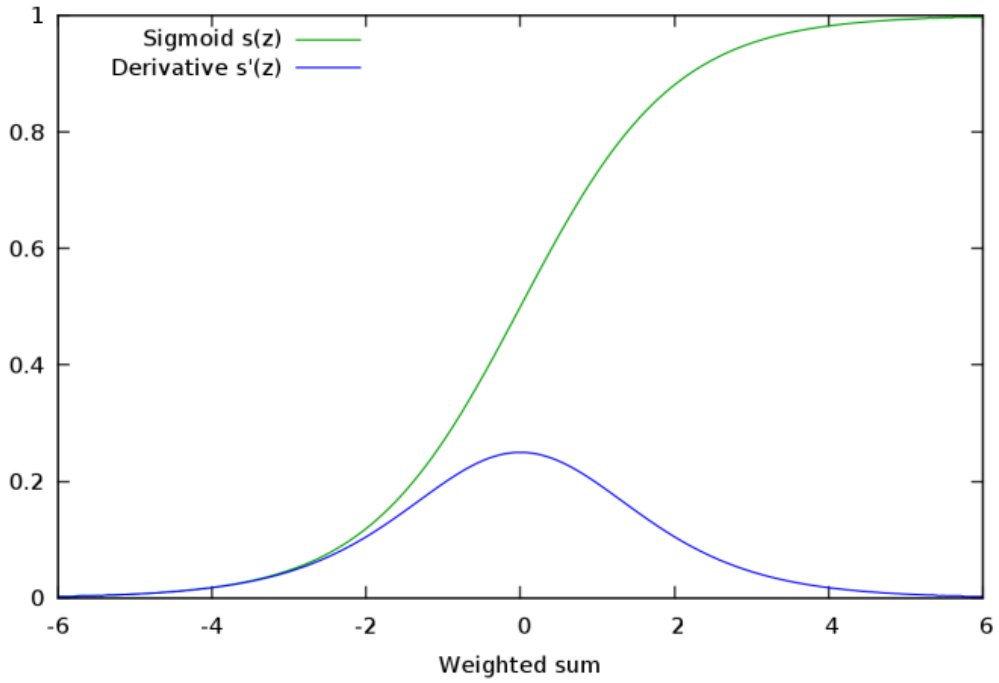

Figure 9-2: Sigmoid function and its derivative. While the sigmoid has a range of 0 to 1 the derivative has a range of 0 to 2.5. These functions were normalized before using them. www.wikipedia.com

For the purposes of this research the abscissa was scaled to ±1 and the ordinate for the derivative was scaled to 0 to 1. This normalization may not have been necessary, but doing so is the best way of keeping the results of calculations near zero and thus provides the best dynamic range when using a digital computer.

9.3 Neural Network Structure

The neural network used in this research is the standard form with an input layer, a hidden layer and an output layer. The name usually given to such a network is the perceptron and it was first used by Rosenblatt (1962). Figure 9-3 shows the network used in this research. The input layer contained 60 nodes of hot flash data and 1 bias node. The hidden layer contained 35 nodes and the output node contained one node.

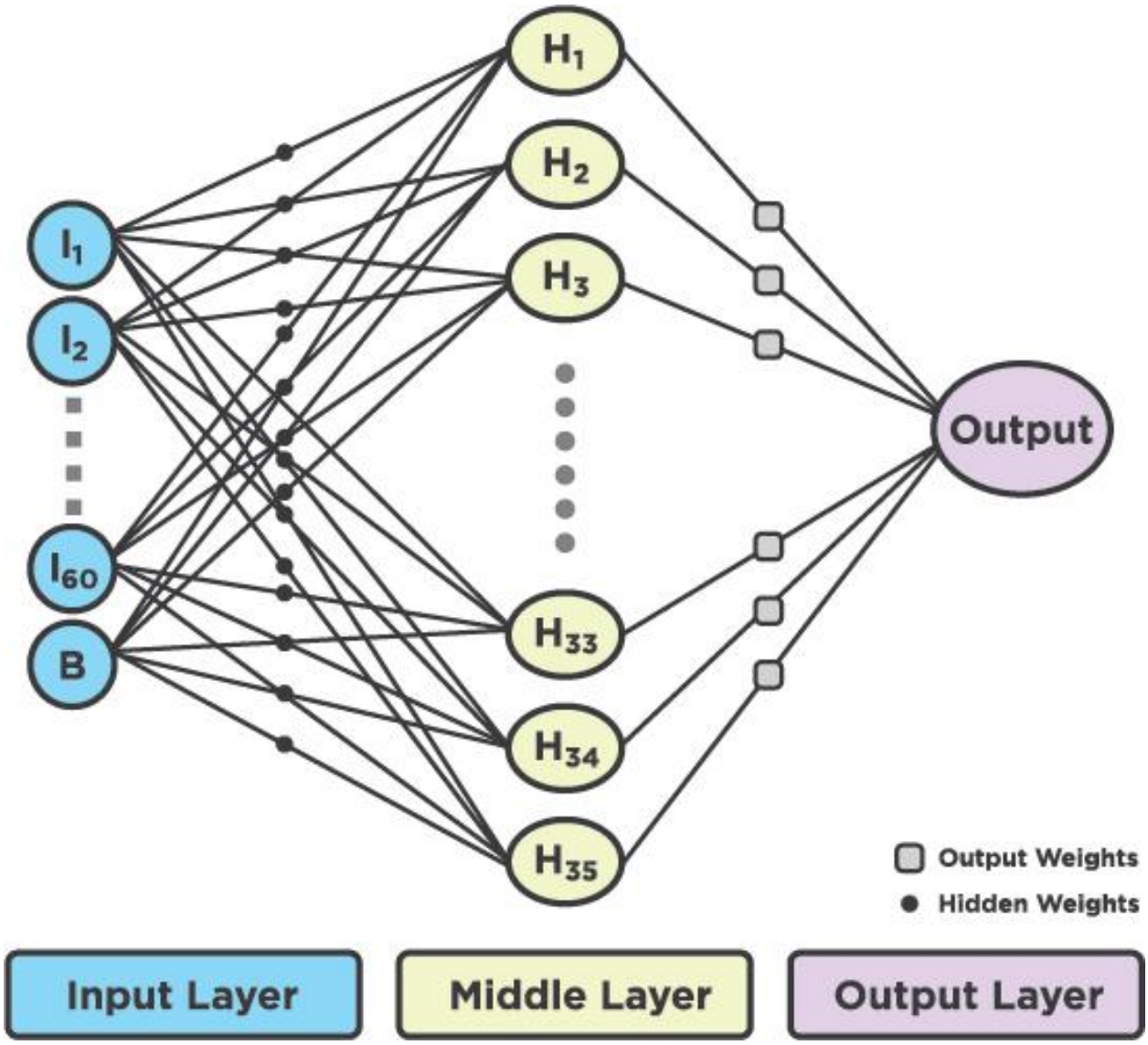

Figure 9-3: A signal flow diagram of the neural network used in this research.

The size of the input was chosen to be 60 nodes because this depicted a 10 minute sample of a hot flash using a 10 second sampling rate. The predominant features of the rapid rise, smooth peak at the top, and the exponential like tail all fall within this 10 min window. A 61st node was added to the input to act as a bias term since the output was to have values between 0 and 1

rather than the usual ±1. The 35 nodes in the hidden layer were chosen empirically using the literature as a guide. (Smith 2003 and Semmlow 2009). They suggest using fewer hidden nodes than there are in the input. The neural network software was written to allow for changes in the size of the hidden layer by changing a single constant. Hidden node sizes between 20 and 60 were used to find results that provided good statistics without excessive computing time. The output layer only needed one node to indicate if the input pattern was classified as a hot flash or not. Values between 0 and 1 indicated the probability of a hot flash event.

9.4 Neural Network Implementation

The greatest effort comes in defining the training data set and in the actual training of the neural network. Training is done by submitting patterns that should elicit a true response along with an indication that the pattern is true and patterns that elicit a false response along with the indication of being false. This training is usually done with hundreds of such patterns and then retrained with the same patterns a few thousand times. A group of such training patterns is called an epoch and if too many epochs (>1000) are used for training, the neural network can become over trained. Should this happen, the development set will have excellent statistics and any evaluation set will have very poor statistics. The idea is to train with enough epochs such that both sets have similar statistical outcomes.

Initially, each of the weights is set to a small random value, in the range between 0.01 and 0.0001. The choice of range was purely empirical and there are no absolute rules to follow. For this research, a flat probability density function (pdf) was chosen with numbers between ±0.04. The training process begins by applying a known hot flash pattern to the input. The input values

are multiplied by the hidden weights, summed and activation functions are applied. These results are modified using the output weights, a single activation function applied, and the result propagated to the output. Equations 9.4, 9.5, and 9.6 are implemented to obtain the forward response where the § symbol represents the sigmoid function.

$$h(i) = \sum_{\substack{i=1,35 \\ j=1,61}} wh_{ij} \times x_j + b \qquad 9.4$$

$$out = \sum_{k=1,35} wo_k \times \S[h(k)] \qquad 9.5$$

$$output = \S[out] \qquad 9.6$$

Figure 9-4 shows the MatLab source code that performs this forward response.

```
%-------------------------------------------------------------------------
% calculate network forward response
%-------------------------------------------------------------------------
for i = 1:hidden_size
    acc1 = 0;Type equation here.
    for j = 1:input_size
        acc1 = acc1 + input(1,j).*Wh(j,i);
    end
    hidden(i) = sigmoid(acc1);
end

acc2 = 0;
for k = 1:hidden_size
    acc2 = acc2 + hidden(k).*Wo(k);
end
output = sigmoid(acc2);
```

Figure 9-4: Forward response of the neural network written in MatLab. The input is a 60 point vector containing the hot flash data. The hidden values are a vector of length 35 while the output is a single value between 0 and 1 that describes the probability of the input being a hot flash event. The variables acc1 and acc2 contain the accumulated weighted sums of the input and hidden layers respectively before the sigmoid discriminators are applied.

Once an input pattern has been processed in the forward direction all of the values for the hidden and output layers are known as well as the weights. A process called back propagation is used to do the actual training. The fastest way to train a network is to use the gradient or steepest descent method to modify the values of the weights. This method changes the network's weights and bias so that the error proceeds towards a minimum along the steepest gradient. The output sigmoid classification is known from the forward response. The derivative of this response ($slope\_output$) is calculated using equation 9.3. Equation 9.7 calculates how the network output will change with respect to a slight change in the output weights.

$$dodw = \frac{\Delta output}{\Delta Wo(m)} \approx hidden(m) \times slope\_output \qquad 9.7$$

The actual network output classification is compared with the desired value of 0 or 1 using equation 9.8 providing an error term describing the amount of error in the output.

$$err = desired - output \qquad 9.8$$

With this knowledge the output weights can be modified by multiplying the gradient by the error term (err) and a learning constant (*mu*) as shown in equation 9.9.

$$Wo(m)_{new} = Wo(m)_{old} + dodw \times err \times mu \qquad 9.9$$

The learning constant has a value between has a value between 0.1 and 0.001 and is used to control the speed of convergence thus preventing the equation from diverging.

Changing the hidden weights is a bit more difficult. The process requires that the output error be distributed to each hidden node to which that output node is connected. The output weights are

included in this back propagation calculation. The derivatives of the outputs from the hidden layer ($slope\_hidden$) can be calculated using equation 9.3 and the results used to calculate the changes in the hidden layer values with respect to changes in the hidden weights.

$$dhdw \approx input(i) \times slope_{hidden(i)} \times Wo(i) \times slope\_output \qquad 9.10$$

The variable $dhdw$ is now multiplied by the learning constant mu and the error (err) and the results are used to find new values for the hidden weights.

$$Wh(m)_{new} = Wh(m)_{old} + dhdw \times err \times mu \qquad 9.11$$

The output error for each input pattern is squared and added to the sum of the pervious squared errors. When an epoch is completed the square root is taken of this sum, displayed on the system console, and used as a measure how well the network is converging. The MatLab source code that performs this back propagation is shown below:

```
%--------------------------------------------------------------------------
% calculate the network back propagation
%--------------------------------------------------------------------------
slope_output = 4.0*output*(1.0-output);
err = desired - output;

for m = 1:hidden_size
    slope_hidden = 4.0*(hidden(m)*(1.0-hidden(m)));
    for n = 1:input_size
        dhdw = input(n)*slope_hidden*Wo(m)*slope_output;
        Wh(n,m) = Wh(n,m) + dhdw*err*mu;
    end
end
for m = 1:hidden_size
    dodw = hidden(m).*slope_output;
    Wo(m) = Wo(m) + dodw*err*mu;
End
```

Figure 9-5: Back propagation algorithm implemented in MatLab using the gradient method.

9.5 Neural Network Training

A neural network only trained on hot flash events will not be able to separate such events from non-events. In fact, it will conclude that everything presented to it is a hot flash. As non-event patterns are added in increasing quantities to the training regimen, the neural network will be able to do a better job of separation. There was a decision that needed to be made as to the number and the proportion of true hot flash events and false hot flash events that should be used during the training process. If a subject had 24 hot flashes a day and each of the hot flashes lasts for 15 min the subject is having a hot flash 25% of the total time. Should the number of true hot flash and false hot flash training patterns be equal or should they be slanted to use more of the false hot flash events that occur more often? After much consideration, it was decided to use the same number of events and non-events and to use as many as possible of both.

To train the artificial neural network 295 hot flash events were selected from the development set by choosing those where more than half of the experts agreed that the event was a hot flash. A definition was established that every one of the experts agreed with and the description can be found in Appendix VI. The true hot flash events had to have occurred within the first three days in each of the conductance records. Next, 165 events were chosen where only one expert thought that the event might be a hot flash but the rest of the experts did not. Not enough of these events could be found in the first three days of the data so the period was extended to five days. After some training runs it was determined that many of the false hot flash events had a morphology that was too similar to a true hot flash producing too many false positives. In general, there were nearly as many false positives as there were true positives. To produce a

better training set, events that resembled true hot flashes were removed from the false hot flash file leaving 118 patterns. I did this at my own discretion. Figure 9-6 shows an overlay of all of the true hot flash events and Figure 9-7 shows an overlay of the false hot flash events.

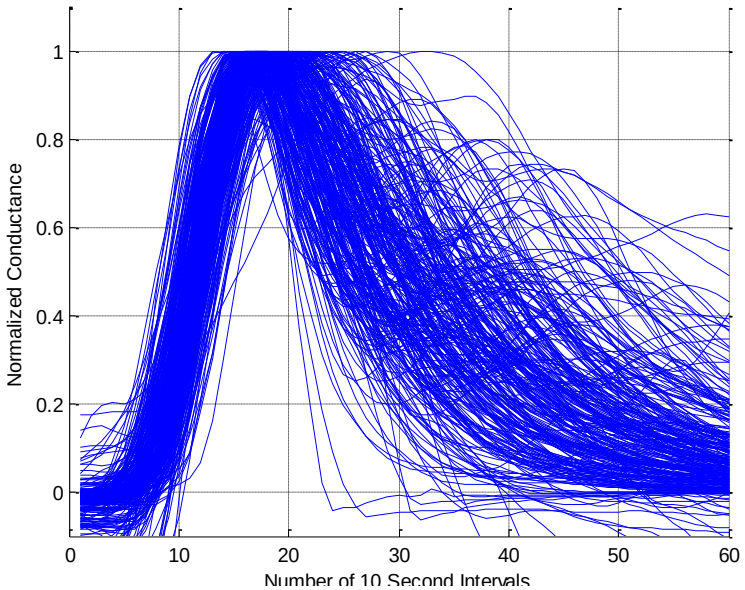

Figure 9-6: An overlay of the 295 true hot flash events used to train the neural network.

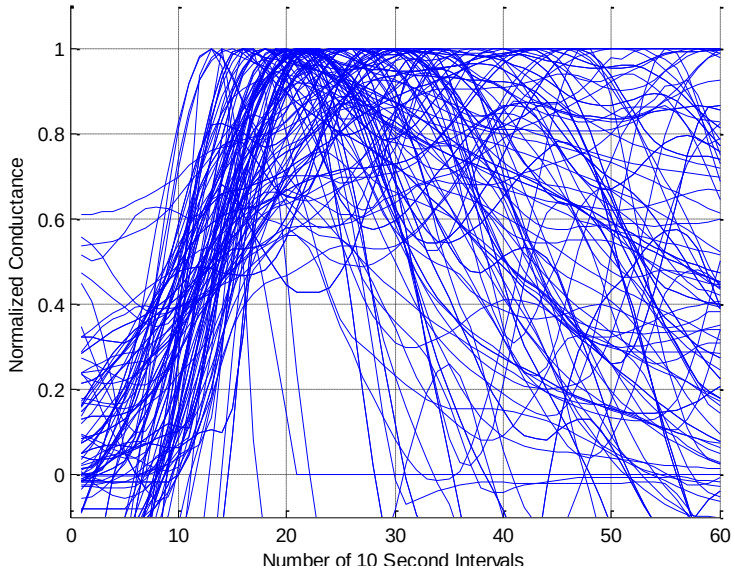

Figure 9-7: An overlay of the 118 false hot flash events used to train the neural network.

The training process uses a MatLab function that processes an entire input pattern of 60 points calculating the forward response and the back propagation. This function returns the squared error of the pattern and the new weight values. The training was done by using alternate records with the even records containing the 'true' events and the odd records containing the 'false' events. Many training runs were executed with the weights set to random values before each run. Approximately 50 training runs were completed using the development cohort and the weights from the run with the best statistical results were considered the trained weights. The results from 5 of the runs using the training data set are compared in Figure 9-8 and the run with the best statistical results is shown in Figure 9-9.

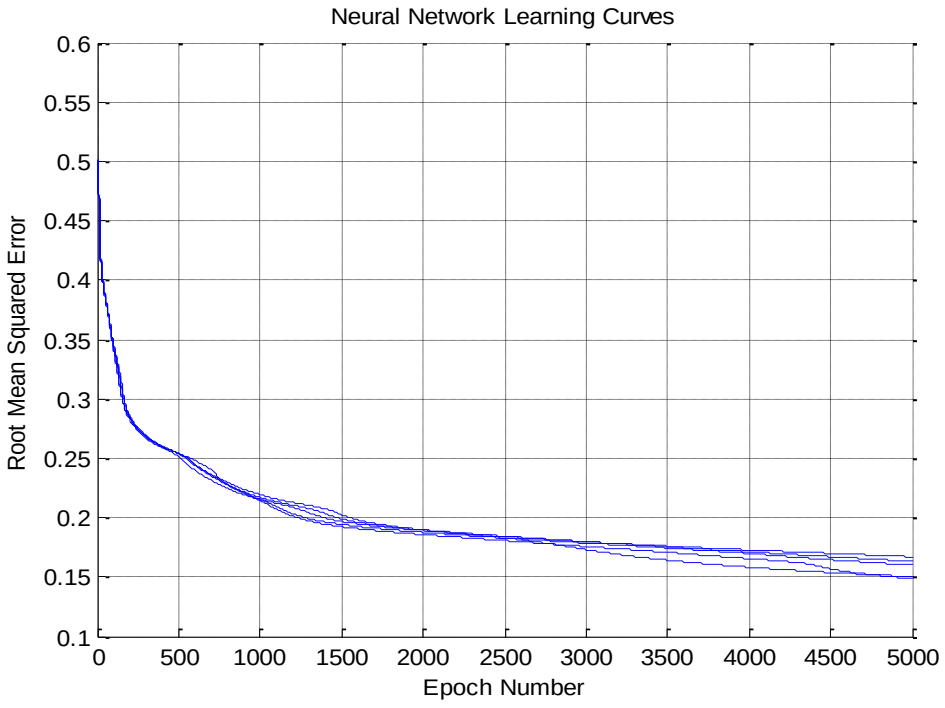

Figure 9-8: Neural network learning curves showing the results from 5 training runs. An epoch is the entire training set having been passed once through the neural network. The rms error is calculated using the errors from the true and false data sets using equations 9.12 and 9.13. The differences in the learning curves are caused by the weights having been randomly initialized.

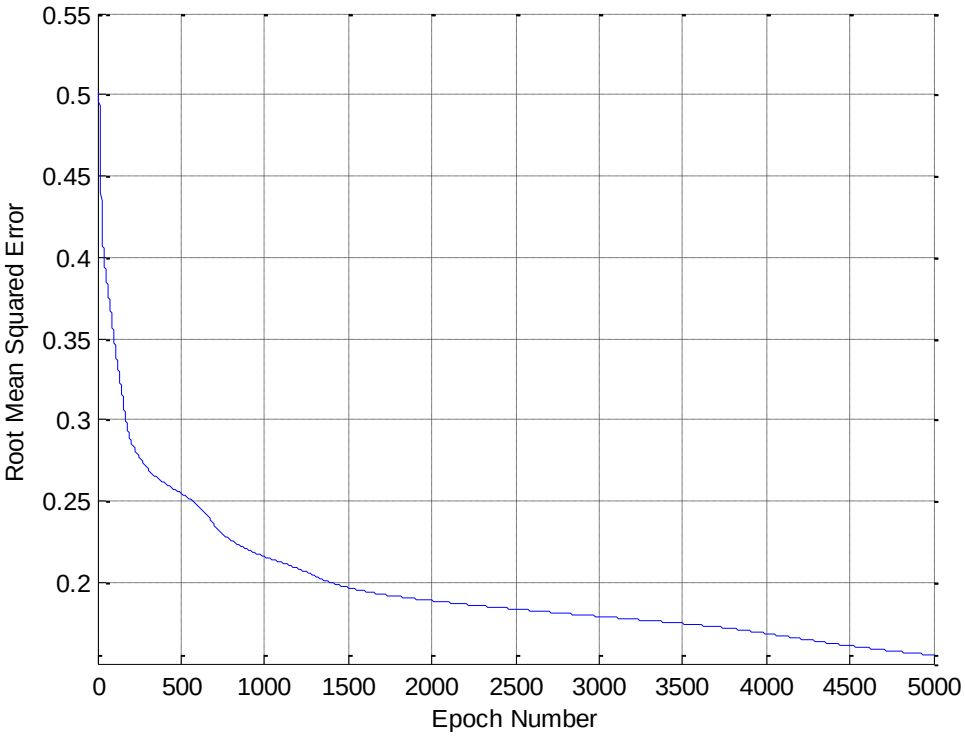

Figure 9-9: Neural network learning curve for the training run that produced the best statistical results. The values of the weights generated from this run were used to process both the development and validation data sets. For this run the learning coefficient was set to 0.0005.

Shown below in table VI are the values of the errors for the best training run. These were printed on the computer console for every 10^{th} epoch that was processed.

Table VII Errors Generated During Best Training Run			
Epoch	**RMS error**	**True error**	**False error**
10	4.968047e-001	4.988561e-001	-4.937071e-001
20	4.556717e-001	4.553123e-001	-4.350747e-001
30	4.147462e-001	3.737136e-001	-3.565410e-001
40	3.992495e-001	3.298267e-001	-3.050228e-001
50	3.901055e-001	3.072069e-001	-2.776055e-001
		↓	
4960	1.556250e-001	6.683414e-002	-6.577620e-002
4970	1.555308e-001	6.639264e-002	-6.562400e-002
4980	1.554373e-001	6.595202e-002	-6.547396e-002
4990	1.553445e-001	6.551243e-002	-6.532603e-002
5000	1.552525e-001	6.507403e-002	-6.518016e-002

The true and false errors start out at approximately 0.5 and end at approximately 0.065. True and false errors were calculated for each of the input patterns. As shown in equation 9.12 these values were squared and summed along with the accumulated sum for that epoch. The RMS errors were calculated using equation 9.13.

$$esum = esum + true\_error^2 + false\_error^2 \tag{9.12}$$

$$rms\ error = \sqrt{esum/(2 \times num\_inputs)} \tag{9.13}$$

A total of 295 true hot flashes and 118 false hot flashes were available. Some elements of the false hot flash patterns were used more than once. As the algorithm processed the true hot flashes, the false hot flash data index simply rolled over providing a total of 295 true and false

hot flashes. Since 295 true and 295 false errors were calculated for each pass through the loop, the denominator was multiplied by 2 to account for this.

If the training is done too aggressively such as using too big a learning constant or by adding extra gain to the error terms the training can became unstable. Sometimes the results were so unstable that the errors continually kept diverging and sometimes the results were somewhat acceptable as shown in Figure 9-10.

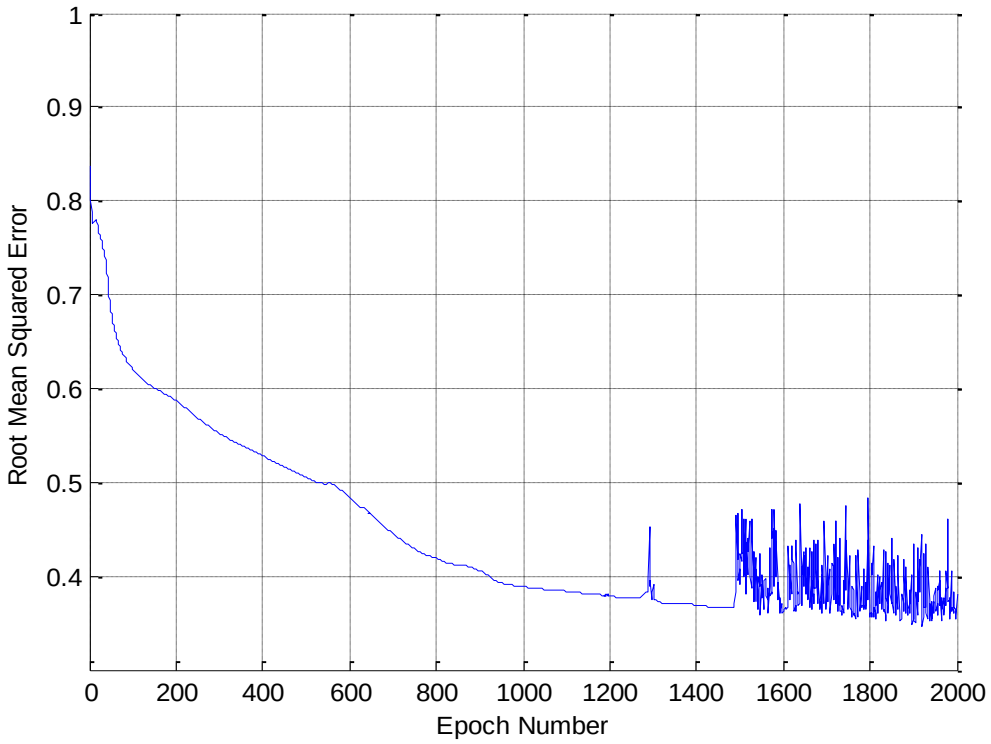

Figure 9-10: Learning curve when a learning constant of 0.01 and a true error gain of 5 were used. The oscillations continued even if more epochs were used in the training process.

9.6 Using the Trained Neural Network

The forward response is used to process data with weight values from the best training set. Sixty data points from the raw data are processed at a time, the data is slid over one data point, and the forward response is run again. This is repeated for the entire data. Figure 9-11 shows the

classification response from the output of the neural network. A cut point of 0.3 was empirically selected to provide the best overall statistics.

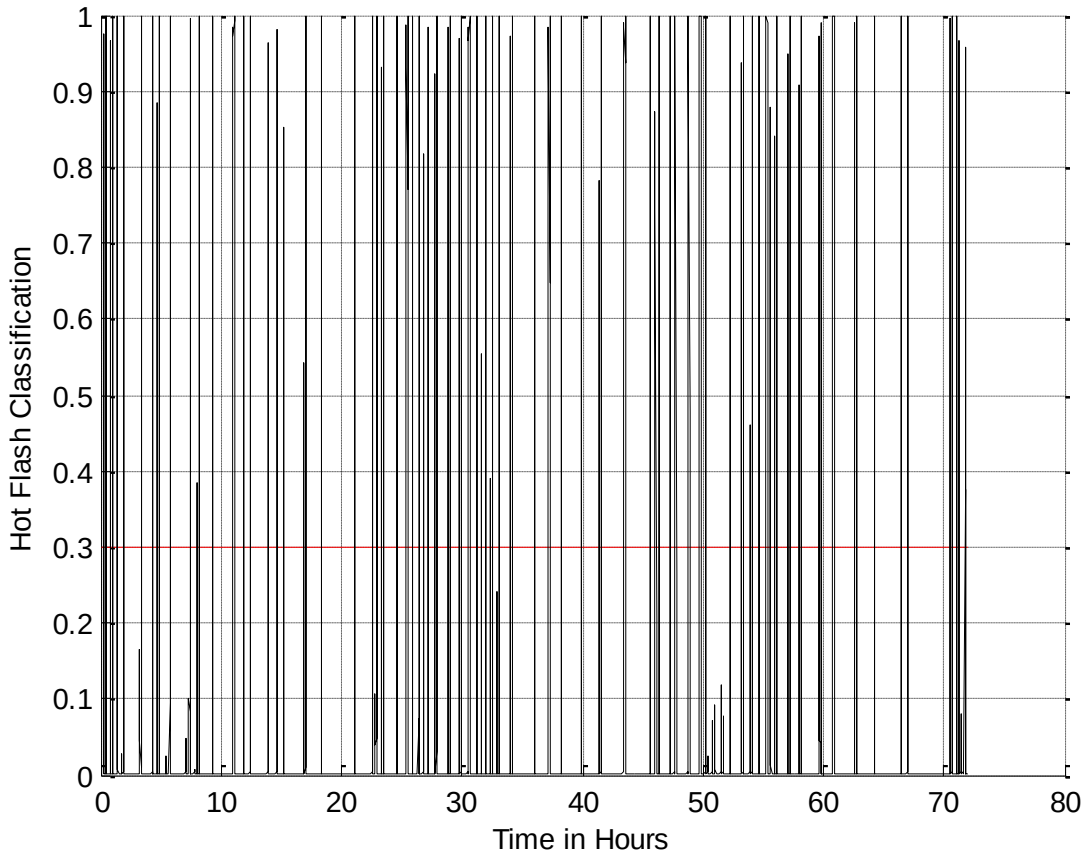

Figure 9-11: The classification from the neural network. The cut point of 0.3 produced the best overall statistics on both the development and validation cohort. The data came from subject 3024.

Figure 9-12 Compares the first eight hours of the data and the classification response and shows a close correlation to the events marked by the experts. Two positive classifiers appear at times for a single hot flash event in the data. It was assumed that this occurred because these hot flash events had a local secondary peak possibly confusing the algorithm.

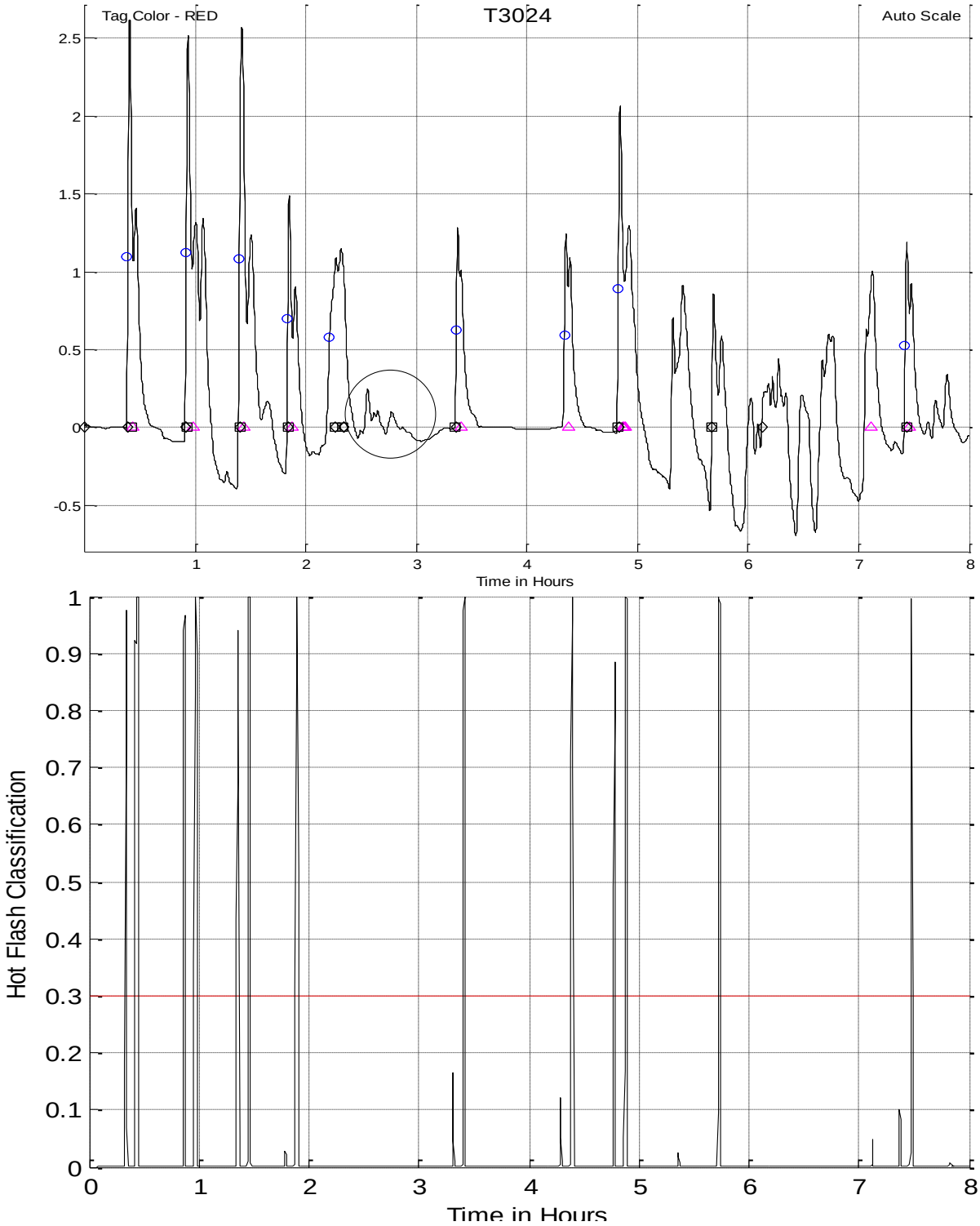

Figure 9-12: Comparison between subject data 3024 and the neural network classification response. The blue circles indicate events that were marked by the experts as a hot flash.

The entire development cohort was processed by the neural network using the weights that produced the best statistical results with the training data set. Figure VIII shows the results using the neural network on the development cohort with a mean sensitivity is 0.93 and a mean specificity is 0.89.

Table VIII Statistics using the Neural Network on the Development Cohort

Subject	TP	TN	FP	FN	SENS	SPEC	PPV	NPV
H3001	13	119	6	6	0.68	0.95	0.68	0.95
H3002	34	90	16	4	0.89	0.85	0.68	0.96
H3003	60	66	13	5	0.92	0.84	0.82	0.93
H3004	53	82	9	0	1.00	0.90	0.85	1.00
H3005	33	91	18	2	0.94	0.83	0.65	0.98
H3008	17	123	3	1	0.94	0.98	0.85	0.99
H3009	28	105	8	3	0.90	0.93	0.78	0.97
H3011	60	75	7	2	0.97	0.91	0.90	0.97
H3012	64	71	9	0	1.00	0.89	0.88	1.00
H3013	45	81	12	6	0.88	0.87	0.79	0.93
H3014	35	98	11	0	1.00	0.90	0.76	1.00
H3016	13	114	15	2	0.87	0.88	0.46	0.98

H3017	23	114	6	1	0.96	0.95	0.79	0.99
H3020	32	90	21	1	0.97	0.81	0.60	0.99
H3022	64	67	12	1	0.98	0.85	0.84	0.99
H3024	59	74	10	1	0.98	0.88	0.86	0.99
H3025	16	127	1	0	1.00	0.99	0.94	1.00
Mean	**38**	**93**	**10**	**2**	**0.93**	**0.89**	**0.77**	**0.92**

The ultimate test was to run the neural network on the evaluation cohort using the weights that produced the best statistical results with the training data set. Table IX shows the results from the validation cohort of 20 individuals with a mean sensitivity of 0.87 and a mean specificity of 0.84.

Table IX Statistics using the Neural Network on the Validation Cohort

Subject	TP	TN	FP	FN	SENS	SPEC	PPV	NPV
H4001	41	75	28	0	1.00	0.73	0.59	1.00
H4002	27	97	17	3	0.90	0.85	0.61	0.97
H4008	20	101	19	4	0.83	0.84	0.51	0.96
H4014	30	96	16	2	0.94	0.86	0.65	0.98
H4015	36	87	16	5	0.88	0.84	0.69	0.95
H4019	11	102	31	0	1.00	0.77	0.26	1.00

H4020	51	84	8	1	0.98	0.91	0.86	0.99
H4021	25	97	13	9	0.74	0.88	0.66	0.92
H4026	48	62	31	3	0.94	0.67	0.61	0.95
H4033	31	99	10	4	0.89	0.91	0.76	0.96
H4041	37	77	26	4	0.90	0.75	0.59	0.95
H4042	19	90	25	10	0.66	0.78	0.43	0.90
H4043	16	114	6	8	0.67	0.95	0.73	0.93
H4044	3	107	34	0	1.00	0.76	0.08	1.00
H4048	61	74	9	0	1.00	0.89	0.87	1.00
H4049	19	112	12	1	0.95	0.90	0.61	0.99
H4051	40	69	34	1	0.98	0.67	0.54	0.99
H4058	3	134	4	3	0.50	0.97	0.43	0.98
H4059	46	79	16	3	0.94	0.83	0.74	0.96
H4062	3	132	7	2	0.60	0.95	0.30	0.99
Mean	**28**	**94**	**18**	**3**	**0.87**	**0.84**	**0.58**	**0.97**

Chapter 10

10 Conclusion and Discussion

10.1 Data Reduction Results

The neural network performed quite well considering its simplicity. As can be seen in Table X, the neural network produced better results than the matched filter when using the development cohort data. However, when applied to the validation data, the results of the neural network were somewhat inferior to the matched filter. The matched filter is the algorithm of choice for all future research and for commercial applications.

Table X Collective Results using the matched Filter and the Neural Network

Matched Filter	Sensitivity	Specificity	PPV	NPV
Development Cohort	0.92	0.90	0.76	0.97
Validation Cohort	0.92	0.87	0.63	0.97
Neural Network	Sensitivity	Specificity	PPV	NPV
Development Cohort	0.93	0.89	0.77	0.92
Validation Cohort	0.87	0.84	0.58	0.97

In all cases the positive predictive value had a poor showing with values in the 50s, 60s, and 70s. This occurred because the team was willing to error on the side of a higher sensitivity compared to specificity. This reasoning created a large number of false positives. However, the experts were conservative in marking the data leaving occasional probable hot flashes unmarked. So, in conclusion with less conservative marking the overall statistical results may actually have been better than shown above.

10.2 Production Hot Flash Monitor

Once the hot flash monitoring system was proven to function properly, a Phase II SBIR grant application was submitted to NCCAM and subsequently funded. This provided enough funds to full commercialize the monitor. Figure 10-1 shows the commercialized monitor.

Figure 10-1: Commercialized Hot Flash monitor. Placement of the monitor is usually done vertically over the sternum but it can be placed on either side.

A poster presented at the North American Menopause Society (NAMS) and a paper that is ready for publication can be found in Appendices IX and X respectively.

Bibliography

Referenced

Boucsein, W., *Electrodermal Activity*, Plenum Series in Behavioral Psychophysiology and Medicine, Plenum Press, 1992.

Creasman J., Wang H., Hot Flash Detection from Sternal Skin Conductance: An Application of Hidden Markov Models. 2009.

Dawson, M. E. & Schell, A. M. (1990). The Electrodermal System, in Cacioppo, J. T. & Tassinary, L.G. (Eds.) *Principles of Psychophysiology: Physical, social, and inferential elements*. The Cambridge Press, Cambridge, UK.

de Talhouet, H., and J. G. Webster, The origin of skin-stretch-caused motion artifacts under electrodes, *Physiol. Meas.*, 17, 81-93. 1996.

Ebling FJG, Eady RAJ, Leigh IM (1992): Anatomy and organization of the human skin. In *Textbook of Dermatology*, 5th ed., ed. RH Champion, JL Burton, FJG Ebling, p. 3160, Blackwell, London.

Fere, C. (1988). Note on changes in electrical resistance under the effect of sensory stimulation and emotion. *Comptes Rendus des Seances de laSociete de Biologie* (Series 9), 5, 217-219.

Freedman, R. R., Biochemical, metabolic, and vascular mechanisms in menopausal hot flashes. Fertility and Sterility, 1998 70: 332-337.

Freedman, R. R., Menopausal hot flashes, in R. A. Lobo, J. Kelsey, R. Marcus (eds.), *Menopause: Biology and Pathobiology*, San Diego, CA: Academic, 2000.

Jossinet, J. and McAdams, E., Hydrogel electrodes in biosignal recording, *Proc. Annu. Int. Conf. IEEE Eng. Med. Biol. Soc.*, 12(4): 1490-1491, 1990.

Kahneman, D. (1973). *Attention and Effort*. Prentice-Hall: Englewood Cliffs, NJ.

Lykken, D. T., and P. H. Venables, Direct measurement of skin conductance: a proposal for standardization, *Psychophysiology*, 8, 656-672, 1971.

McCullough, W.S., & Pitts, W.H. (1943). A logical calculus of the ideas immanent in nervous activity. Bulletin of Mathematical Biophysics,5, 115-133.

Miller, H. G., Li, R.M., "Measuring Hot Flashes: Summary of a National Institutes Health Workshop", Conference Report, Mayo Foundation for Medical Education and Research, 2004.

Neuman, M. R. 1998. Biopotential Amplifiers. In Webster, J. G. (ed.). *Medical Instrumentation: Application and Design.* 3rd ed. New York: John Wiley & Sons.

Olson, W. H., Schmincke, D. R., and Henley, B. L. 1979. Time and frequency dependence of disposable ECG electrode-skin impedance. *Medical Instrumentation*. 13(5): 269-272.

Rosenblatt, F, The perceptron: "A probabilistic model for information storage and organization in the brain. Psychol. Rev. 65:386-408, 1958.

Semlow, J.L., Biosignal and Medical Image Processing, Second Edition, CRC Press, 2009.

Smith, S.W., Digital Signal Processing a Practical Guide for Engineers, Second Edition, Newnes, 2003.

Thurston, R. C, Matthews, K. A., Hernandez, J., De La Torre, F. (2009), Improving the performance of physiologic hot flash measures with support vector machines, *Psychophysiology* **46**: 285-292

Young, T., Finn, L., Austin, D., and Peterson, A., Menopausal status and sleep-disordered breathing in the Wisconsin sleep cohort study (2003). *Am. J. Respir. Crit. Care Med*., 167, 1181-1185.

Related Research

Bromberger JT, Assmann SF, Avis NE, Schocken M, Kravitz HM, Cordal A. Persistent mood symptoms in a multiethnic community cohort of pre- and peri-menopausal women. *Am J Epidemiol* 2003;158:347–56.

Brown DE, Sievert LL, Morrison LA, Reza AM, Mills PS. Do Japanese American women really have fewer hot flashes than European Americans? The Hilo Women's Health Study. *Menopause*. 2009;16:870–6.

Burbank, D. P., and J. G. Webster, Reducing skin potential motion artifact by skin abrasion, *Med. Biol. Eng. Comp.*, 16, 31–38, 1978.

Carpenter JS, Azzouz F, Monahan PO, Storniolo AM, Ridner SH. (2005) Is sternal skin conductance monitoring a valid measure of hot flash intensity or distress? *Menopause*. Sep-Oct; 12(5):512-9.

Collins A, Landgren BM. Reproductive health, use of estrogen and experience of symptoms in peri-menopausal women: a population-based study. *Maturitas* 1994; 20:101–11.

Das, D. P., and J. G. Webster, Defibrillation recovery curves for different electrode materials, *IEEE Trans. Biomed. Eng.*, BME-27, 230–233, 1980.

Dennerstein L. Well-being, symptoms and the menopausal transition. *Maturitas* 1996;23:147–57.

Einerson, N.J., Stevens, K.R., Kao, W.J. Synthesis and physiochemical analysis of gelatin-based hydrogels. Biomaterials. 24, 509, 2002.

Freedman RR (1989) Laboratory and ambulatory monitoring of menopausal hot flashes. *Psychophysiology*. Sep;26(5):573-9

Freedman, R R. Biochemical, metabolic, and vascular mechanisms in menopausal hot flashes. *Fertility and Sterility* 70: 332-337, 1998

Freedman, R. R. and S. Wasson (2007). "Miniature hygrometric hot flash recorder." *Fertil Steril* **88**: 494-6.

Getzel, W. A., and J. G. Webster, Minimizing silver-silver chloride electrode impedance, *IEEE Trans. Biomed. Eng.*, BME-23, 87–88, 1976.

Gold, E. B., B. Sternfeld, et al. (2000). "Relation of demographic and lifestyle factors to symptoms in a multi-racial/ethnic population of women 40-55 years of age." *Am J Epidemiol* **152**: 463-73.

Grady, D. (2006). "Management of menopausal symptoms." *N Engl J Med* **355**: 2338-47.

Hua, P., E. J. Woo, J. G.Webster, and W. J. Tompkins, Using compound electrodes in electrical impedance tomography, *IEEE Trans. Biomed. Eng.*, 40, 29–34, 1993.

Hua, P., E. J. Woo, J. G.Webster, and W. J. Tompkins, Finite element modeling of electrode–skin contact impedance in electrical impedance tomography, *IEEE Trans. Biomed. Eng.*, 40, 335–343, 1993.

Kronenberg, F. (1990). "Hot flashes: epidemiology and physiology." *Ann N Y Acad Sci* **592**: 52-86.

Lee G., Choi J., Differential method against motion artifacts in skin conductance measurement, Electronics Letters, Vol. 43, No. 7, March 29, 2007.

Mayotte, M. J., J. G. Webster, and W. J. Tompkins, A comparison of electrodes for potential use in pediatric/infant apnoea monitoring, *Physiol. Meas.*, 15, 459–467, 1994.

McKinlay, J., S. McKinlay, et al. (1987). "The relative contributions of endocrine changes and social circumstances to depression in mid-aged women." *J Health Soc Behav* **28**: 345-63.

Miller, EH (2004) Women and insomnia. *Clin Cornerstone*. 6 Suppl 1B:S8-18.

Molnar G.W., Body temperatures during menopausal hot flashes, *J Appl Physiol*, Vol. 38, No. 3, March 1975

Panescu, D., K. P. Cohen, J. G. Webster, and R. A. Stratbucker, The mosaic electrical characteristic of the skin, *IEEE Trans. Biomed. Eng.*, 40, 434-439, 1993.

Panescu, D., J. G. Webster, and R. A. Stratbucker, A nonlinear electrical–thermal model of the skin, *IEEE Trans. Biomed. Eng.*, 41, 672–680, 1994.

Panescu, D., J. G. Webster, and R. A. Stratbucker, A nonlinear finite element model of the electrode–electrolyte–skin system, *IEEE Trans. Biomed. Eng.*, 41, 681–687, 1994.

Qu, M., Y. Zhang, J. G. Webster, and W. J. Tompkins, Motion artifact from spot and band electrodes during impedance cardiography, *IEEE Trans. Biomed. Eng.*, BME-33, 1029–1036, 1986.

Rosell, J., J. Colominas, P. Riu, R. Pallás-Areny, and J. G. Webster, Skin impedance from 1 Hz to 1 MHz, *IEEE Trans. Biomed. Eng.*, 35, 649–651, 1988.

Rossouw, J. E., G. L. Anderson, et al. (2002). "Risks and benefits of estrogen plus progestin in healthy postmenopausal women: principal results from the Women's Health Initiative randomized controlled trial." *JAMA* **288**: 321-33.

Shanafelt T. D., Barton D. L., and Adjei A. A., Pathophysiology and Treatment of Hot Flashes, *Mayo Clin Proc.* 2002;77:1207-1218

Sahakian, A. V., W. J. Tompkins, and J. G. Webster, Electrode motion artifacts in electrical impedance pneumography, *IEEE Trans. Biomed. Eng.*, BME-32, 448–451, 1985.

Shumaker, S. A., C. Legault, et al. (2003). "Estrogen plus progestin and the incidence of dementia and mild cognitive impairment in postmenopausal women: the Women's Health Initiative Memory Study: a randomized controlled trial." *JAMA* **289**: 2651-62.

Shumaker, S. A., C. Legault, et al. (2004). "Conjugated equine estrogens and incidence of probable dementia and mild cognitive impairment in postmenopausal women." *JAMA* **291**: 2947-58.

Sloan, J. A., C. L. Loprinzi, et al. (2001). "Methodologic lessons learned from hot flash studies." *J Clin Oncol* **19**(23): 4280-90.

Stone, A. A. (2002). "Patient non-compliance with paper diaries." *BMJ* **324**: 1193-4.

Swanson, D. K., and J. G. Webster, A model for skin-electrode impedance, in H. A. Miller and D. C. Harrison (eds.), *Biomedical Electrode Technology*, Academic Press, New York, 1974, pp. 117–128.

Swanson, D. K., and J. G. Webster, Pressure-induced changes of electrode impedance cause negligible errors in impedance plethysmography, *J. Clin. Eng.*, 8, 229–233, 1983.

Tam, H. W., and J. G. Webster, Minimizing electrode motion artifact by skin abrasion, *IEEE Trans. Biomed. Eng.*, BME-24, 134–139, 1977.

Thakor, N. V., and J. G. Webster, Electrode studies for the long-term ambulatory ECG, *Med. Biol. Eng. Comp.*, 23, 116–121, 1985.

Thurston R. C., Blumenthal J. A., Babyak, M.A., and Sherwood A., Emotional Antecedents of Hot Flashes During Daily Life, *Psychosomatic Medicine* 200567:137–146

Webster J. G. , Bahr D. E., Shults M. C., Grady D. G., Macer J., A miniature skin-attached hot flash recorder: *IFMBE Proc.*, 15, 1-4, 2006

Wiese, S. R., P. Anheier, R. D. Connemara, A. T. Mollner, T. F. Neils, J. A. Kahn and J. G. Webster, Electrocardiographic motion artifact versus electrode impedance, *IEEE Trans. Biomed. Eng*., 52, 136-139, 2005.

Women's Health Initiative Steering Committee (2004). "Effects of conjugated equine estrogen in postmenopausal women with hysterectomy: The Women's Health Initiative Randomized Controlled Trial." *JAMA* **291**: 1701-12.

Woo, E. J., P. Hua, J. G. Webster, W. J. Tompkins, and R. Pallás-Areny, Skin impedance measurements using simple and compound electrodes, *Med. Biol. Eng. Comput.*, 30, 97–102, 1992.

Appendix I

Shown are the Hot Flash Monitor Schematics. The first two drawings show the diagnostic grade monitor and the last drawing is a schematic of the hot flash commercialized monitor.

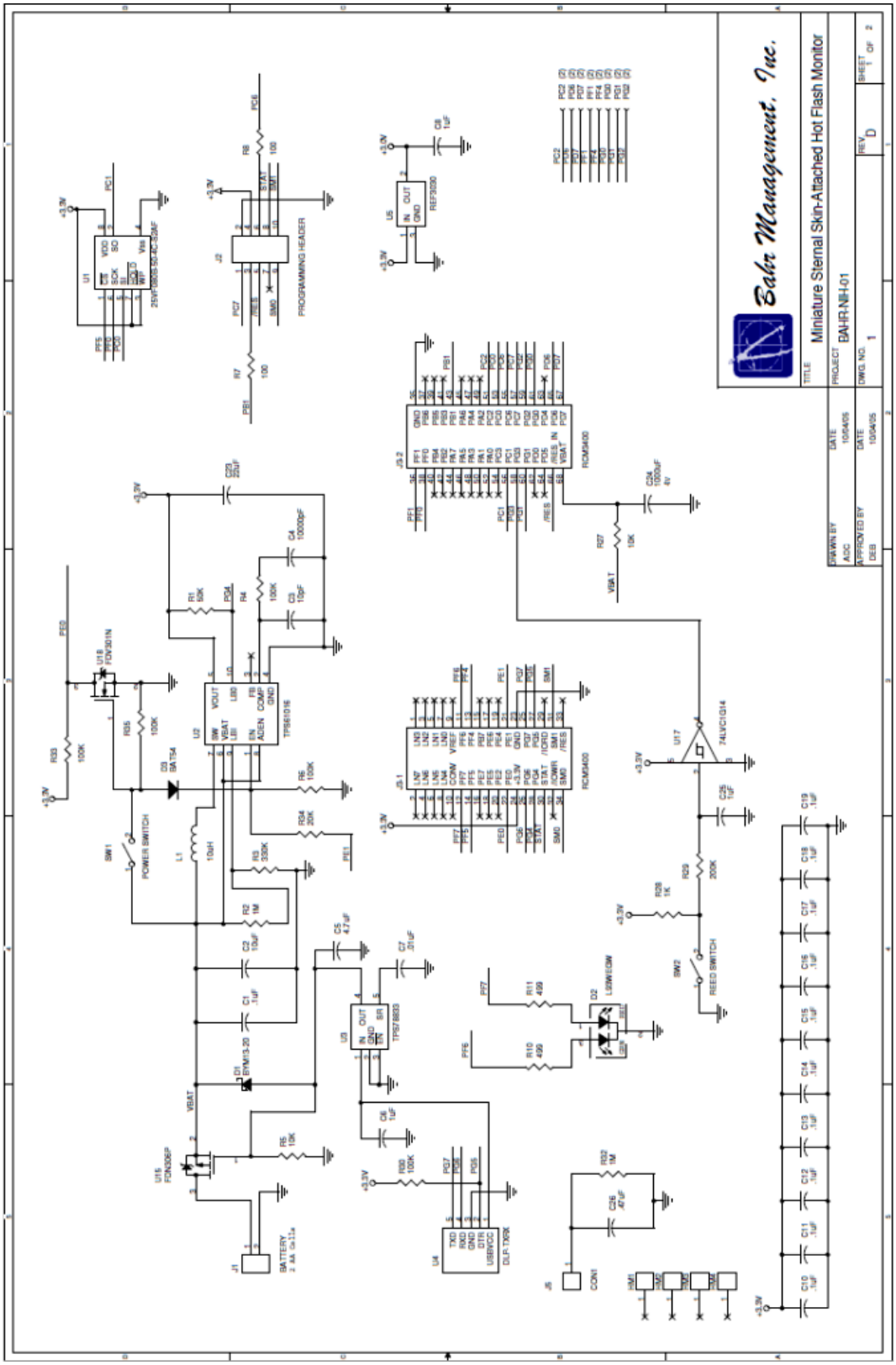

Figure I-1: Schematic of the microprocessor and control circuitry for the diagnostic grade monitor.

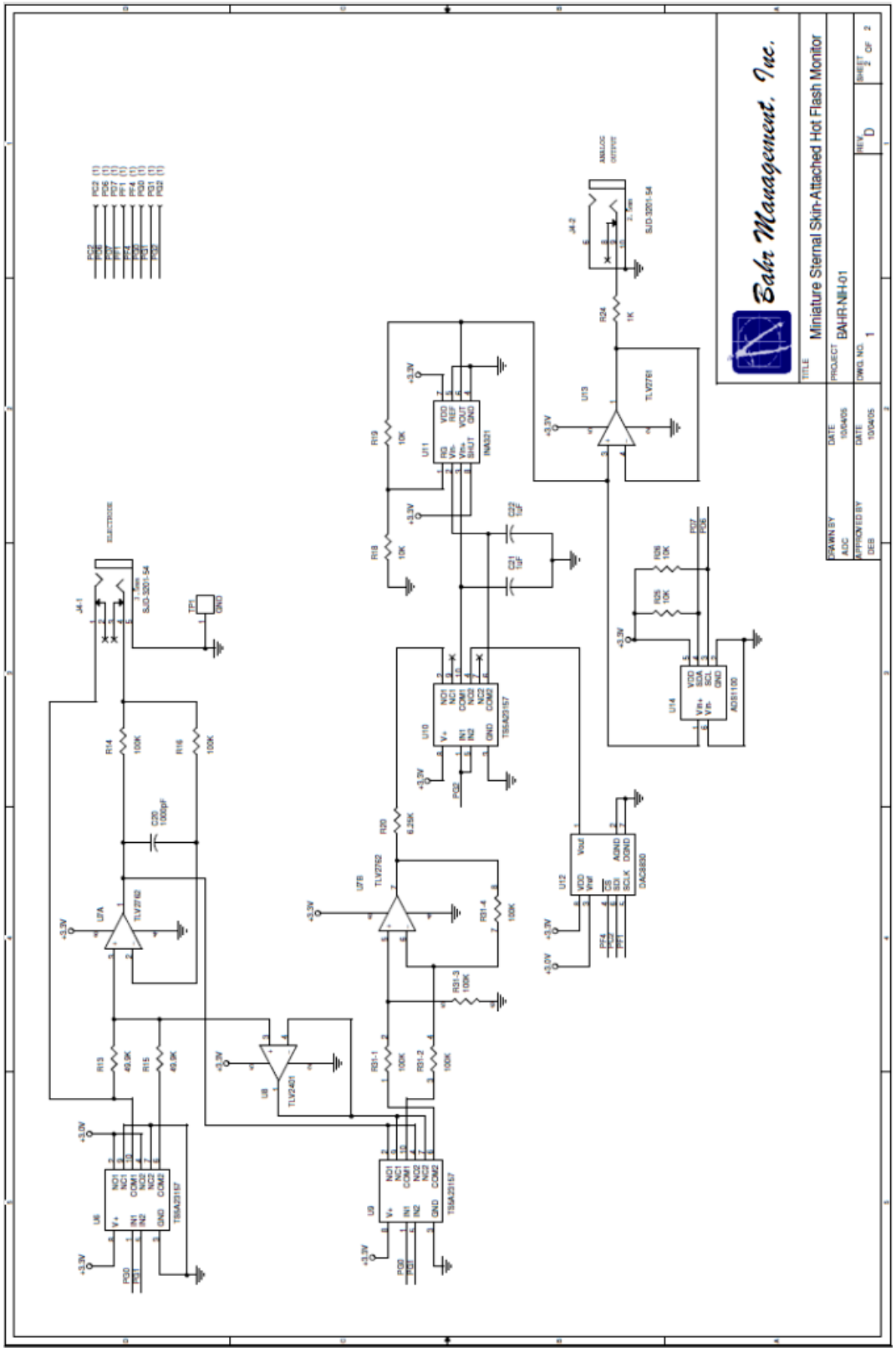

Figure I-2: Schematic of the analog and storage circuitry for the diagnostic grade monitor.

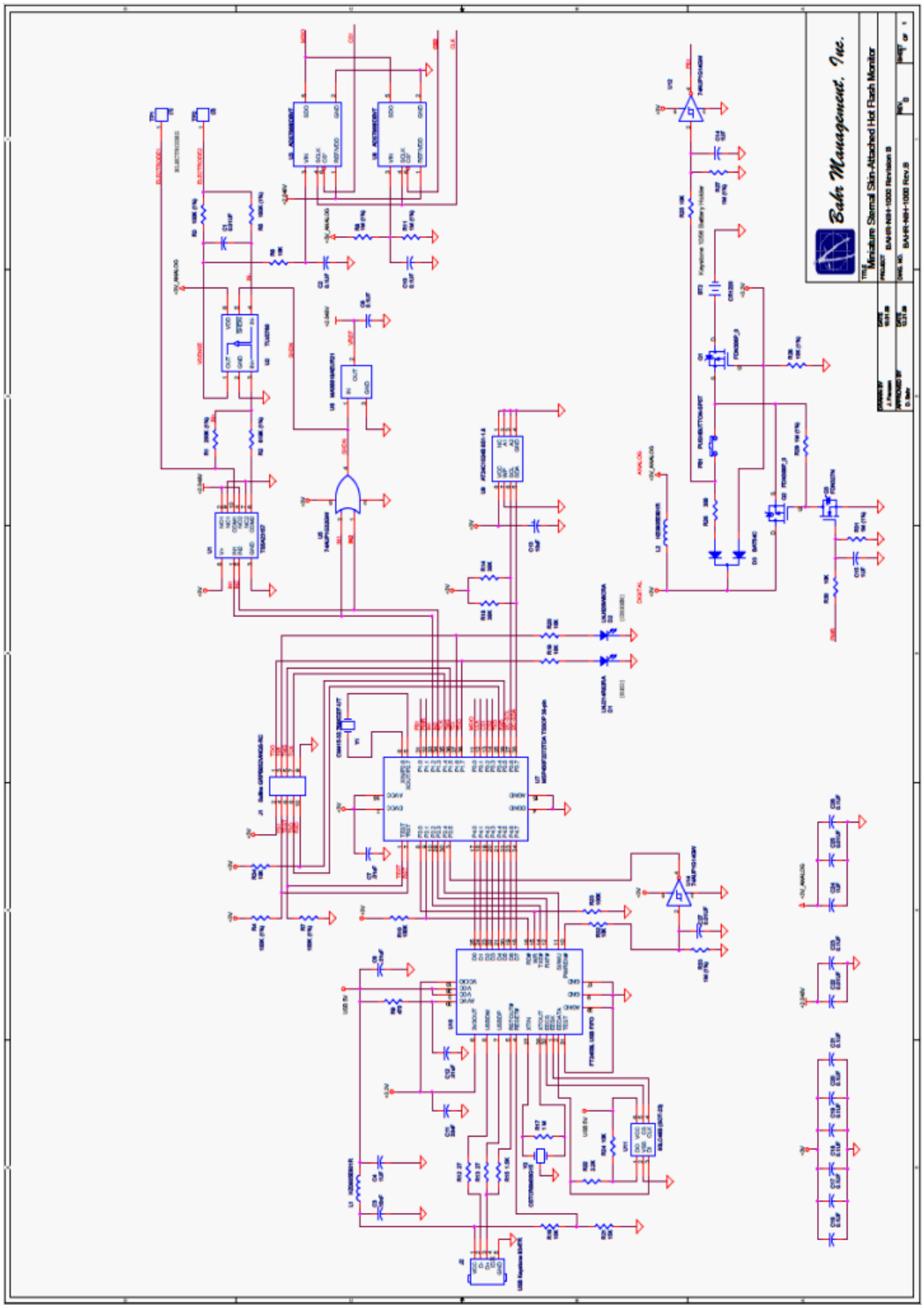

Figure I-3: Schematic of the commercialized hot flash monitor

Appendix II

Participant/Staff Instructions for Wearing the Bahr Hot Flash Monitor

1. Follow the directions on the envelope containing the electrode patch, cleaning the skin with alcohol prior to use. **Do not use body lotion, suntan oil, powder or any other product under or near the area of the patch.** Place the patch on the chest (sternum), centrally, or off to the one side if necessary to be able to cover it up more easily with clothing. Do not wear a strap across the monitor such as a purse strap, a seat belt or side bag strap. It might press on the electrode and cause motion artifacts.

2. Please wear the monitor all the time except when you bathe or shower. Check from time to time to make sure the little green light is flashing (about every 5 seconds). If you want to move the monitor to a different location on the chest remove the monitor from the electrode, peel off the electrode and place a new electrode in the desired position. **Don't try to re-use an electrode once you take it off** - it may not adhere properly again.

3. When you feel a hot flash starting push the button on the monitor firmly to "mark" the time of the hot flash. The small flashing light will flash red a couple of times and then resumes flashing green automatically.

4. Just before you go into the bathroom to bathe or shower, carefully hold down the top and bottom of the hot flash electrode patch against the skin and unsnap the white plastic monitor. Leave the monitor outside the bathroom or shower room so it does not get wet or exposed to moisture. Leave the electrode patch on when you bathe or shower but do not rub or scrub the patch. When drying, blot the electrode patch as dry as possible but do not rub or wipe it. Let the patch air dry thoroughly for at least 5 minutes then snap the monitor firmly back onto the electrode patch. It will automatically resume recording (green light flashing).

5. When re-attaching the monitor you may find it easier to turn the monitor sideways, push on the bottom snap, then twist it upright and push firmly on the top snap. Make sure both snaps are tightly in place.

6. If the patch falls off, starts to peel at the edges, leaks gel or becomes unsightly you can replace it with a new electrode. To avoid irritation to the skin place the new electrode a little higher or lower (or on the other side of the chest) than the original one. You can discard the old electrode. Redness at the sight of the electrode is fairly common but generally disappears within a couple of hours.

7. You may experience a little itchiness at the site of the patch for the first day or two but this generally disappears.

Appendix III

FLASH Monitor Evaluation Studies II

(FLAMES II)

Clinical Trial Protocol

TABLE OF CONTENTS

A. Brief Summary

B. Background and Purpose of the Study

C. Study Design Overview

D. Study Participants

E. Ethics

F. Study Visits and Procedures

G. Study Measures

H. Data Management

I. Data Analysis

J. Data and Safety Monitoring

APPENDIX A. The Hot Flash Monitor

APPENDIX B. The Motion logger Actigraph

APPENDIX C. Visit Schedule

A. Brief Summary

In 2005, we received funding from the National Center for Complementary and Alternative Medicine for Small Business Innovation Research (SBIR) to develop and test a prototype miniature hot flash monitor. Working with biomedical engineers at Bahr Management in Wisconsin, the prototype monitor has been developed and is currently being tested at the UCSF Women's Health Clinical Research Center (WHCRC) in women with hot flashes (FLASH Monitor Evaluation Studies: FLAMES, CHR #H5287-27894-02). The monitor is a small device (approximately 3″x 1″x 1/8″) with two short wires attached by two electrodes over the sternum. The monitor can be worn for up to 7 days and characterizes hot flashes by recording the frequency, timing, and amplitude of changes in sternal skin conductance. Hot flashes are detected by custom designed pattern recognition software. The monitor also incorporates an event marker that is triggered by the participant passing a small magnet over the monitor when a hot flash is experienced. The magnet is worn as a ring or embedded in a wristwatch band. The accuracy of the monitor compared to participant self-report (both on a diary and using the event marker) is excellent. (See Appendix A for a technological description of the miniaturized hot flash monitor).

We have been funded by a second SBIR grant to expand the capabilities of the monitor (FLAMES II). The biomedical engineers have expanded the capabilities of the hot flash monitor by adding heart rate monitoring to improve the accuracy of hot flash monitoring and help clinical researchers explore the etiology of hot flashes. The new hot flash/heart rate monitor is about 50% larger than the monitor developed in FLAMES I. The engineers will develop pattern recognition software for changes in heart rate

associated with hot flashes and will provide a lightweight cable that can be used to download data to a personal computer at the Women's Health Clinical Research Center (WHCRC) directly from the hot flash/heart rate monitor. This system will be tested in synchrony with a commercially available wristwatch-type actigraph to record sleep parameters during hot flash monitoring. Participants will be asked to record their hot flashes on a 3 day hot flash diary while wearing the monitor and the actigraph.

Testing of technological components at the UCSF-WHCRC for feasibility and accuracy will be done as the Hot Flash/Heart Rate (HF/HR) monitor is developed by the engineers. Up to 75 peri- or post-menopausal women with hot flashes will be recruited for this cross-sectional study. Data collection for all participants will include demographics, medical history, concomitant medications, menopausal symptoms, body mass index, chest dimensions and participant satisfaction.

B. Background and Purpose of the Study

Two of the major symptoms associated with the menopause transition are hot flashes and trouble sleeping {Nelson, 2005}. Measurement of the frequency and severity of these symptoms has typically relied on self-report by recall over a defined time period or daily reporting on a paper diary. These approaches are inaccurate, because recall is imperfect and women may forget to complete paper diaries in real time, especially when awakened from sleep.

B.1. Changes in Heart Rate

Hot flashes can be detected by measuring the increase in skin conductance that occurs due to sweating. However, it can be difficult to distinguish the sweating that occurs with exercise or emotional stress from that which occurs due to hot flashes. Several

laboratory-based studies have found that heart rate increases at the onset of a hot flash. {Molnar, 1975}{James, 2004}. Engineers will modify the miniature hot flash monitor to record heart rate simultaneously with skin conductance with the goal of using changes in heart rate to contribute to hot flash pattern recognition. We believe that correlating the rate of change and pattern of change in skin conductance due to hot flashes and to activity-induced sweating may provide better discrimination of the two.

B.2. Sleep Symptoms

Sleep symptoms are commonly measured in menopause research using standardized questionnaires including the Pittsburg Sleep Index {Buysse, 1989} and the Insomnia Severity Index {Bastien, 2001}. These scales have been found to be reproducible and valid, but do not allow researchers to correlate sleep disturbance with hot flashes. We propose to test a commercially available wrist-watch actigraph that is synchronized with the miniature HF/HR monitor to provide detailed information on the correlation between hot flashes, heart rate, sleep time and time of awakenings. We will use the Octagonal Motionlogger Sleep Watch 2.0 (catalog no. 26.100 Ambulatory Monitoring, Inc, Appendix B), a small watch-like device that is worn on the wrist for up to seven days. The actigraph contains a piezoelectric linear accelerometer (sensitive to 0.003 *g* and above), a microprocessor, 32K RAM memory, and associated circuitry. The orientation and sensitivity of the accelerometer are optimized for highly effective sleep-wake inference from wrist activity, which has been shown to be reproducible {Blackwell, 2005} and valid compared to polysomnography {Lichstein, 2006}. Actigraphy parameters allow objective, ambulatory measurement of sleep symptoms associated with stages of the menopause transition, and can monitor changes in menopausal sleep symptoms related to treatment. Synchronizing actigraphy with the

miniature HF/HR monitor will allow us to determine if sleep disturbances are temporally associated with hot flashes.

B.3. Self-reported Menopausal Symptoms Recorded on a Diary

Early testing of the prototype hot flash monitor suggests that changes in skin conductance correlate well with self-reported occurrence of hot flashes, although participants appear to under report symptoms, particularly during sleeping hours. Severity of hot flashes is reported on the diary using a Likert scale of 1 – 5, with 1 being the least severe and 5 being the most severe. We will explore the correlation of self-reported severity of the hot flash and measures of sternal skin conductance (amplitude of change in sternal skin conductance, duration of elevation of sternal skin conductance above baseline, rate of increase in sternal skin conductance) and heart rate to identify an objective measure of severity that is valid and accurate. Most ambulatory studies currently use a 7-day self-report hot flash diary (Sloan, 2001). However, participant compliance with diary recording tends to diminish over time and it has been shown that reducing the duration of diary recording leads to greater accuracy {Tincello, 2007}. Participants will be asked to keep a hot flash diary for the first 3 days while wearing the HF/HR monitor, and to focus on describing the intensity of the hot flash on a numerical scale and recording other activities such as exercise and showering.

B.4. Our specific aims are:

To further characterize hot flashes in women by testing the following measures synchronized with sternal skin conductance monitoring:

a. heart rate monitoring technology incorporated into the skin conductance monitor
b. a commercially available wrist watch-type actigraph to monitor sleep patterns
c. a 3 day diary to record occurrence and severity of hot flashes

C. Study Design Overview

The study will be cross-sectional in design. Eligible participants will be generally healthy peri- or postmenopausal women without known cardiac arrhythmias who report experiencing at least 4 hot flashes per day that can occur during the day and/or at night. Up to 25 women will be asked to wear the miniaturized hot flash monitor, updated to include technology to measure and record heart rate, for up to 7 days, to determine feasibility of the new device. Up to 25 more participants will be asked to wear both the miniaturized HF/HR monitor and, during bedtime, the actigraph, for up to 7 days to develop the hot flash/heart rate pattern recognition algorithm for hot flash detection. A third group of up to 25 participants will be asked to wear both the miniaturized HF/HR monitor and during bedtime, the actigraph, for up to 7 days to test the algorithm that is developed.

Participants will be asked to self-report hot flashes in two ways. They will record the occurrence and intensity (on a scale from 1 – 5) of hot flashes for the first three days they wear the monitor by recording in a 3-day diary. They will also mark every hot flash for 7 days by triggering the event marker on the monitor with a magnet worn as a ring or embedded in a wristwatch band. All participants will be provided with a digital wristwatch set to display military time and synchronized with the monitor. They will use the watch to accurately record on the diary the time they feel a hot flash.

ID-coded data from all the devices will be downloaded at the WHCRC and posted to the trial's secure website for viewing by the biomedical engineers and project team. The time and severity of hot flashes recorded by the miniaturized hot flash

monitor, changes in heart rate and sleep patterns will be compared to self-reported hot flash data to determine the feasibility and accuracy of the simultaneous recordings.

D. Study Participants

Participants will be generally healthy females who are peri- or postmenopausal and bothered by hot flashes.

D.1. Inclusion Criteria

- peri- or postmenopausal women
- 4 or more hot flashes per day occurring during the day or night
- able to read and understand English and willing to sign informed consent

D.2. Exclusion Criteria

- known sensitivity to surgical adhesive tape
- have a pacemaker or implanted defibrillator
- report that a physician has diagnosed cardiac arrhythmia
- are planning to travel via plane during the course of wearing the monitor
- use of medications within the past three months that may cause variations in the frequency or severity of hot flashes (hormone therapy, selective estrogen receptor modulators, selective serotonin reuptake inhibitors, gabapentin, clonidine etc.)
- any condition that, in the opinion of the investigator, would interfere with the candidate's ability to complete the study

E. Ethics

E.1. Institutional Review Board

The study protocol, informed consent form, study questionnaires, educational and recruitment materials will be approved by the Committee for Human Research (CHR) at UCSF prior to the start of the study. Protocol amendments generated during the study will also be submitted to the CHR for approval prior to implementation. Copies

of all CHR approval letters will be maintained at the WHCRC in the study files. Any serious adverse events that occur during the trial will be reported to the CHR. The collaborating engineers at Bahr Management will not have access to any individual identifying data.

Before individuals may participate in any study visits, informed consent will be obtained. The consent form explains in lay language the goals of the study, the visits and procedures and the risks and benefits of participating. Any amendment to the protocol during the study that impacts participants will be reflected in a revised consent form that must be approved by the CHR and signed again by the participant.

F. Study Visits and Procedures:

F.1. Recruitment

Participants will be recruited at the University of California, San Francisco using a multi-component UCSF CHR-approved recruitment approach, beginning with an existing list of women interested in research on hot flashes who have consented to be contacted regarding new studies. If necessary, we will expand to community-based media efforts (newspaper notices, radio advertising, brochures in local clinics and businesses, community centers, notices in churches, and direct recruitment from physician and practitioner offices). We will attempt to enroll minority women (especially African-American women who may suffer from hot flashes more commonly than White women) from the extensive ethnic minority population of San Francisco. In previous studies of treatments for hot flashes, we have successfully enrolled about 35% minority women, including about 25% African-American women.

F.2. Screening

Interested women who have provided consent for contact or who contact us will undergo an initial interview by telephone to explain the study further and determine if candidates meet entry criteria and are willing to complete study procedures. If women are uncertain about the number of hot flashes they have, they will be asked to keep track of their episodes for two days and call back if they have 4 or more per day. Up to 75 participants will be recruited to take part in testing one or more of the following phases:

- heart rate/hot flash monitoring for feasibility
- actigraphy and hot flash/heart rate monitoring to develop a pattern recognition algorithm
- actigraphy and hot flash/heart rate monitoring to test the pattern recognition algorithm

Women will be allowed to participate in all testing stages if they wish since no treatment intervention is involved.

F.3. Clinic Visits (see Appendix C for Visit Schedule)

F.3.1 Baseline Visit

Eligible candidates will be scheduled for a Baseline Visit. At this time, all study procedures, risks and potential benefits will be explained and the candidate will be given adequate time to read the "FLAMES II" informed consent document and ask questions. The consent form will indicate which device/s the participant will be asked to wear and what the specific procedures are. Once the consent has been signed and witnessed, the participant will be given a copy of the signed consent and the original will be a part of the research record. All data will be stored confidentially following

HIPPA rules. The participant will complete baseline questionnaires regarding demographics, basic health habits, concurrent medications, menopause status and menopausal symptoms. Height, weight and chest dimensions will be recorded. Participants will be asked to wear the hot flash monitor continuously but to remove the monitor and actigraph during bathing, showering, swimming or other activities that may soak the devices. After bathing or showering, they will pat dry the electrode patches and surrounding areas and re-attach the monitor as soon as possible. Electrodes should be replaced at any time they fall off or begin to detach from the skin at the edges.

F.3.1.1 Testing the Hot Flash/Heart Rate Monitor for Feasibility

After completing the FLAMES II informed consent and study questionnaires, the participant will be provided the following items:

1. the miniature hot flash monitor which includes heart rate monitoring technology, attached to a single patch containing 2 electrodes placed centrally on the sternum and to a third electrode (single patch) placed beneath the heart, under the left breast
2. a digital watch displaying military time
3. a magnet worn as a ring or embedded in a wristwatch band
4. a 3-day hot flash diary
5. extra electrode patches

The study coordinator will synchronize the time on the monitor with the computer and with the digital watch. She will turn the monitor on and attach it to the participant's chest. The participant will be asked to wear the monitor and to pass the magnet close to the monitor to trigger the event marker whenever she feels a hot flash. She will be asked to record the occurrence and severity of each hot flash she feels on a hot flash diary for the first three days that she wears the monitor, using the digital watch to enter time.

She will begin the diary at midnight the day she leaves the clinic and stop recording at midnight three days later.

The participant will wear the monitor and mark her hot flashes with the magnet continuously until her next clinic visit in approximately 7 days. She will be asked to replace the electrode patches any time they fall off or begin to lift at the edges. The study coordinator will demonstrate all procedures.

Heart rate will also be documented by clinic staff during the visit by measuring the participant's radial pulse. The participant will be seated and asked to rest for 5 minutes. The nurse will observe the digital watch and note the time she starts counting the pulse. The pulse will be measured for 1 minute. Then the participant will be asked to walk briskly down a hall and back. The pulse rate will be counted again for one minute and the nurse will record the time she begins counting using the participant's digital watch as a reference. Before the participant leaves the clinic, an appointment will be made for a return clinic visit up to 7 days later.

F.3.1.2. Testing Actigraphy and the Hot Flash/Heart Rate Monitor

After completing the FLAMES II informed consent and study questionnaires, the participant will be provided the following items:

1. the miniature HF/HR monitor and electrodes
2. a digital watch
3. a wristwatch-type actigraph that will record sleep patterns
4. a Sleep Log to record the time of going to bed and the time of arising
5. a magnet worn as a ring or embedded in a wristwatch band
6. a 3-day hot flash diary
7. extra electrode patches

The study coordinator will synchronize the time on the monitor with the computer and with the digital watch. She will turn the monitor on and attach it to the participant's chest. The participant will be asked to wear the monitor continuously and to pass the magnet close to the monitor whenever she feels a hot flash to trigger the event marker in the monitor. She will be asked to wear the actigraph from the time she goes to bed until the time she arises. She will be asked to record daily in a Sleep Log the time she went to bed and the time she woke up and to record the occurrence and severity of each hot flash she feels on a hot flash diary for the first three days that she wears the monitor, using the digital watch to enter time. She will begin the diary at midnight the day she leaves the clinic and stop recording at midnight three days later. She will be asked to remove the monitor during bathing or showering to avoid getting it wet, and to record in the log until her next clinic visit, approximately 7 days later. She will be asked to replace the electrode patches any time they fall off or begin to lift at the edges. The

study coordinator will demonstrate all procedures.

Heart rate will also be documented by professional clinic staff during the visit by measuring the participant's radial pulse. The participant will be seated and asked to rest for 5 minutes. The nurse will observe the digital watch and note the time she starts counting the pulse. The pulse will be measured for 1 minute. Then the participant will be asked to walk briskly down the hall and back. The pulse rate will be counted again for one minute and the nurse will record the time she begins counting using the participant's digital watch as a reference. Before the participant leaves the clinic, an appointment will be made for a return clinic visit up to 7 days later.

F.3.2 Final Visit

The participant will return to the clinic up to 7 days after her baseline visit. All devices will be collected and the electrode patches she is wearing will be removed. The study coordinator will assess the skin at the site of the patches. The participant will be asked to complete satisfaction questionnaires to describe her experience with the devices she has used. She will also be invited to provide comments about any other study procedures. Any severe adverse events will be documented and will be reported immediately to the Data and Safety Monitor, to the sponsor and to the UCSF-Committee for Human Research.

The study staff will download data identified only by ID# from the monitor and the actigraph to a secure desktop computer for analysis.

G. Study Measures

G.1 Anthropometric measurements

Weight will be recorded in kilograms using a calibrated scale. Participants will be measured in light clothing (without shoes) to the nearest 0.5 kg. Standing height, which is measured at the Screening Visit, will be measured in millimeters with a wall-mounted Harpenden Stadiometer. Body mass index will be calculated from body weight and height as weight in kg divided by the square of height in meters. Since adherence or conductivity of the electrode patch may be affected by the anatomy of the sternum, chest dimensions will be recorded as self-reported bra size.

G.2 Menopausal Symptoms

The brief Menopausal Symptom Questionnaire ascertains information on the bothersomeness of typical symptoms experienced by menopausal women such as hot flashes, breast tenderness, vaginal dryness and discharge, and trouble sleeping. This questionnaire has been used and validated in multiple major trials including the Postmenopausal Estrogen-Progestin Interventions trial, the Heart and Estrogen/progestin Replacement Study and the Women's Health Initiative randomized trials. Each symptom is rated on a 5-point Likert scale ranked 0 (not bothersome) to 4 (very bothersome).

G.3 Hot Flash Diary

Hot flash includes hot flash episodes or night sweats classified by severity (on a scale of 1 to 5, with 1 being the least severe and 5 being the most severe) along with time of occurrence. Simple written instructions and a sample of a completed diary will be given

to participants. Study staff will review instructions for completion of the diary with the participant to ensure proper understanding. Participants will also be asked to record activity that may cause sweating such as exercise or yard and house work. Diaries will be provided to the participant at the Baseline Visit and participants will be asked to bring the completed diary with them to the Final Visit. The clinic staff will review diary entries for completeness, summarize the information and the summary data will be entered into the database.

G.4 Sleep Patterns

The commercially available Octagonal Motionlogger Sleep Watch 2.0 (catalog no. 26.100 Ambulatory Monitoring, Inc) is a small watch-like device, also called an actigraph, worn on the wrist for up to seven days. The actigraph contains a piezoelectric linear accelerometer (sensitive to 0.003 *g* and above), a microprocessor, 32K RAM memory, and associated circuitry. The orientation and sensitivity of the accelerometer are optimized for highly effective sleep-wake inference from wrist activity, which has been shown to be reproducible {Blackwell, 2005} and valid compared to polysomnography {Lichstein, 2006}. The output from the actigraph supplies information about percent of time in bed asleep and percent of time awake, number and timing of awakenings per night and length of awakenings at night. Data collection requires the participant to keep a simple Sleep Log that notes when they go to bed at night and when they arise. Participants will put the actigraph on before they go to bed and take it off when they arise.

G.5 Other Measurements

Variables that may be associated with the frequency or severity of hot flashes will be measured. These include demographic characteristics, health habits, general health,

menopause status, and medication use. We will also assess participant satisfaction with the monitor and tolerance of the electrodes.

H. Data Management

H.1 Data Collection

Data will be collected on machine-readable data forms using Cardiff Teleform software. Data forms identified by ID# and acrostic will be filled out at the clinical site and sent to a database managed by the San Francisco Coordinating Center (CC) via standard fax machines. The clinical site retains hard copies of the data forms. At the CC, the forms will be received on a secure server that will use optical character reader (OCR) technology to acquire the data. A CC operator will verify the data manually on screen. This important step corrects many misinterpretations in the automated data input. Verified data are then sent over the local area network (LAN) at the CC to a database on a secure Microsoft SQL Server. Analog images of the forms are stored in an image-management system on optical disk. The CC does not receive any paper in the process of data acquisition.

H.2 Data Processing

A password-protected website has been established for the original development phase of the hot flash monitor and this will be the study's data collection hub. The CC will provide user accounts and security-enabled web browsers for the clinical center staff, the biomedical engineers and the study project team to access data displays, study documents and printable teleforms.

The study data are subject to a set of daily error-checking programs. This routine includes checks for completeness, data consistency, and invalid ranges. The results are

posted to the study website where clinical site personnel check daily to confirm that the CC has received all of the faxed forms and to address any queries. The clinical staff responds to queries and edits data forms on the website producing a permanent and irrevocable electronic audit trail. As part of the data editing system, the website includes pages that closely resemble the questionnaires so that clinical staff can view the data that have been accepted into the data system. The web server provides continually updated routine and customized data summary reports.

I. Data Analysis

I.1 Heart Rate

The heart rate monitor will be incorporated into the miniature hot flash monitor and will continuously record heart rate for up to 7 days. Heart rate variability will be calculated by a predetermined algorithm. We will examine the correlation between heart rate, heart rate variability and the presence and severity of the hot flash detected by the hot flash monitor.

I.2. Actigraphy

The Motionlogger Sleep Watch 2.0 uses a piezoelectric linear accelerometer (sensitive to 0.003 *g*) to distinguish sleep from wakefulness based on activity of the wrist. The actigraph records data including percent of time in bed asleep and awake, number and timing of awakenings per night and length of awakenings at night. The device does not detect stage of sleep. The Motionlogger has been shown to be reproducible {Blackwell, 2005} and valid compared to polysomnography {Lichstein, 2006 #22}. Thus, we do not plan to repeat tests of reproducibility and accuracy, but will ensure that it is feasible to

use the device as part of our total system, and that the Motionlogger can be properly synchronized to the HF/HR monitor.

J. Data and Safety Monitoring

The progress of this study and participant safety will be evaluated by an independent Data and Safety Monitor, Dr. Andrew Avins, Senior Researcher at Kaiser Permanente of Northern California, who is the Data Safety Monitor for our currently funded testing of the miniature hot flash monitor (FLAMES I). Dr. Avins is a clinical researcher with experience in study design, research ethics and statistics. He will periodically review the timeline, conduct and outcomes of the study and provide feedback to the NIH and study investigators on the overall performance of the study with particular attention to protecting the safety of participants. Dr. Avins is entirely independent of the institutions and investigators participating in the study, has no financial ties to the outcome of the study and no financial ties to other companies developing medical devices.

Appendix A: The Hot Flash Monitor

Technical electronic design:

We present our most recently developed prototype electronic design. Because miniaturization of electronics is proceeding at a rapid pace, we will thoroughly review the latest devices available to ensure an optimal miniature, low-power design.

Theory of operation:

1. Fig. 1 shows a simplified device. It is actuated with a magnet pulse and/or input/output data ports. After startup, additional magnetic inputs are counted as user subjective input of hot flash times.

2. The crystal time base starts and the number of seconds since activation is stored in a register.

3. At intervals of 10 seconds a measurement sequence begins.

4. P_0 and P_1 are set to V_{BATT} and ground respectively. Divider R_2/R_3 derives an electrode bias voltage of 0.5 V.

5. The op amp establishes a virtual drive voltage with skin electrode current provided by R_1. The current is measured with the A/D. R_F/C_F may be needed to store enough charge for the A/D sampling capacitance.

6. P_0 and P_1 are reversed and step 5 repeated for the identical reverse polarity.

7. A/D comments: For $P_0 = V_{BATT}$, $P_1 = 0$ V. With no skin contact current the A/D baseline is $V_{BATT}(R_3)/(R_2 + R_3)$ or for example 0.5 V = 2.85 V(1)/(1 + 4.7). Then R_3 = 1 MΩ. R_2 = 4.7 MΩ. With skin contact R_1 will experience a skin current of 0.5 V + (0.5 V)$(R_1)/(R_{E1} + R_T + R_{E2})$ which is presented to the A/D. R_1 needs to be selected for the best use of the A/D

range during the device operating life. This range is 2.85 – 0.5 = 2.35 V or 2.35/2.85 = 82% of the available A/D range. For P_0 = 0 V, $P_1 = V_{BATT}$ current is reversed in the electrodes and the A/D range is V_{BATT} – 0.5 V down to 0 V. Maximum skin current is limited by R_1. For example for R_1 = 250 kΩ and 1 cm2 electrodes, maximum current will be (2.85 V – 0.5 V)/250 kΩ or 9.4 μA/cm2.

8. Port P_2 provides ~2 mA to light an LED to acknowledge user magnetic input.

9. For data download the device will be placed in a cradle providing for I/O pin alignment with PCB I/O pads P_{3-5}.

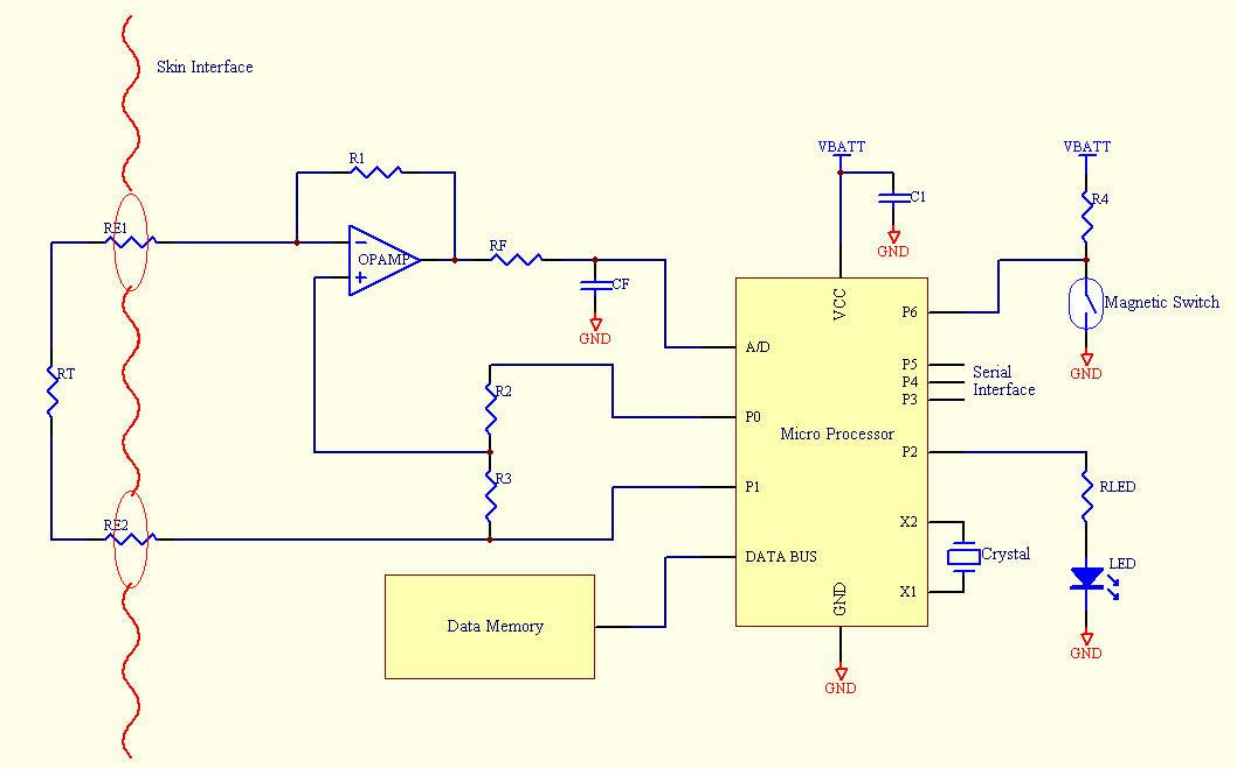

Fig. 1. Microprocessor provides current to tissue R_T through electrodes on the skin.

Suitable microprocessor choices could come from the TI MPS 430 family. An average current requirement for the entire circuit is less than 5 μA, so a small coin cell can provide power for many months of use. For data memory a separate chip may be

needed. For example Microchip offers the 24AA512 64K (8-bit word) low-voltage EEPROM with I2C serial interface. I2C to PC serial adaptors are readily available for download of data to a PC file.

We have developed software for measuring, storing, processing, and displaying the data. See Fig. 2. We display skin conductance changes as absolute changes and also as relative changes. Software will provide hot flash conductance changes, hot flash duration, and the product of conductance change and duration.

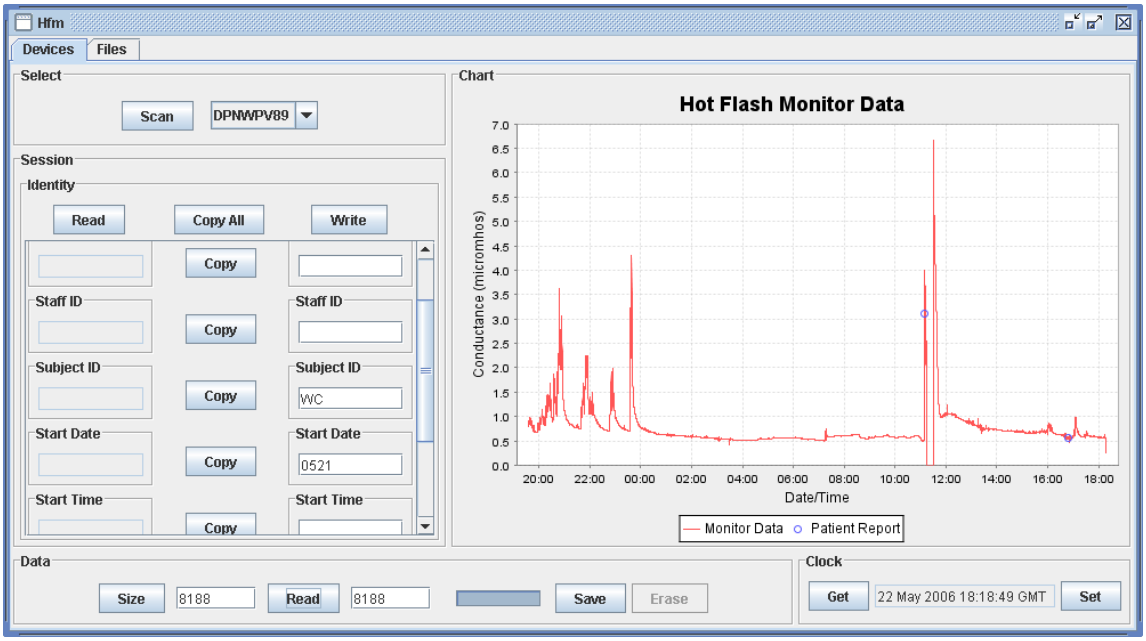

Fig. 2. Desktop computer software scans the monitor serial number, provides file labeling, downloads the data, saves them, displays them, erases the memory, and sets the clock. At the end of a 7-day test shown here, the conductive adhesive gel gives results as good as for day 2 of the same electrode (Shown below in Fig. 5 right).

Electrode gel development and testing

Our philosophy is that if we use an excellent sensor, then we will be able to use signal processing software to yield optimal results. If the sensor is poor, no signal processing software can correct the problem. Thus we have performed extensive testing on electrodes.

We tested ECG electrodes, but they do not work because they are designed to make good skin contact. Their approximately 4% salt content diffuses into the skin and deliberately increases the conductance. Then when the hot flash opens the sweat ducts, the incremental parallel added conductance is a small fraction of the total and is unnoticeable. We tested the cream recommended by BIOLOG and found that it yielded poor and erratic results. (Fig. 5 left). We used Medi-Trace silver/silver chloride electrodes (S'offset; Graphic Controls, Buffalo, NY). Electrodes were 1.5 cm in diameter and filled with 0.05 M potassium chloride Velvachol/glycol gel (Carpenter, 2005).

We tested conductive adhesive gels and found they yield excellent results. (Fig. 3 right). We tested these same electrodes for 7 days and got the same excellent results on day 7 (Fig. 4) as we did on day 2 (Fig. 3 right). We have tested electrodes with various tacks to ensure that the electrodes make good contact for several days, yet do not cause skin irritation when removed. We tested backing materials that breathe so that that sweat does not accumulate in the solid gel. We have tested vinyl backing materials that do not breathe to prevent shower or bath water from entering and accumulating within the solid gel.

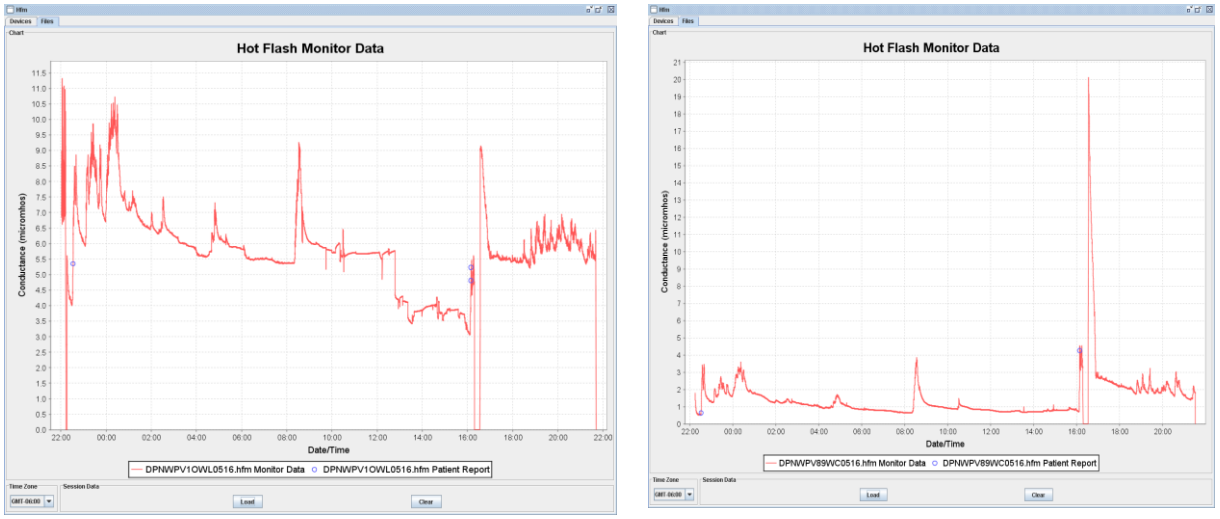

Fig. 3. Side-by-side comparison of two electrodes worn by the same subject at the same time. Left: Biolog cream causes about 6 micromho (μS) baseline conductance. Sweating caused by exercise (marked by circles) causes about 30% change. Right: Conductive adhesive gel causes about 0.8 μS baseline conductance and has less motion artifact. Sweat caused by exercise causes 400% change. During shower, the recorder was detached (0 μS). After shower, electrode was wet, recording about 20 μS and recovering in about 1 h.

Appendix B: The Motionlogger Actigraph

The UCSF Coordinating Center has used the Motionlogger Sleep Watch 2.0 actigraph. The Sleep Watch to collect sleep parameters several multicenter studies in community dwelling elderly, demented elderly {Blackwell, 2006}, and is currently using the device in a multicenter trial of a Chinese herbal preparation for treatment of hot flashes. Coordinating Center staff, including Drs. Katie Stone and Terri Blackwell, have conducted many of the studies of the reproducibility and validity of actigraph sleep measures {Blackwell, 2005; Lichstein, 2006 #22} and have scored over 6,000 actigraphy files during more than 5 years of experience.

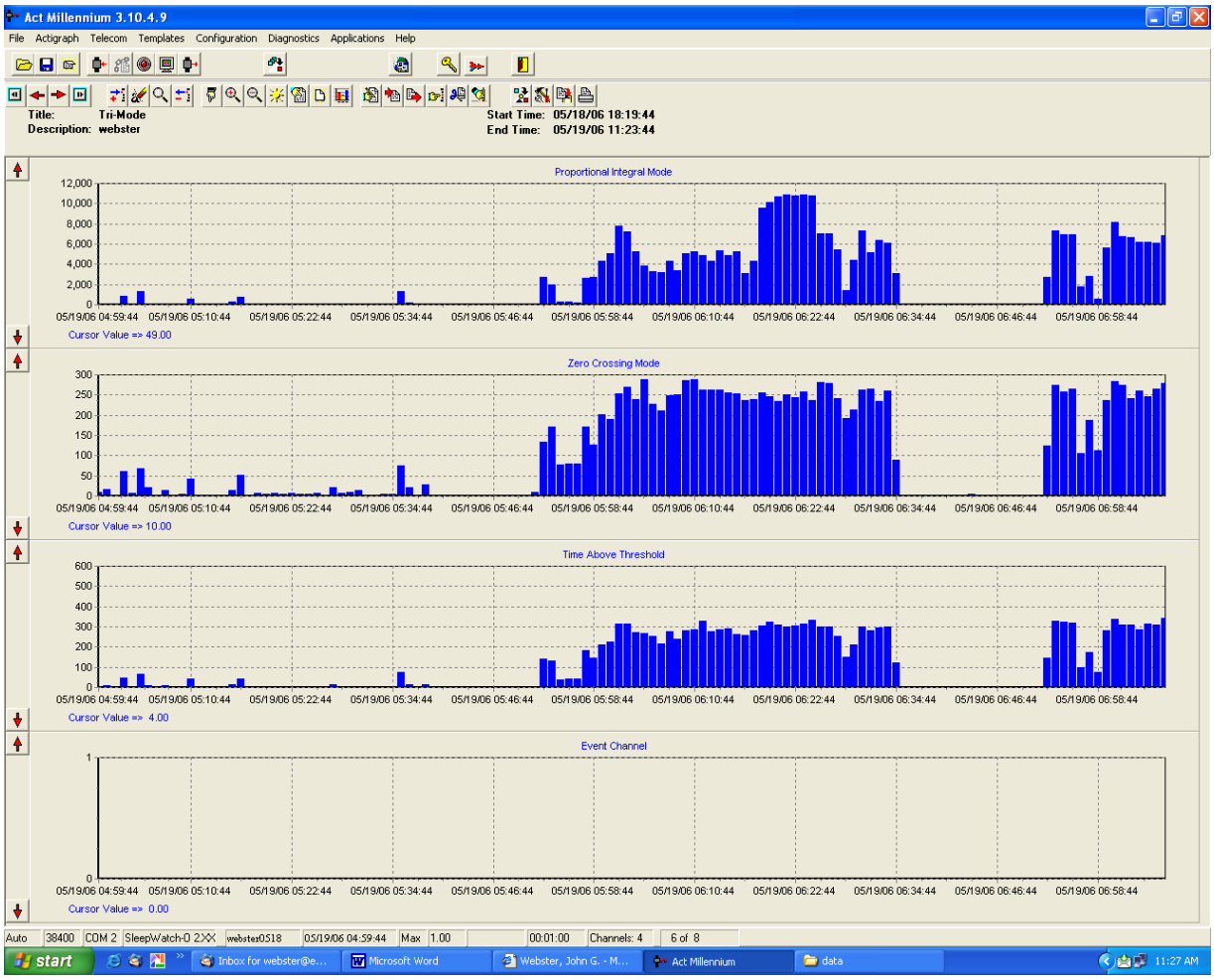

Fig 4. Desktop computer actigraphy data show low motion during sleep, followed by higher activity after awakening, zero activity when the actigraph was removed during showering, followed by higher daily activity.

Appendix C: Visit Schedule

Form/Procedure	**Baseline Testing Hot Flash and Heart Rate Monitor**	**Baseline Testing Including Actigraph**	**Final Visit**
Telephone Eligibility Screening Form (Prior to all visits)			
Detailed description of Study/Informed Consent	X	X	
Collect Contact Information	X	X	
Demographics	X	X	
Basic Health & Menopause Status Questionnaire	X	X	
Menopausal Symptoms Questionnaire	X	X	
Anthropometric measures: Height, Weight, Chest	X	X	
Concurrent Medications	X	X	

Inclusion/Exclusion	X	X	
Attach Hot Flash/Heart Rate Monitor	X	X	
Give extra supply of electrodes	X	X	
Provide magnet/event marker	X	X	
Provide 3-day hot flash diary	X	X	
Provide Motionlogger actigraph		X	
Provide Sleep Log		X	
Review Diary and Sleep Log			X
Participant Satisfaction Questionnaires			X
Skin Site Assessment			X
Serious Adverse Events (Probe/Document)			X

Appendix IV

UCSF COMMITTEE ON HUMAN RESEARCH October 13, 2005
APPLICATION SUPPLEMENT

NON-SIGNIFICANT RISK DETERMINATION
FOR AN INVESTIGATIONAL DEVICE

Principal Investigator of CHR Application:	CHR # (if issued):
Deborah Grady, MD, MPH	05027894
Study Title (may not exceed 500 characters):	
Evaluation of a Miniature Ambulatory (Hot Flash) Monitor (E-MAM)	

Complete and attach this appendix to your CHR application if

- you are using an investigational device which does not have an Investigational Device Exemption (IDE) number, and
- you believe the use of investigational device in this study poses non-significant risk.

A Significant Risk device is one that presents potential for serious risk to the health, safety, or welfare of a subject and the device (1) is intended an implant; (2) is used in supporting or sustaining human life; (3) is of substantial importance in diagnosing, curing, mitigating or treating disease, or prevents impairment of human health; or (4) otherwise presents a potential for serious risk to the health, safety, or welfare of a subject. A non-significant risk (NSR) device is one that does not pose significant risk. For more information see Guidance On Significant And Non-Significant Risk Device .

In the space below, please explain why the use of the device in this study poses non-significant risk, and attach any other supporting information (e.g., any reports of prior investigations). Please also explain whether the FDA or any other IRB has determined the device to be significant or non-significant risk.

We believe this monitor poses no significant risk to humans.

Co- principal Investigator Dr. John Webster searched the FDA site http://www.fda.gov/cdrh/d861.html and reports that the closest NSR devices are:

- Functional Electrical Neuromuscular Stimulators
- Transcutaneous Electric Nerve Stimulation (TENS) Devices for treatment of pain
- Nonimplantable Electrical Incontinence Devices

Dr. Webster also searched the UCSF-CHR web link at http://www.research.ucsf.edu/chr/Guide/chr12D_FDA.asp#Decision. Transcutaneous Electric Nerve Stimulation (TENS) Devices for treatment of pain were the most similar devices listed as having no significant risk (NSR).

All these NSR devices involve electrodes placed on the skin and use electric currents so large that the wearer is aware of the electric current. In contrast, our hot flash monitor, like the FDA-approved Biolog monitor, will use electric currents so small that there is no perception of electric current. The amount of electricity produced by both monitors is similar, below the level that can be sensed, and has no known risks.

The miniature monitor patch and the Biolog electrodes may cause skin rash or discomfort due to the adhesive. Irritation or allergic reactions to the miniature monitor and BIOLOG electrodes will be carefully evaluated objectively by the clinic nurse as well as subjectively by participant questionnaire. The Biolog monitor has been used in studies at UCSF for a total of 57 twenty-four hour periods to date, with 3 mild adverse skin reactions reported so far. None of the skin reactions caused the participant to remove the electrodes.

Dr. Webster routinely uses commercially available electrocardiographic (ECG) electrodes in teaching laboratories in his courses. As part of his course work he has varied salt concentrations in the electrodes to learn how they change skin resistance. There has been no skin irritation or other adverse events reported, nor observed.

Ordinary ECG electrodes supplied by electrode companies are made several different ways:

1. A small piece of kitchen sponge filled with 4% conductive gel.
2. A more solid hydrogel soaked in 4% saline. The conductive hydrogel inside the electrode is made of gelatin and Polyethylene Glycol (PEG). PEG is used for various skin treatments such as wound healing and surface skin medical coatings and is FDA approved.
3. Conductive adhesive polymer
4. A cup-shaped electrode filled with gel (used with the Biolog monitor)

We will use electrodes similar to those sold commercially, but will likely use a more dilute electrolyte, for example, 0.1% NaCl (approximating sweat) instead of the more concentrated 4% NaCl used by ECG electrode manufacturers. This will reduce the lowering of skin resistance to make the hot flash more detectable and should make the electrode even less irritating.

There have been no communications with the FDA about this monitor, since it is non-invasive and uses less current than other NSR devices. A study independent of our study was submitted to the IRB at the University of Wisconsin for approval. It deals only with research on the change in skin resistance for variation of salt concentration in the electrode gel, does not use a continuous monitor, and is still in the review queue.

The technology of the patch electrode is not new. What is most innovative about this monitor is the data processing software being developed to store and download data post-testing to a PC.

COMMITTEE ON HUMAN RESEARCH
OFFICE OF RESEARCH, Box 0962
UNIVERSITY OF CALIFORNIA, SAN FRANCISCO
www.research.ucsf.edu/chr/Apply/chrApprovalCond.asp
chr@ucsf.edu
(415) 476-1814

CHR APPROVAL LETTER

TO: Deborah G. Grady, M.D., M.P.H.
Box 1793

RE: FLAMES: Flash Monitor Evaluation Studies

The Committee on Human Research (CHR) has reviewed and approved this application to involve humans as research subjects. This included a review of all documents attached to the original copy of this letter.

Specifically, the review included but was not limited to the following documents:
Consent Form, Dated 6/2008

The CHR is the Institutional Review Board (IRB) for UCSF and its affiliates. UCSF holds Office of Human Research Protections Federalwide Assurance number FWA00000068. See the CHR website for a list of other applicable FWA's.

APPROVAL NUMBER: H5287-27894-04. This number is a UCSF CHR number and should be used on all correspondence, consent forms and patient charts as appropriate.

APPROVAL DATE: June 24, 2008 **EXPIRATION DATE:** July 17, 2009 **Full Committee Review**

GENERAL CONDITIONS OF APPROVAL: Please refer to www.research.ucsf.edu/chr/Apply/chrApprovalCond.asp for a description of the general conditions of CHR approval. In particular, the study must be renewed by the expiration date if work is to continue. Also, prior CHR approval is required before implementing any changes in the consent documents or any changes in the protocol unless those changes are required urgently for the safety of the subjects.

HIPAA "Privacy Rule" (45CFR164): This study does not involve access to, or creation or disclosure of Protected Health Information (PHI).

Sincerely,

Emily K. Bergsland, M.D.
Acting Chair, Committee on Human Research

cc: Judith Macer, Box 1793

Appendix V

Instructions for Expert Rating of Hot Flashes from the Development Set

6-17-10

To download the file go to https://filestogo.com/loginS.htm

Log in as follows:
Log in : Hotflash
Password : HFM001

1. Select "Download" from the menu bar at the top of the page.
2. Select one of the two files shown there and download it:

   HFM_Expert_PC_Full_pkg.exe

   HFM_Expert_PC_pkg.exe

3. The large file (Expert_PC_Full) is a single self extracting file and contains the MatLab program, the MatLab Compiler Runtime software, and the data. The smaller file contains the program and the data in a separate folder. To use the program copy it to folder and open it. The file will unpack everything, install the run time compiler, and expose the run time executable. If you are asked questions in a DOS window just answer with the letter 'A'.

4. When the download is complete and the software has been unpacked open the runtime executable with the extension exe. Make sure that the exe file and the hfm data are in the same folder. The easiest thing to do is to copy the exe file into the data sub-folder. The two files HFM_Expert_PC_Full.exe and HFM_Expert_PC.exe are the same file with different names. You can use either one of the two files to process the data.

5. After a few seconds a black screen will appear. Wait for a box to open that will ask for a key. Type in your initials or first or last name. Use this same key every time you open the file in the future. This key is used by the program to label the tag files that are produced when you mark the data.

6. The next box will display a list of individual participant data files. Start with H3001. Click on the file and once the graphic user interface opens you should be ready to go. Be patient as the main window may take some time to open.

7. Use the left and right arrow keys to move through the data. The vertical scale is automatic, but can be set to self scale by using the **S** key on the keyboard. When set to self scale you can use the up and down arrow keys to expand or contract the data vertically. To go back to automatic type the **A** key. To mark a HF use the left mouse button and to delete the mark use the right mouse button. To quit simply type a **Q**. You can type a **W** at any time to write the HFs that you have marked without exiting the program. To exit the program and discard all of the changes that you have made for the current participant just press an **E**.

8. A black diamond or square indicates where the participant marked a hot flash. A ledged on the bottom of the screen describes which is which. These symbols are always located on the zero line.

9. To mark a HF use the left mouse button. This will produce a red circle. To delete the circle (if you change your mind) right click on top of the circle. You will notice at the top of the GUI a description of the color of the small circles for the expert marked HFs. The default is red. The colors that are available are **R**-red, **C**-cyan, **B**-blue, **M**-magenta, **G**-green, and **K**-black. Type the key corresponding to the color you want to use next. John and I looked at the colors and we thought that using red for a true HF (classic HF and marked by participant), and black (marked by participant but not a classic HF) was a good color combination.

10. The files can be opened and closed as many times as you wish. Any marked data will be automatically updated. When you are done marking the data send Dennis all the tagged files.

Appendix VI

Rules for Marking Hot Flashes

1. The purpose of the expert markers is to identify a "real" or "classic" hot flash.
2. Look at each hot flash that the woman marked by diary or monitor (black diamonds or black triangles).
3. If you agree it is definitely a hot flash position the cursor half way up the upslope and then use your mouse to place a red circle on the data.
4. If you're unsure or it isn't a "classic" mark that with a black circle and then move to the next hot flash.
5. To leave the program (quit) simply type a **Q**. The file will be saved with your initials at the end of it.
6. Re-open the HFM Expert file to get another participant data display.

Definition of a Classic Hot Flash

- A quick increase in slope, reaching a peak within 30 - 60 seconds and with almost a 90° slope
- After the data reaches its peak, the slope returns to within about 10% of baseline after about 10 minutes.
- Height or amplitude of peak, is not as important as the degree of upward slope
- The width of the peak at about the halfway point will be about 4 – 5 minutes wide (1 inch = 60 minutes)

Tracings uncharacteristic of hot flashes

- Tracings that are flat that do not show at least a 2 µSiemens change in skin conductance
- Curves that do not return to baseline within 10 minutes of an initial steep increase in skin conductance
- Tracings that have a gradual or shallow slope to the peak.

Appendix VII

Hot Flash Data Storage

November 2006

Version #1

Data as stored on the Monitor and sent to the PC – 17 bytes

	Time		SR Flag	HF Data	
Bytes	9	b	1	5	b

Version #2

Data as stored on the Monitor – 16 bits

	SR Flag	HF Data
Bits	1	12

Time is implicit since the data is stored every 10 seconds

Formatted ASCII data sent to the PC – 32 bytes

	Time		HF Data		HR Data		SD		SR Flag	EOL	NL
Bytes	9	b	5	b	5	b	5	b	1	1	2
Byte	(0)	(9)	(10)	(15)	(16)	(21)	(22)	(27)	(28)	(29)	(30)

Where b represents a blank or 0x20, EOL = 0x13, and NL = 0x13, 0x10

Time – Time is seconds since 1970 / 10 starts at Jan 1, 2006

Hot Flash – HF is stored as 12 bits where the range is 0 to 40.95 uSiemens

Heart Rate – HR is stored as 15 bits where the resolution is 1ms representing a range from 20.0 to 180.0 beats per minute stored in 1ms increments. The rates are averaged over the 10-second interval.

SD – Standard deviation of HR data during last 10 sec where the range is 0.0 – 99.9.

SR Flag – Self-Report Flag HR Flag – Heart Rate Flag

EOL – End of Line NULL NL – New Line CRLF

Appendix VIII

Derivation of Sigmoid Derivative Equation 9.3

$$y(z) = \frac{1}{1+e^{-z}}$$

$$y'(z) = \frac{1}{(1+e^{-z})^2} \times \frac{e^{-z}}{1}$$

$$y'(z) = \frac{1}{1+e^{-z}} \times \frac{1}{1+e^{-z}} \times e^{-z}$$

$$y'(z) = \frac{1}{1+e^{-z}} \times \frac{e^{-z}}{1+e^{-z}}$$

$$y'(z) = \frac{1}{1+e^{-z}} \times \frac{1+e^{-z}-1}{1+e^{-z}}$$

$$y'(z) = \frac{1}{1+e^{-z}} \times \left(\frac{1+e^{-z}}{1+e^{-z}} - \frac{1}{1+e^{-z}}\right)$$

$$y'(z) = \frac{1}{1+e^{-z}} \times \left(1 - \frac{1}{1+e^{-z}}\right)$$

$$y'(z) = y(z) \times [1 - y(z)]$$

Appendix IX

Principal Investigator/Program Director: Webster, John Goodwin

BACKGROUND

Hot flashes are common in peri- and postmenopausal women and negatively impact quality of life. The frequency and severity of hot flashes are generally measured by self-report, which may not be complete, especially during sleep. We designed and tested the accuracy of a miniature hot flash monitor that measures changes in skin conductance to automatically detect hot flash frequency in ambulatory women over a 7-day period.

METHODS

We conducted focus groups with clinical researchers, menopausal women with hot flashes, and engineers to determine the optimal characteristics of a miniature ambulatory hot flash monitor. We tested and selected a conductive adhesive polymer electrode that yields baseline skin conductance less than 1 µS, which yields a larger hot flash-to-baseline ratio. (Figure 1).

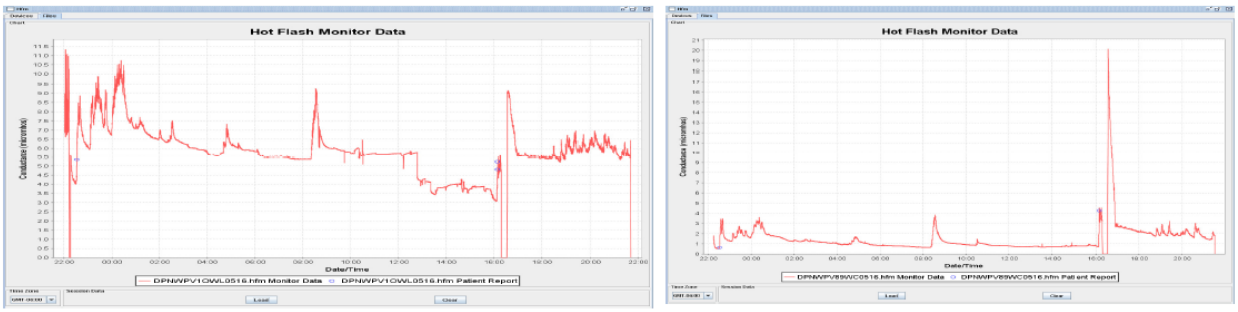

Figure 1: Side-by-side comparison of two types of electrodes worn by the same subject at the same time. Left: Biolog cream produces about 6 µS baseline conductance. Sweating caused by exercise (marked by circles) causes about 30% change. Right: Conductive adhesive gel produces about 0.8 µS baseline conductance and has less motion artifact. Sweat caused by exercise causes 400% change.

A belt-worn prototype recorder was tested on 11 women to optimize the placement of electrodes, adhesion of the electrodes, conductance of the gel, and to minimize effects of the electrodes on the skin. Subsequently, we built a miniature monitor (Figures 2 and 3) and developed pattern recognition software to automatically detect hot flashes compared to self-report by a diary or by an event marker built into the monitor that is triggered by a magnetic ring, (Figures 4, 5 and 6). We developed and optimized the pattern recognition software using data from 20 women. Participants were healthy peri- and postmenopausal women aged 45-60 with 2 or more hot flashes per day by self-report.

Participants could not have had a menstrual period in the past 6 months and had no known allergy to adhesive or tape. There were no restrictions on medications but women with pacemakers or implantable defibrillators were not included. Participants agreed not to travel by airplane during the study. Women attended a clinic visit then wore the monitor continuously for 7 days, except for bathing or showering, and replaced electrodes whenever they became loose or dirty. They recorded all hot flashes on a diary for only the first 3 monitoring days, since our experience and that of others [1,2] indicated that adherence with keeping the diary and the accuracy of self-recording decreases after a few days. Measurements included demographics and health habits, a brief medical history, menopausal symptoms, height, weight and chest dimension, skin site assessment and participant satisfaction questionnaires.

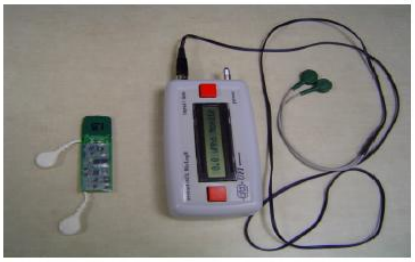

Figure 2: Miniature monitor compared to commercially available Biolog Hot Flash Monitor

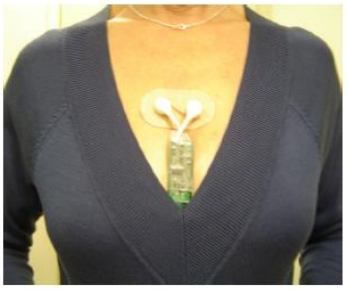

Figure 3: Subject wearing the miniature monitor

Figure 4: Magnetic ring used to trigger event marker

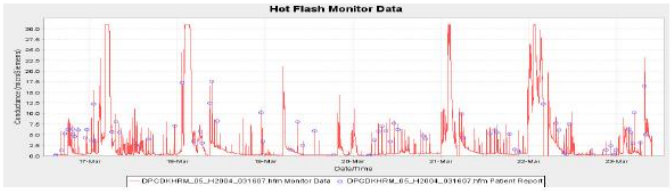

Figure 5: Seven day recording on the miniature hot flash monitor (blue circles are self-recorded hot flashes using the magnet-activated event recorder built into the monitor)

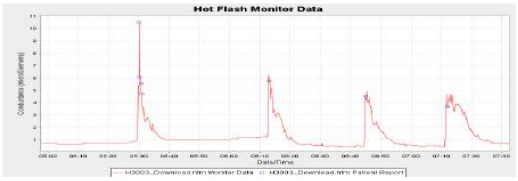

Figure 6: Two-hour recording of hot flash activity on the miniature hot flash monitor

RESULTS

The miniature ambulatory monitor is 70 x 22 x 5 mm, weighs 14 g, is worn on the anterior chest either above or between the breasts and is not visible under clothing. The monitor was reported by participants to be comfortable, unobtrusive and easy to attach and remove. Research staff reported that the monitor is easy to start, attach and remove, data are easy to download via a wire attached to a personal computer USB port. Battery life is about 3 weeks.

During 7 days of use in this cohort, the electrode patch came off and had to be replaced by 5 participants and there were 15 reports of the patch loosening but not falling off. Effects of the electrode adhesive on the skin were mild and reversible. Nine participants reported reddening on the skin at the site of the electrode while research staff observed a moderate (bright pink) reaction in 2 participants and a mild (faint pink) reaction in 18 participants.

During 3 days of diary keeping, 20 participants in the development cohort reported a total of 887 hot flashes. The mean number of hot flashes reported per day was 14.8 (±9.6). Measures of the accuracy of the miniature hot flash recorder compared to self reported hot flashes (either on the diary or by activation of the event marker in the monitor) are presented in Table 1. Sensitivity was 0.93 (±0.05), specificity was 0.98 (±0.013), the positive predictive value was 0.87 (±0.13), and the negative predictive value was 0.99 (±0.013).

Table 1. Accuracy of the miniature hot flash recorder compared to self-reported hot flashes.

	Self-reported Hot Flash	No Self-reported Hot Flash
Monitor Detected Hot Flash	814	91
No Monitor Detected Hot Flash	73	5669

PPV and specificity are artificially low since participants are not always compliant with self-report. Figure 7 is an example of a 7 day recording where multiple hot flashes were reported in the first two days of recording and correlated with the monitor recording. Subsequently fewer hot flashes were self-reported.

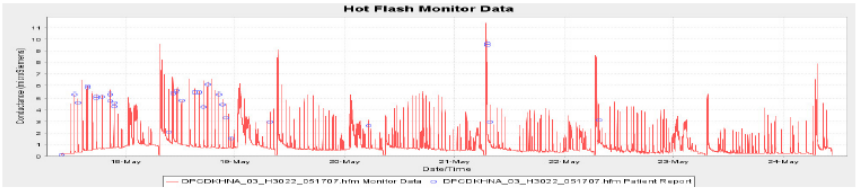

Figure 7: 7 day recording with diminishing self-report markers

CONCLUSIONS

In conclusion, a miniature ambulatory hot flash monitor that uses a conductive adhesive polymer electrode and measures changes in skin conductance accurately identifies menopausal hot flashes over a 7-day period.

Acknowledgement: This hot flash monitoring system was developed under National Institutes of Health, National Center for Complementary and Alternative Medicine grant 1R43AT003180-01.

REFERENCES

1. Tincello DG, Williams KS, Joshi M, Assassa RP, Abrams KR. Urinary diaries: a comparison of data collected for three days verses seven days. *Obstet Gynecol. 2007 Feb;109(2 Pt 1):277-80*
2. Dmochowski RR, Sanders SW, Appell RA, Nitti VW, Davila GW. Bladder-health diaries: an assessment of 3-day vs 7-day entries. *BJU Int. 2005 Nov;96(7):1049-54*

Appendix X

Miniature ambulatory skin conductance monitor and algorithm for investigating hot flash events

Dennis E Bahr[1,2], John G Webster[1,2,5], Deborah Grady[3], Fredi Kronenberg[4], Jennifer Creasman[3], Judy Macer[3], Mark Shults[1], Mitch Tyler[2], and Xin Zhou[2]

[1]Bahr Management, Inc., Middleton, WI, 53562 USA
[2]University of Wisconsin, Madison, WI, 53706 USA
[3]University of California, San Francisco, CA, 94115 USA
[4]Stanford University, Palo Alto, CA, 94305 USA
[5]King Abdulaziz University, Jeddah, Saudi Arabia

Abstract - A skin conductance monitoring system was developed and was shown to accurately acquire and record hot flash events in both supervised laboratory and unsupervised ambulatory conditions. The monitor consists of a disposable adhesive patch supporting two hydrogel electrodes and a reusable, miniaturized, enclosed electronic circuit board that snaps onto the electrodes. The monitor measures and records the skin conductance for three or more days without external wires or telemetry and has an event marker that the subject can press whenever a hot flash is experienced.

The efficacy of the system was proven by comparing the results from algorithms developed during this research and from experts who had years of experience doing hot flash studies. Two different processing algorithms were used. One was an Artificial Neural Network and the other a Matched Filter technique with multiple kernels implemented as a sliding form of the Pearson Product-Moment Correlation Coefficient. Both algorithms were developed and/or trained on a development cohort of 17 women and then validated using a second similar cohort of 20. All subjects were between the ages of 40 and 60 and experienced 10 or more hot flashes per day over a three day period. The Matched Filter had the best statistics with a mean sensitivity of 0.92 and a mean specificity of 0.90 using the data from the development cohort and a mean sensitivity of 0.92 and a mean specificity of 0.87 using the data from the validation cohort.

Keywords: Hot flash, hot flush, recorder, monitor, template matching, matched filter, electrode, hydrogel, Pearson, correlation.

1. Introduction

A hot flash event is the sudden onset of intense flushing in the upper torso and face, often followed by profuse sweating and chills [1]. The etiology of hot flashes is thought to be related to abnormalities of thermoregulation associated with changes in hormone levels that occur at menopause, but the mechanism is not clearly understood [2]. There are about 45 million American women between the ages of 45 and 65 years. At least two thirds of these women will experience hot flashes and approximately 20% will seek medical relief for debilitating symptoms [1].

Postmenopausal hormone therapy is a highly effective treatment for hot flashes [3] and 10 million

women in the US are currently taking some form of estrogen, either alone or in combination with progestin [4]. However, large randomized trials have recently shown that standard-dose hormone therapy is associated with increased risk for cardiovascular disease, venous thromboembolic events, and dementia [4, 5, 6, and 7]. Given the increased risks for serious diseases and other common side effects such as uterine bleeding and breast tenderness [8], many women seek to avoid using hormone therapy for treatment of hot flashes. Clinicians are continually turning to other means to manage hot flashes, including Complementary and Alternative Medicine (CAM) therapies. There is a long history of the use of CAM therapies for hot flashes, but the empirical base to assess safety and efficacy is neither extensive nor very strong. The FDA has recommended that hormones for the treatment of hot flashes be used at the lowest dosage and for the shortest period of time. However, little is known about risks and benefits for smaller doses, shorter treatment times, and different routes of administration. Thus, investigators who are conducting research on a range of treatments to reduce hot flashes are searching for methods to objectively measure hot flash events as a result of intervention treatments.

As reflected in recent NIH-sponsored seminars (Women's Health Seminar Series-2010), and numerous conferences on menopause there is intense interest in the research community regarding the etiology of hot flashes and in finding effective and safe treatment. However, research is currently hindered by the lack of a feasible, reliable and accurate objective measure of hot flash frequency and severity. Most studies currently use a 7-day self-reported hot flash diary [9]. This measure is subjective and can be inaccurate and unreliable because participants forget or fail to enter hot flashes in the diary (especially at night when many hot flashes occur), severity is self-reported on a coarse scale (mild, moderate, severe), and the exact timing of the hot flash is not recorded [10]. In addition, keeping a daily diary is labor intensive and inconvenient so most participants are unwilling to do this for more than about a week.

The objectives were quite clear as to the requirements for a good hot flash system. The first and most important objective was to develop an electrode that provided artifact free signals with little or no base line drift. Secondly, develop an improved measurement device that is reliable, user-friendly, accurate, and could collect data for three to seven days under ambulatory conditions. The monitor would need to be able to collect data under conditions of daily life, during waking and sleeping hours, without interfering with daily activities. Such a device should be able to be used to evaluate the efficacy of various therapies, including complementary and alternative medicine (CAM) modalities, to record hot flashes under ambulatory conditions in clinical studies, and to monitor subjects in intervention studies.

2. Hot flash events

There are two well known mechanisms that the human body uses to cool itself. One is vasodilatation and the other is sweating when vasodilatation alone cannot accomplish the task. An increase in sternal skin

conductance due to sweating has been shown to be an accurate measure of the occurrence of hot flashes in temperature controlled laboratory settings [2]. Molnar [11] demonstrated in extensive studies that the temperature of the upper anterior torso increased during a hot flash event causing mild to profuse sweating. Thus, the upper torso was chosen as the best place to monitor skin conductance and the sternum was chosen because it was easy to affix electrodes over the bone like structure.

Sweat duct activity is initiated and modulated by body temperature, hormones, and neural activity. Sweat is generated in the sweat glands and carried to the surface through the sweat ducts. Immediately after the initiation of the hot flash event, the pores on the skin surface begin opening and exuding sweat that has been channeled to the surface by the sweat ducts from the sweat glands below the surface. Full sweat pore recruitment takes approximately 1 min. Once the skin surface is covered in a layer of fluid the skin begins to cool and the pores close over in a period of 5 to 10 min.

The action of the sweat pores opening provides electrical access to the layers below the epithelium. A small voltage of less than 1 V applied to the surface of the skin by a pair of closely spaced electrodes will cause a current to flow. It is postulated that the current flows from electrode to electrode mostly through the sweat pores under the electrode surfaces. This current is typically 10 to 30 times the baseline leakage and roughly proportional to the cross-sectional area of the recruited sweat pores. There is also a small surface leakage current due to the layer of sweat on the skin below the electrode. Fig. 1 shows how the skin conductance rising sharply at the onset of a hot flash, and then slowly returning back to the baseline.

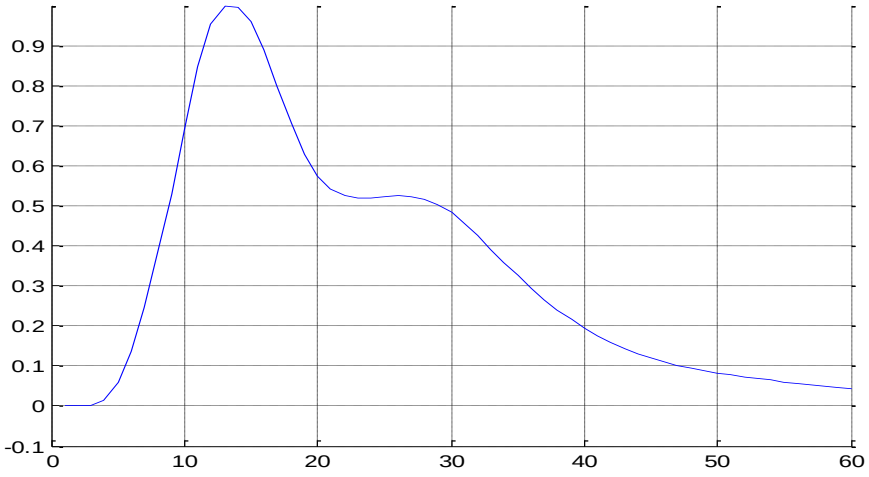

Fig. 1: A normalized example of the electrical conduction of a hot flash event. The abscissa units are shown as the sample number. Since samples were taken every 10 seconds the full scale represents 10 minutes. Typically the conductance values range from 1to10 μS. The plateau between sample numbers 20 and 30 occurred in approximately 15% to 20% of the hot flash waveforms that were collected during this research. No explanation as to what caused this could be found in the literature or could the cause be determined during this research.

The three most important characteristics of hot flash events are the rapid rise in the conductance, the gently rounded peak, and the exponential like fall. These common characteristics were the most useful in detecting the hot flash events in the conductance data.

3. Electrode design

One method that is still used to measure hot flashes is to use an isotonic sodium chloride based semi-liquid gel or cream that approximates perspiration (0.1 to 0.3% NaCl). This formula is substituted for the higher salt content (~5% NaCl) gel and sponge in a standard ECG electrode. A constant 0.5 V was applied to a pair of these electrodes and the conductivity is measured as a function of time. These modified electrodes have a number of major limitations. The gel between the skin and the electrode will begin migrating almost immediately causing motion artifacts and the conductance to drift without physiological involvement. A second major limitation is that the impermeable plastic patches containing the semi-liquid gels trap sweat under the electrode increasing hydration causing a continual rise in conductance over time thus rendering the electrode essentially useless after a few days of use. A third problem is that the stickiness or tack is designed for a few days of use and is very aggressive often leaving a large welt on the skin after removal.

Jossinet and McAdams [12] showed that when electrodes using semi-liquid gels as the skin electrode interface, were used the skin was well hydrated and skin resistance decreased (conductance increased) with time. They also showed that for hydrogel electrodes, the skin resistance did not decrease with time because these materials do not actively hydrate the skin. Their investigations demonstrated that skin conductivity is best measured using a hydrogel (or very mild wet gel) electrode interface. Hydrogels are water-containing polymers that incorporate either natural or synthetic hydrocolloids and are therefore “solid” and hydrophilic.

There are many manufactures of hydrogel materials and there many types of hydrogel materials. It was decided to acquire hydrogel samples from AmGel, Inc. a major manufacturer of medical hydrogel materials. Samples were chosen from three of AmGel’s major hydrogel Series and included AG603, AG703, and AG803. Samples in the AG900 series were not chosen because of the high volume resistivity of that material. Fig. 2 shows the hydrogel materials were cut into 1.5 cm^2 squares and placed in pairs on a 4 cm by 7 cm oval skin-colored polyester containing two pre-assembled Ag/AgCl metal electrodes.

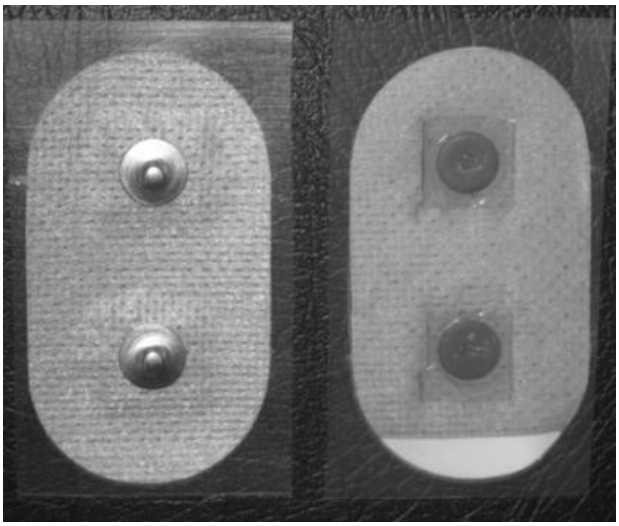

Fig. 2: An assembled hydrogel electrode patch used during early experimentation to provide data on hydrogel formulations. The design uses spunlaced polyester coated with an acrylic adhesive, Ag/AgCl metal electrodes with snaps on the back, and a special formulated hydrogel metal-to-skin interface.

In order to find the best hydrogel material specific attention was paid to baseline values, baseline drift, and signal-to-noise ratios when measuring hot flash episodes. The AmGel AG703 and AG803 adhesive hydrogels were found to be superior to AG603 hydrogel, BIOLOG gels, or 0.1% or 0.9% saline in hydrogels. Both AG703 and AG803 showed the best results as to low baseline drift, low artifact, and fast recovery back to baseline. The best overall results were obtained using AG803 which is a specially formulated hydrogel material usually used for electrophoresis. Fig. 3 shows graphs of some of the results of the experimental studies.

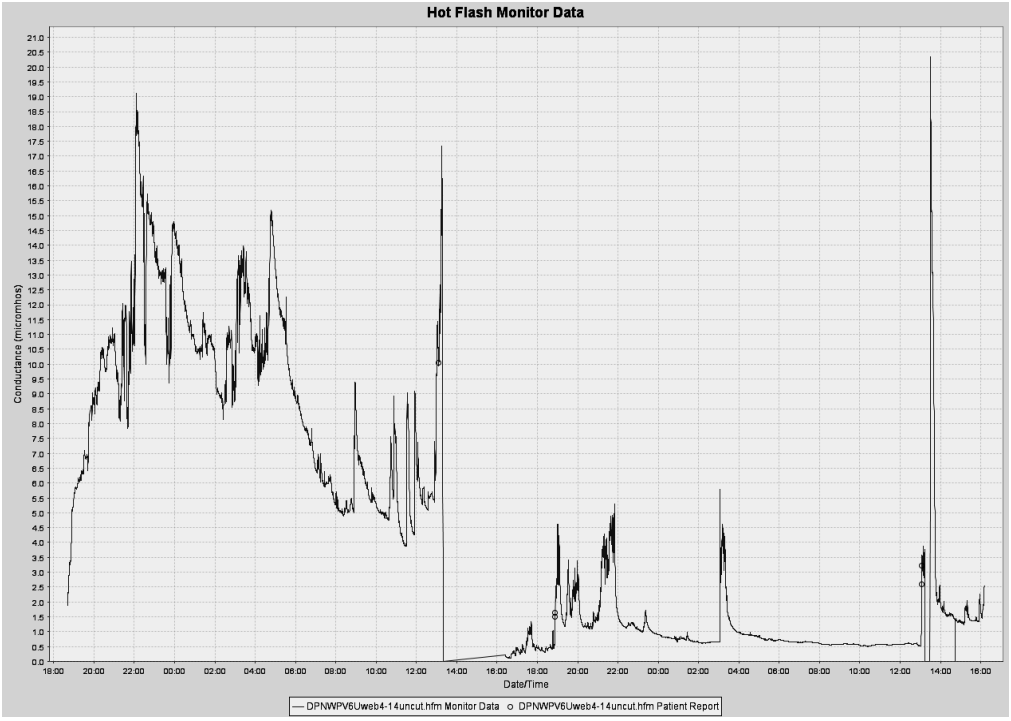

Fig. 3: Left half shows AG603 hydrogel gel with a conductance averaging 10 μS and erratic recordings. Right half shows AG803 hydrogel yielding a conductance averaging 1.0 μS with clean recordings.

The patch material is spunlaced polyester (MacTec, Inc - TM-9478). The patch is coated on one side with 594 acrylic-based hypoallergenic pressure-sensitive adhesive. The adhesive material is a medical grade adhesive and is formulated for sustained contact with human skin. It is protected by a 70# dense, semi-bleached Kraft release liner. The TM-9478 material is designed for use as a breathable medical tape. The hydrogel and the polyester absorb the sweat from the skin and the breathable feature allows the sweat to evaporate. This prevents the accumulation of sweat and provides for a low amplitude base line that does not wander over time. The baseline conductance changed a few μSiemens over the 3 day testing periods usually increasing in magnitude. This was assumed to be caused by the accumulation of salt content under the electrode. If the electrode patch became wet as in taking a shower, it dried off in about 1 h and was ready to continue collecting hot flash data. Fig. 4 compares an electrode using semi-liquid gel with the new hydrogel electrode shows significant improvement in base line offset and base line wandering.

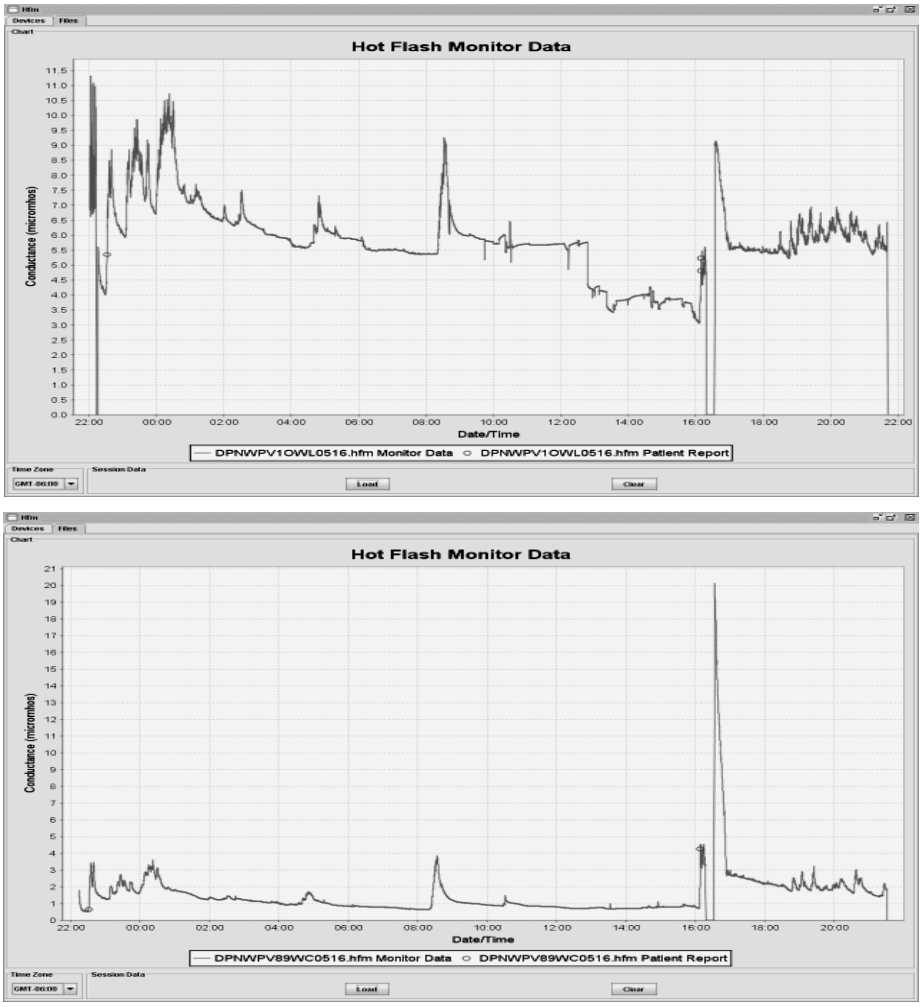

Fig. 4: Comparison of two electrodes worn by the same subject at the same time. Top: The cream used with the Biolog monitor causes about 6 μS baseline conductance. Sweating caused by exercise (marked by circles) causes about 30% change. Bottom: Conductive adhesive gel causes about 0.8 μS baseline conductance and has less motion artifact. Sweat caused by exercise causes 400% change. During shower (at about 16:00 h), the recorder was detached (0 μS). After shower, electrode was wet, recording about 20 μS and recovering in about 30 min.

4. Data Processing

During hot flash events the conductance rises rapidly as the sweat pores open and begin exuding sweat. The conductance reaches a peak with full sweat pore recruitment and then the conductance falls slowly as the sweat pores close and the sweat evaporates from the electrode. This morphological shape varies in rise time, height, width, and fall time within subject records and across subject records. The hot flashes have a rise time of approximately 1 min and duration of no more than 10 min. The task was to locate the hot flashes events int the data among the motion artifacts such as those produced by exercise and bathing.

The miniature ambulatory monitor and software were tested by collecting data on two cohorts of 20 subjects who had an average of 10 hot flashes per day over a three day period. The results from the first or development cohort had three subjects discarded because the electrodes were clearly intermittent and not making proper contact with the surface of the skin. Because the skin conductance data usually contained artifacts and noise and often had a slow drift, the data was first filtered with two separate filters. The noise is minimized without significant distortion by using a centered moving average convolution filter with a width of 7 points (±1 min). To minimize the base line drift in the data, it is then filtered using a 361 point (±30 min) centered median filter. This type of filter has the characteristic of eliminating drift without distorting the sharp peaks. Since the data was post processed using stored causal data, it was possible to use centering on both filters to eliminate all phase shift error. This is done by passing the filter kernel over the data in one direction and then in the other, doing half of the required math operations in each of the directions. Fig. 5 shows the results were marked by experts as to where they thought a hot flash had occurred since it is known that subject marked data cannot be considered to be reliable [10].

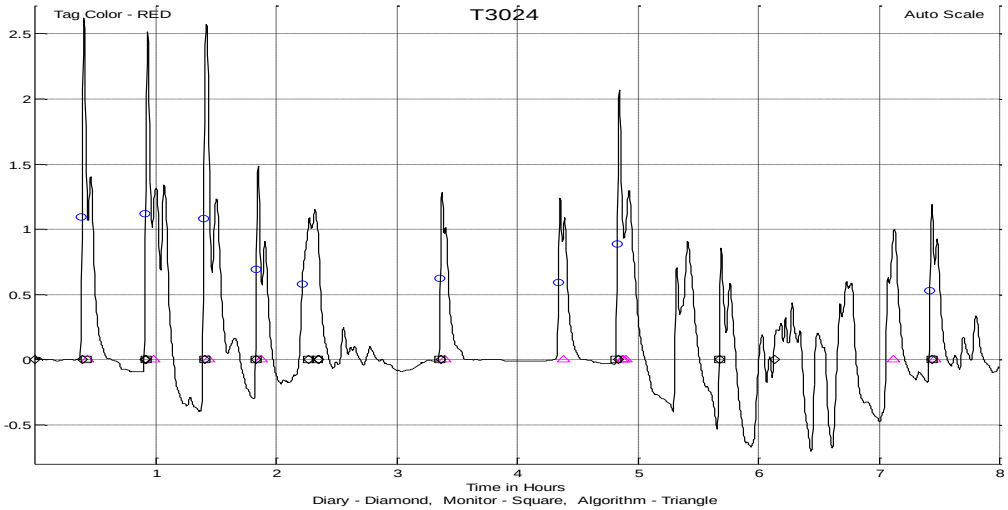

Fig. 5: Sample of the Hot Flash data that was marked by the experts.

Any detection method would need to perform properly with the development data set, the evaluation data set, and data collected during future work. Three methods of detecting hot flash events were evaluated and two were chosen and ultimately implemented as computer programs. One method that was considered was to select known hot flash events from the development data set and average these data producing one or more representative patterns. The patterns could then be matched using statistical methods. Such a choice may have generated great statistics for the development cohort population but may not have functioned properly over other population samples. This is akin to overtraining an algorithm.

A second choice was a parameterized model where the shape of the model could be altered by modifying the model parameters in order match the shape of known hot flash events. For this research the log-normal function was chosen as the model because of its shape and the Pearson Product-Moment Correlation Function was chosen to determine goodness-of-fit of the kernel. This method proved to be the best of the three.

A third method was to use an algorithm that could *learn* what the shape of a true hot flash event looked like using samples from the development data set. The method chosen was the Artificial Neural Network. This is a mathematical model that simulates the biological neuron by multiplying the inputs to the network using a series of weights and then summing these weights to produce a single output that is either true or false. This is similar to how the dendrites and axons function in our brains. The dendrites collect electrical signals from other neurons often applying a *weight* to these signals, summing the results, and sending the resultant signal along the neuron axon to other neurons. In the model the weights are adjusted during a training procedure to obtain the best statistics dependent on some error criteria determined by the user.

5. The matched filter

Hot flash events have a shape that can be recognized as similar to a constant with a squared exponent squared and skewed to the right. There are many functions with this characteristic but it was decided to limit the search to the Poisson distribution and the log-normal distribution since they are well known. Even though these functions are considered *probability density functions*, it is possible to morph them into functions of time or position using a substitution of variables. The problem with the Poisson distribution function was that the variance and the mean are equal to each other in all cases. This made it all but impossible to alter the rise time, width, and fall time independently as was needed so this function was discarded as a candidate.

The log-normal function is useful in modeling naturally occurring variables that are the *product* of many independent variables rather than the *sum* of these variables. Since the hot flash event is modulated by body temperature, hormones, and neural activity this function seemed to be a natural fit. The equation for the one dimensional log-normal function is shown in equation (1).

$$fx(x;\ \mu,\sigma) = \frac{1}{x\sigma\sqrt{2\pi}}\ e^{\frac{-(lnx-\mu)^2}{2\sigma^2}}\ ,\ x > 0 \tag{1}$$

The symbol σ is the standard deviation and the square σ^2 is the variance. The symbol μ is the mean value and the x symbol is the independent variable and can range from $-\infty$ to $+\infty$. The term $\frac{1}{x\sigma\sqrt{2\pi}}$ in front of the exponential is the normalization constant and comes from the fact that the integral over the exponential function is not unity but rather $x\sigma\sqrt{2\pi}$. What was needed was a simpler equation that had a similar shape but where the mean and standard deviation could be replaced with two terms, such as center and width. An empirical equation was developed using the log-normal as a model and is shown in equation (2).

$$template(x + offset) = \exp\left[-0.8 * \left(\frac{\ln\left(\frac{x}{center}\right)}{width}\right)\right]^2 \tag{2}$$

The term *x* is the independent variable and has a range from 0 to 90 since the data was sampled and stored every 10s the range spans $[90 * 10/60]$ or 15 min. The term *center* is where the peak occurs and the *width* is a measure of the width and skew or drop in the tail. The *Offset* term is the amount of time from zero to where the function's rising edge begins since there is usually a flat baseline just before the rise. It was readily determined that the slope of the rising edge, the width of the kernel, and the length of the tail were the most important parameters. The variables *center* and *width* in equation (2) were chosen to produce the best statistical results when compared with experts who marked the data sets for true hot flash events. Initially, it was hoped that a single pattern or kernel could be developed with fixed constants for the *center* and *width* that could be used for all subjects. But, this was not to be and it was necessary to use five separate kernels all with unique values for the center and width. The *width* was varied between 0.1 and 4.0 in steps of 0.1 and the *center* was varied between 1 and 25 in steps of 1 providing 1000 filter kernels.

The kernels were correlated with the data one at a time by sliding the kernel along the data one sample point at a time and using the Pearson correlation coefficient to determine how well the kernel and the data matched. It was found that there was an abundance of false negatives when data were used that had Pearson correlation coefficients above 90%. A decision was made to use multiple kernels and to mark a hot flash as positive if any one of the kernels provided an 85% or better match. By varying these one at a time and keeping the others constant it was possible to choose the best values to use for these parameters. Fig. 6 shows the log-normal templates used for the kernels.

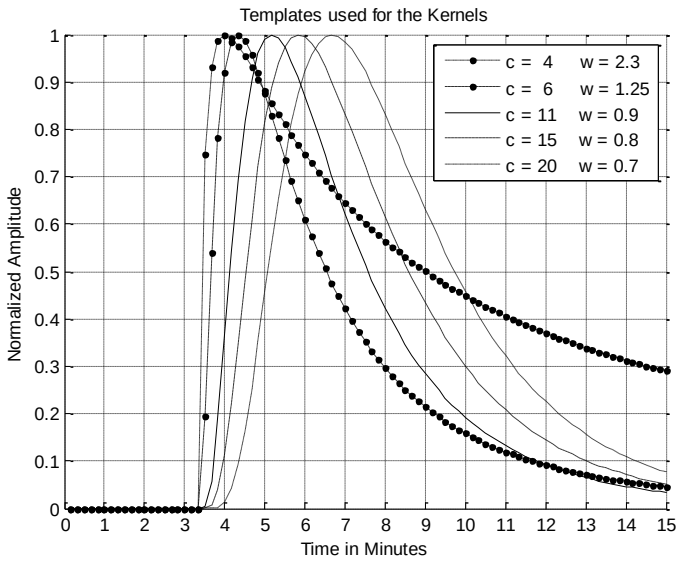

Fig. 6: The five templates used for the kernels, where *c* is the center parameter and the *w* is the width parameter.

The Pearson Product-Moment Correlation Function was implemented in MatLab as a sliding or moving algorithm and this was used to determine the best values for the center and width parameters. Extensive use was made of Receiver Operating Characteristic (ROC) curves to determine what values to use for the center and width for the parameterized kernels. Fig. 7 shows an example of one of these curves.

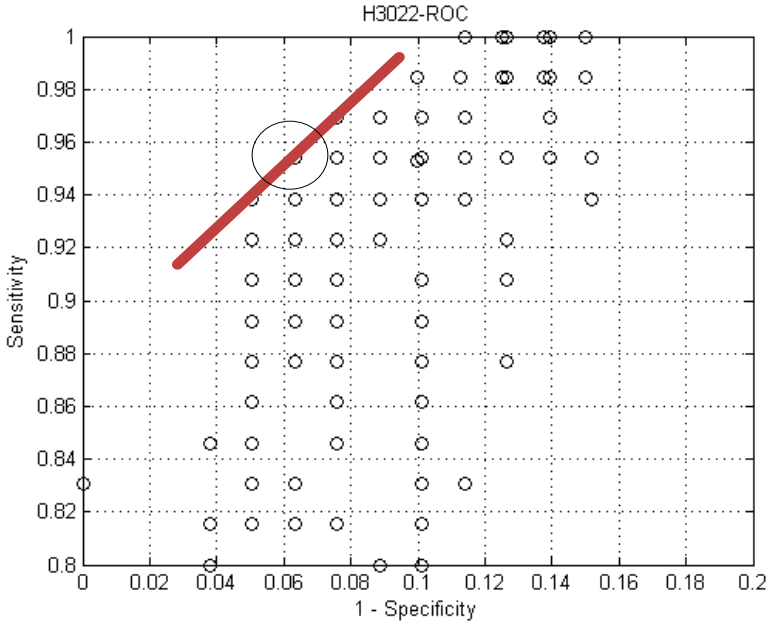

Fig. 7: A ROC curve shows the results of scanning the parameters for the kernel. Each small circle represents the results of processing the data with a fixed *center* and *width*. The best *center* and *width* generated the circled point.

ROC curves were run for each of the 17 subjects in the development set and the points (circles on the graph) that were clustered in the upper left hand corner were considered likely candidates. The parameters of the kernels that generated these points and were common across the subjects were the values chosen as the working parameters. This method was shown to produce good results with a mean sensitivity of 0.92 and a

mean specificity of 0.90 using the development cohort.

Subject	TP	TN	FP	FN	SENS	SPEC	PPV	NPV
H3001	16	111	14	3	0.84	0.89	0.53	0.97
H3002	36	90	16	2	0.95	0.85	0.69	0.98
H3003	65	64	10	5	0.93	0.86	0.87	0.93
H3004	54	81	9	0	1.00	0.90	0.86	1.00
H3005	33	93	14	4	0.89	0.87	0.70	0.96
H3008	17	119	5	3	0.85	0.96	0.77	0.98
H3009	22	104	9	9	0.71	0.92	0.71	0.92
H3011	61	77	5	1	0.98	0.94	0.92	0.99
H3012	62	72	8	2	0.97	0.90	0.89	0.97
H3013	44	77	16	7	0.86	0.83	0.73	0.92
H3014	35	100	9	0	1.00	0.92	0.80	1.00
H3016	13	114	15	2	0.87	0.88	0.46	0.98
H3017	22	116	4	2	0.92	0.97	0.85	0.98
H3020	30	91	20	3	0.91	0.82	0.60	0.97
H3022	65	69	10	0	1.00	0.87	0.87	1.00
H3024	59	76	8	1	0.98	0.90	0.88	0.99
H3025	16	124	4	0	1.00	0.97	0.80	1.00
Mean	**38**	**93**	**10**	**3**	**0.92**	**0.90**	**0.76**	**0.97**

Using the same algorithms on the evaluation cohort of 20 individuals produced an average sensitivity is 0.92 and the average specificity is 0.87.

Subject	TP	TN	FP	FN	SENS	SPEC	PPV	NPV
H4001	42	84	18	0	1.00	0.82	0.70	1.00
H4002	27	96	17	4	0.87	0.85	0.61	0.96
H4008	23	94	27	0	1.00	0.78	0.46	1.00
H4014	28	101	11	4	0.88	0.90	0.72	0.96
H4015	33	88	16	5	0.88	0.85	0.69	0.95
H4019	11	116	16	1	0.92	0.88	0.41	0.99
H4020	47	84	9	4	0.92	0.90	0.84	0.95
H4021	29	100	10	5	0.85	0.91	0.74	0.95
H4026	47	63	30	4	0.92	0.68	0.61	0.94
H4033	34	102	7	1	0.97	0.94	0.83	0.99
H4041	38	90	13	3	0.93	0.87	0.75	0.97
H4042	24	92	23	5	0.83	0.80	0.51	0.95
H4043	19	116	5	4	0.83	0.96	0.79	0.97
H4044	3	126	15	0	1.00	0.89	0.17	1.00
H4048	57	71	13	3	0.95	0.85	0.81	0.96
H4049	20	110	14	0	1.00	0.89	0.59	1.00
H4051	38	79	24	3	0.93	0.77	0.61	0.96

H4058	5	136	2	1	0.83	0.99	0.71	0.99
H4059	51	81	12	0	1.00	0.87	0.81	1.00
H4062	4	131	8	1	0.80	0.94	0.33	0.99
Mean	**29**	**98**	**15**	**2**	**0.92**	**0.87**	**0.63**	**0.97**

6. The artificial neural network

The signals entering the dendrites of a neuron are modified by various chemical and electrical processes before being *summed* and sent along the axon where the signal is presented to other neurons. Modifications of the input signals are done continously as the biological system adapts to various local and external stimuli. The neural network, on the other hand, uses weights to modify the input signals, but only does this during a training session and usually does not modify these weights when the neural network is being used to classify signals. In a neuron the connection to the dendrite can be either excitatory or inhibitory while in the artificial neural network this is accomplished using weights that are numbers less than one and can be either positive or negative. The neural network used in this research is of the standard form with an *input* layer, a *hidden* layer and an *output* layer. The name usually given to such a network is the *perceptron* and was first used by Rosenblatt [13]. The artificial neural network had an input layer containing 60 nodes of hot flash data and 1 bias node. The hidden layer contained 35 nodes and the output node contained one node. Fig. 8 shows the signal flow diagram of the artificial neural network used in this research.

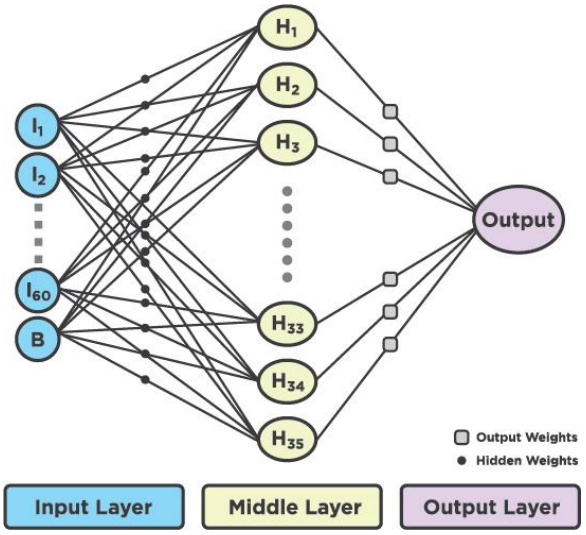

Fig. 8: A signal flow diagram of the artificial neural network used in this research.

The size of the input was chosen to be 60 nodes because this depicted a 10 min sample of a hot flash using a 10 s sampling rate. The predominant features of the rapid rise, smooth peak at the top, and the exponential like tail all fall within this 10 min window. A 61st node was added to the input to act as a bias term since the output will have values between 0 and 1 rather than the usual ±1. The 30 nodes in the hidden layer were chosen empirically using the literature as a guide. [14, 15]. They suggest using fewer hidden nodes than there are in the input. Hidden node sizes between 20 and 60 were evaluated and a value of 35 was chosen because it provided sufficiently good results without requiring lengthy computation times. An equation that describes the neural network process is:

$$a = \sum_{i=1}^{N} w_i x_i + b \tag{3}$$

Where x is the input symbol, w is the multiplier weights, i is the input sample number, b is a bias term, N is the total number of inputs, and a is the output or activation. The output a is often passed to a non-linear discrimination or activation function with an output of ±1, 0 to 1, or some non-linear mathematical function. There are a number of such discriminator functions each with its own special characteristics including a vertical line with a range from 0 to 1, a sloped line, the hyperbolic tangent, and the sigmoid function. The sigmoid is usually the function of choice because it is a monotonic function and has the ability to compress the output giving its networks greater stability. The sigmoid also happens to be a differentiable function where the derivative is easy to calculate.

(Sigmoid function) $$y(z) = \frac{1}{1+e^{-z}} \tag{4}$$

(Sigmoid derivative) $$y'(z) = y(z)[1 - y(z)] \tag{5}$$

For the purposes of this research the sigmoid abscissa was scaled to ±1 and the ordinate for the sigmoid derivative was scaled to 0 to 1. This normalization may not have been necessary, but doing so is the best way of keeping the results of calculations near zero and thus provides the best dynamic range using a digital computer.

The greatest effort comes in defining the training data set and in the actual training of the neural network. Training is done by submitting patterns that should elicit a true response along with an indication that the pattern is true and patterns that elicit a false response along with the indication of being false. This training is usually done with hundreds of such patterns and then retrained with the same patterns a few thousand times. A group of such training patterns is called an epoch and if too many epochs (>1000) are used for training, the neural network can become over trained. Should this happen, the development set will have excellent statistics and any evaluation set will have very poor statistics. The idea is to train with enough epochs such that both sets have similar statistical outcomes.

Initially, each of the weights is set to a small random value, usually in the range between 0.01 and 0.0001. The choice of range is purely empirical and there are no absolute rules to follow. For this research, a flat probability density function (pdf) was chosen with numbers between ±0.01. The training process begins by applying a known hot flash pattern to the input. The input values are multiplied by the hidden weights, summed and activation functions are applied. These results are modified using the output weights, a single activation value applied, and the result propagated to the output. Figure 9 shows the MatLab source code that performs this forward response.

```
%--------------------------------------------------------------------------
% calculate network forward response
%--------------------------------------------------------------------------
for i = 1:hidden_size
    acc1 = 0;
    for j = 1:input_size
        acc1 = acc1 + input(1,j).*Wh(j,i);
    end
    hidden(i) = sigmoid(acc1);
end

acc2 = 0;
for k = 1:hidden_size
    acc2 = acc2 + hidden(k).*Wo(k);
end
output = sigmoid(acc2);
```

Figure 9: The forward response of the neural network written in MatLab. The *input* is a 60 point vector containing the hot flash data. The *hidden* values are a 30 point vector while the output is a single value between 0 and 1 describing the probability of the input being a hot flash. The variables `acc1` and `acc2` contain the accumulated weighted sums of the *input* and *hidden* layers respectively before the sigmoid discriminator is applied.

Once an input pattern has been processed in the forward direction all of the values for the hidden and output layers are known as well as the weights for both layers. A process called *back propagation* is now used to do the actual training. The fastest way to train a network is to use the gradient method to modify the values of the weights. This method is often called the method of steepest descent or the delta rule. The gradient method changes the network's weights and bias so that the error proceeds towards a minimum along the steepest gradient.

The output sigmoid classification is known from the forward response. The derivative of this response ($slope\_output$) can be calculated using equation 9.3 Equation 9.4 is used to calculate how the network output will change with respect to a slight change in the output weights.

$$dodw = \frac{\Delta output}{\Delta Wo(m)} \approx hidden(m) * slope\_output \tag{6}$$

The actual network output is compared with the desired value using equation 9.4 providing the degree of error of the output classification.

$$err = desired - output \tag{7}$$

With this knowledge the output weights can be modified by multiplying the gradient by the *err* and the learning constant (*mu*) which has a value between 0.1 and 0.001.

$$Wo(m)_{new} = Wo(m)_{old} + dodw * err * mu \tag{8}$$

The learning constant is used to control the speed of convergence and prevents the equation from diverging. Changing the hidden weights is a bit more difficult. The process requires that the error be distributed to each hidden node to which the output node is connected to. The output weights are included in the calculation. The derivatives of the outputs from the hidden layer ($slope\_hidden$) can be calculated using equation 9.3 and the results used to calculate the changes in the hidden layer values with respect to changes in the hidden weights.

$$dhdw \approx input(i) * slope\_hidden(i) * Wo(i) * slope_{output} \tag{9}$$

The variable $dhdw$ is now multiplied by the learning constant mu and the error err and the results are used to find new values for the hidden weights.

$$Wh(m)_{new} = Wh(m)_{old} + dhdw * err * mu \tag{10}$$

The error for each input pattern is squared and added to the sum of the pervious squared errors. When an epoch is completed the square root is taken of this sum and used as a measure of how well the network is converging and displayed on the system console. The MatLab source code that performs this back propagation is shown below:

```
%--------------------------------------------------------------------------
% calculate the network back propagation
%--------------------------------------------------------------------------
slope_output = 4.0*output*(1.0-output);
err = desired - output;

for m = 1:hidden_size
    slope_hidden = 4.0*(hidden(m)*(1.0-hidden(m)));
    for n = 1:input_size
        dhdw = input(n)*slope_hidden*Wo(m)*slope_output;
        Wh(n,m) = Wh(n,m) + dhdw*err*mu;
    end
end

for m = 1:hidden_size
    dodw = hidden(m).*slope_output;
    Wo(m) = Wo(m) + dodw*err*mu;
end
```

Figure 10: The back propagation algorithm implemented in MatLab.

The results using the neural network on the development cohort showed a mean sensitivity is 0.93 and a mean specificity is 0.89.

Subject	TP	TN	FP	FN	SENS	SPEC	PPV	NPV
H3001	13	119	6	6	0.68	0.95	0.68	0.95
H3002	34	90	16	4	0.89	0.85	0.68	0.96
H3003	60	66	13	5	0.92	0.84	0.82	0.93
H3004	53	82	9	0	1.00	0.90	0.85	1.00
H3005	33	91	18	2	0.94	0.83	0.65	0.98
H3008	17	123	3	1	0.94	0.98	0.85	0.99
H3009	28	105	8	3	0.90	0.93	0.78	0.97
H3011	60	75	7	2	0.97	0.91	0.90	0.97
H3012	64	71	9	0	1.00	0.89	0.88	1.00
H3013	45	81	12	6	0.88	0.87	0.79	0.93
H3014	35	98	11	0	1.00	0.90	0.76	1.00
H3016	13	114	15	2	0.87	0.88	0.46	0.98
H3017	23	114	6	1	0.96	0.95	0.79	0.99
H3020	32	90	21	1	0.97	0.81	0.60	0.99
H3022	64	67	12	1	0.98	0.85	0.84	0.99
H3024	59	74	10	1	0.98	0.88	0.86	0.99
H3025	16	127	1	0	1.00	0.99	0.94	1.00

Mean	**38**	**93**	**10**	**2**	**0.93**	**0.89**	**0.77**	**0.92**

The results from the validation cohort of 20 individuals showed a mean sensitivity of 0.87 and a mean specificity of 0.84.

Subject	TP	TN	FP	FN	SENS	SPEC	PPV	NPV
H4001	41	75	28	0	1.00	0.73	0.59	1.00
H4002	27	97	17	3	0.90	0.85	0.61	0.97
H4008	20	101	19	4	0.83	0.84	0.51	0.96
H4014	30	96	16	2	0.94	0.86	0.65	0.98
H4015	36	87	16	5	0.88	0.84	0.69	0.95
H4019	11	102	31	0	1.00	0.77	0.26	1.00
H4020	51	84	8	1	0.98	0.91	0.86	0.99
H4021	25	97	13	9	0.74	0.88	0.66	0.92
H4026	48	62	31	3	0.94	0.67	0.61	0.95
H4033	31	99	10	4	0.89	0.91	0.76	0.96
H4041	37	77	26	4	0.90	0.75	0.59	0.95
H4042	19	90	25	10	0.66	0.78	0.43	0.90
H4043	16	114	6	8	0.67	0.95	0.73	0.93
H4044	3	107	34	0	1.00	0.76	0.08	1.00
H4048	61	74	9	0	1.00	0.89	0.87	1.00

H4049	19	112	12	1	0.95	0.90	0.61	0.99
H4051	40	69	34	1	0.98	0.67	0.54	0.99
H4058	3	134	4	3	0.50	0.97	0.43	0.98
H4059	46	79	16	3	0.94	0.83	0.74	0.96
H4062	3	132	7	2	0.60	0.95	0.30	0.99
Mean	**28**	**94**	**18**	**3**	**0.87**	**0.84**	**0.58**	**0.97**

7. Conclusion

The results of this research produced a commercial hot flash monitoring system that included a monitor and the software to upload and process the data. The monitor was designed to collect data on skin conductance from ambulatory research subjects for up to seven days. The monitor clips directly unto the self-adhesive electrode patch eliminating the need for any cables. It is worn unobtrusively on the sternum hidden under clothing and is easy to remove and replace. The housing of the monitor is water resistant so when bathing the monitor is unclipped from the electrode, which is left in place. After bathing the electrode patch is simply patted dry and the monitor reconnected. Fig. 9 shows the front centered push button and the offset red and green LED. The two snaps on the back connect directly to the electrode patch. Fig. 10 shows how the monitor is worn.

Fig. 9: The size of the monitor is 7.2 cm × 3.8 cm × 1.2 cm and it has a mass of 16 g - 0.56 oz including the battery. The battery has a life of more than 1 week. The conductance range is 0 to 30 µS

Fig. 10: Placement of the monitor is usually vertically over the sternum but it can be placed on either side of the sternum without affecting the data.

Acknowledgements

We wish to thank Professor Willis J. Tompkins from the Biomedical Engineering Department at the University of Wisconsin in Madison for proof reading this paper and for his helpful and constructive feedback. This research and development was funded by two SBIR Phase I grants R43AT3183-01, R43AT4070-01, and by a SBIR Phase II grant 2R44AT3183-02 from the National Institutes of Health National Center for Complementary and Alternative Medicine (NCCAM).

References

[1] KRONENBERG F, 1990 Hot flashes: epidemiology and physiology *Ann. N. Y. Acad. Sci.* **592** 52–86

[2] FREEDMAN R, 1998 Biochemical, metabolic, and vascular mechanisms in menopausal hot flashes *Fertility and Sterility* **70** 332–7

[3] MACLENNAN A, LESTER S, MOORE V.(2001): 'Oral estrogen replacement therapy versus placebo for hot flushes: a systematic review', *Climacteric*. **4**(1) 58-74

[4] ROSSOUW JE, ANDERSON GL, PRENTICE RL, ET AL. (2002): 'Risks and benefits of estrogen plus progestin in healthy postmenopausal women: principal results From the Women's Health Initiative randomized controlled trial', *JAMA*. Jul 17 **288**(3) 321-33

[5] SHUMAKER SA, LEGAULT C, RAPP SR, ET AL. (2003): 'Estrogen plus progestin and the incidence of dementia and mild cognitive impairment in postmenopausal women: the Women's Health Initiative Memory Study: a randomized controlled trial', *JAMA*. May 28 **289**(20) 2651-62

[6] ANDERSON GL, LIMACHER M, ASSAF AR, ET AL. (2004): 'Effects of conjugated equine estrogen in postmenopausal women with hysterectomy: the Women's Health Initiative randomized controlled trial', *JAMA*. Apr 14 **291**(14) 1701-12

[7] SHUMAKER SA, LEGAULT C, KULLER L, RAPP SR, ET AL. (2004): 'Conjugated equine estrogens and incidence of probable dementia and mild cognitive impairment in postmenopausal women: Women's Health Initiative Memory Study', *JAMA*. Jun 23 **291**(24) 2947-58

[8] REENDALE GA, REBOUSSIN BA, HOGAN P, ET AL. (1998): 'Symptom relief and side effects of postmenopausal hormones: results from the Postmenopausal Estrogen/Progestin Interventions Trial', *Obstet. Gynecol.* Dec **92**(6) 982-8

[9] SLOAN JA, LOPRINZI CL, NOVOTNY PJ, ET AL. (2001): 'Methodologic lessons learned from hot flash studies', *J. Clin. Oncol.* Dec 1 **19**(23) 4280-90

[10] MILLER H. G., LI, R. M. (2004): 'Measuring hot flashes: Summary of a national institute of health workshop', *Mayo Clinic Proc*. June **79**(6) 735-7

[11] MOLNAR G.W., Body temperatures during menopausal hot flashes, *J Appl Physiol*, Vol. 38, No. 3, March 1975

[12] JOSSINET, J. and McADAMS, E., Hydrogel electrodes in biosignal recording, *Proc. Annu. Int. Conf. IEEE Eng. Med. Biol. Soc.*, 12(4): 1490-1491, 1990.

[13] ROSENBLATT F, The perceptron: "A probabilistic model for information storage and organization in the brain. Psychol. Rev. 65:386-408, 1958.

[14] SEMLOW J.L., Biosignal and Medical Image Processing, Second Edition, CRC Press, 2009.

[15] SMITH S.W., Digital Signal Processing a Practical Guide for Engineers, Second Edition, Newnes, 2003.